AN INVESTIGATION OF THE ACTIVITY OF ZONAL

CATALYST BEDS FOR HYDRODESULFURIZATION

AND HYDRODENITROGENATION OF A

COAL-DERIVED LIQUID

By

OPINDER KISHAN BHAN

Bachelor of Engineering
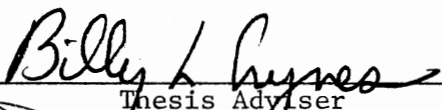
University of Kashmir

Srinagar, India

1978

Submitted to the Faculty of the Graduate College
of the Oklahoma State University
in partial fulfillment of the requirements
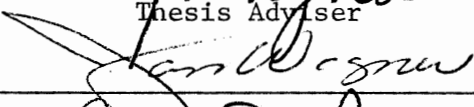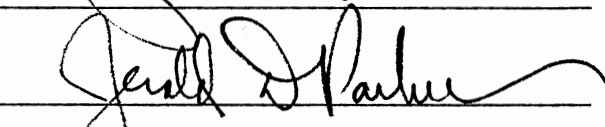for the Degree of
MASTER OF SCIENCE
May, 1981

AN INVESTIGATION OF THE ACTIVITY OF ZONAL

CATALYST BEDS FOR HYDRODESULFURIZATION

AND HYDRODENITROGENATION OF A

COAL-DERIVED LIQUID

Thesis Approved:

Billy L. Crynes

Thesis Adviser

Jan W. Cogan

Jerald D. Parker

Norman N. Durham

Dean of the Graduate College

1084845

PREFACE

Two different catalysts, Ketjenfine-124 (Co-Mo-alumina) and HDN-30 (Ni-Mo-alumina) were studied for hydrotreatment of Pamco Solvent (a coal-derived liquid) separately and in a zonal bed combination. Experiments were conducted at a pressure of 1500 psig and temperatures of $615^{\circ}F$ $(324^{\circ}C)$ and $815^{\circ}F$ $(435^{\circ}C)$. Data were obtained for liquid volume hourly space times in the range of 0.5 to 2.5 hours. Five experimental runs were conducted with run durations up to 120 hours.

I am deeply indebted to my thesis adviser, Professor B. L. Crynes, for his guidance and help in the completion of this study. My special appreciation and thanks are due to him for his inspiration, support, and patience during the entire project. I would also like to thank Dr. M. Seapan and Mr. H. J. Chang for their valuable suggestions and constant cooperation in completing this work. I am very grateful to Messrs. Warren Price, Andrew Tayrien, Steve Mahaffey, Mike Redmund, Pawan Tomkoria, Kevin Bloomer, Gene Haub, Tom Wiles, Cathy Tharp, and Steve Wilkinson for their help in operating the equipment.

A special note of thanks is due Mr. E. E. McCroskey, the store manager, and all of the office secretaries in the School of Chemical Engineering for their cooperation in completing this research and the needed paper work. I would also like to thank Mr. Mike Remmington for completing the drawings and Mrs. Grayce Wynd for typing this thesis.

Finally, I express my deepest gratitude to my parents and my brother for their constant support, inspiration, and encouragement in making this achievement a reality.

TABLE OF CONTENTS

LIST OF TABLES

LIST OF FIGURES

CHAPTER I

INTRODUCTION

The United States' domestic energy production has not been able to keep pace with energy consumption. As a result, the United States has been importing energy, mainly in the form of crude oil. Recent political events have demonstrated the vulnerability of foreign supplies. Accordingly, a massive effort has been launched in this country to develop alternate energy sources which would reduce the crushing dependence on foreign oil. Coal has been cited as the fuel of the future; the utilization of coal in spite of its abundance has been limited, due mainly to the environmental restrictions and due to the difficulty of transporting it. Major research effort is being directed toward making coal-burning efficient, environmentally acceptable, and economically competitive. Table I presents statistics of the United States energy consumption, production, and imports for the year 1979.

Production of coal liquids can be categorized under four major types; the main concepts of these processes are described below:

Pyrolysis

Coal is heated to high temperatures to yield solid (char), liquid and gaseous products, resulting in reduction of the carbon content of the solid. Gas from the process can be sold as fuel gas or converted by application of additional technology to pipeline gas or hydrogen.

1

TABLE I

UNITED STATES ENERGY PRODUCTION, CONSUMPTION, AND
NET IMPORTS[1] BY TYPE, 1979

Type	Production	Consumption	Net Imports
	(Quadrillion $[10^{15}]$ BTU)		
Coal	17.406	15.079	[1.729]
Natural gas	19.238	19.914	1.228
Crude oil	18.064	37.135	13.223
Natual gas plant liquids	2.398	-	-
Hydropower	2.957	3.163	0.206
Nuclear power	2.750	2.750	-
Refined petroleum products	-	-	-
Others[2]	0.089	0.066	-
Total	62.903	78.197	13.233

[1]Net imports = imports minus exports. (Brackets indicate exports greater than imports.)

[2]Includes geothermal power and electricity produced from wood and waste.

Source: Monthly Energy Review, U. S. Department of Energy, May, 1980.

The residual char is used as powerplant fuel, or gasified. A typical
example of this process is Occidental Research Corporation's flash
pyrolysis coal liquefaction process (Coal Liquefaction, April, 1980).

Solvent Extraction

In these processes, coal is reacted with a coal-derived liquid.
This liquid, high in hydrogen content, transfers the hydrogen to the
coal, thus increasing the yield of liquid products. Typical processes
under this category are the Solvent Refined Coal (SRC) process and the
Exxon Donor Solvent (EDS) process (Coal Liquefaction, April, 1980).
In the EDS process, coal, recycle solvent, and hydrogen are reacted to
produce gas, raw coal liquids, and a heavy bottoms stream that con-
tains coal and mineral matter. The liquefaction step effluent is sep-
arated via distillation, and the recycle solvent is catalytically
hydrogenated to produce rejuvenated solvent. Heavy bottoms from the
distillation section are further processed to produce additional
liquids and hydrogen. A 250 ton-per-day coal liquefaction plant is
operated at Baytown, Texas. In the SRC-I process, the coal is extracted
with recycle solvent in a hydrogen atmosphere to produce a solid
product, low in ash and sulfur. In the SRC-II process, the severity
of operating conditions is increased to yield a liquid distillate fuel
with a 350°F (175°C) - 800°F (427°C) boiling range. A 50 ton-per-day
plant is in operation at Fort Lewis, Washington. This plant has been
operated in both SRC-I and SRC-II modes.

Catalytic Liquefaction

In these processes, coal is hydrogenated in the presence of a

catalyst to form a low sulfur feed oil. The typical process under this category is the H-coal process. The H-coal process employs an ebullated-bed reactor. The catalyst activity is maintained by periodic addition of fresh catalyst and withdrawal of spent catalyst. A 600-TPD plant employing the H-coal process has been started at Catlettsburg, Kentucky.

Indirect Liquefaction

Here coal is reacted with steam and oxygen in fluidized bed reactors to produce raw synthesis gas, which is mostly a mixture of hydrogen and carbon monoxide. These gases are treated to remove impurities and then subjected to catalytic reduction to produce various hydrocarbons. This process was commercialized in Germany during World War II. The only commercial plants operating presently are at Sasolburgh, South Africa. Sasol I plant has been operating since the the 1950s. The Sasol II plant went into operation this year. The project was engineered and constructed by Flour Engineering and Construction, Inc., at a total cost of $2.9 billion. Sasol II will be duplicated by the Sasol III Plant (C. E. P., March, 1980).

Coal-derived liquids have been shown to be quite different in composition and properties than petroleum fuels. Coal liquids possess higher concentrations of polynuclear aromatics and relatively high concentrations of hetero-atoms. The concentration of the polynuclear aromatics and hetero-atom compounds is dependent upon the initial coal liquefaction technique (i.e., catalytic, noncatalytic, pyrolytic, etc.) and coal types. Due to these differences, the chemistry of upgrading the coal-derived liquids is different from that of petroleum crudes.

Coal liquids possess high nitrogen, sulfur, and oxygen. The C/H ratio is twice that of petroleum fuels due to the higher aromaticity. Some of the aromatics present in coal liquids are benzenes, tetralins, napthalenes, anthracenes, phenanthrenes, acenapthylenes, etc. Oxygen-containing hetero-cyclic compounds common among coal liquids are phenols, dibenzofurans, benzonapthofurans, and indanols. Compounds containing nitrogen are quinolines, acridines, carbazoles, and indoles. Common sulfur containing compounds are thiophenes, benzothiophenes, dibenzothiophenes, and benzonapthothiophenes. This is in contrast to petroleum fuels, wherein sulfur and organomettalic compounds are invariably the heteroatoms of concern.

It is imperative that hydrotreating of coal liquids precedes catalytic cracking or reforming in an upgrading scheme. This is due to the inability of the catalyst employed in the latter processes to withstand irreversible metal poisons, coking, basic adsorption, as well as heteroatom containing polyaromatics.

During hydrotreatment, sulfur, nitrogen and oxygen are removed as hydrogen sulfide, ammonia, and water, respectively. Sulfur must be removed from the products to meet the low level required for further catalytic processing and to meet the environmental requirements. Nitrogen removal from coal liquids is necessary for the following reasons:

1) These fuels cannot otherwise be burned without exceeding NO_x emission restrictions.

2) Nitrogen-containing compounds severely reduce the activity of cracking, reforming, hydrocracking, hydrodesulfurization, hydrogenation and isomerization catalysts. (The catalysts used in these processes are acidic and are thus poisoned by various nitrogen-containing

compounds, which are strongly basic.)

3) The stability of the product is affected by the high nitrogen concentration.

4) The coal liquids can be quite carcinogenic due to the high aromatic nitrogen content; hydrogenation is required to reduce the nitrogen content and hence the carcinogenicity.

Certain oxygen-containing compounds are acidic, and their presence is unwelcome. Further, it has been observed that upon storage, coal liquids increase in viscosity and gum deposits occur. This probably occurs due to the unstable species present in coal liquid. Hydrotreatment prior to storage results in a stable product; this may be due to the reaction of unstable products to form high molecular weight compounds.

Experience with petroleum feedstocks has led to the development of catalytic hydrotreatment processes. The commercial catalysts developed for hydrotreatment in the petroleum industry have been developed to process mostly paraffins and olefins. The catalyst type mostly employed in the petroleum industry for hydrotreatment is cobalt-molybdenum on an alumina support. Industrially, hydrotreatment is carried out in trickle-bed or fluidized (ebullated) bed reactors.

The present study is part of the research program currently underway at the School of Chemical Engineering, Oklahoma State University, Stillwater, Oklahoma, to develop catalysts and to determine optimum process conditions for upgrading coal-derived liquids. The objectives of the present study were as follows:

1) to design, construct, and test a trickle-bed reactor system for hydrotreatment of coal-derived liquids;

2) to study the effect of zonal-catalyst-beds (employing two different catalysts) for hydrotreatment of coal liquids;

3) to lay groundwork for future study of the concept of guard chambers and "throw away" type catalysts for coal liquid upgrading;

4) to investigate the activity of nickel-molybdenum and cobalt-molybdenum catalysts for hydrodesulfurization, hydrodenitrogenation of a coal liquid.

CHAPTER II

LITERATURE REVIEW

Hydroprocessing of coal-derived liquids will become increasingly important in the future as they enter the commercial market as a substitute feedstock for petroleum refineries. Hydrodesulfurization and hydrodenitrogenation of petroleum feedstocks are practiced commercially in trickle-bed reactors. Considerable research is being conducted by the various organizations in this country to commercialize the production of synthetic fuels from coal.

Trickle-Bed Reactors

Trickle-bed reactors have been used extensively in industry for hydrodesulfurization of petroleum feedstocks. The first trickle-bed hydrodesulfurization unit employing cobalt-molybdenum catalyst was put into commercial operation in 1951 (Van Deemter, 1964). In trickle-bed reactors, liquid and gas flow concurrently over a bed of catalyst particles. The ebullating-bed reactor is the principal alternative to using trickle-bed reactors. The trickle-bed reactor offers the following advantages:

1) The flow pattern is close to that of plug-flow, allowing high conversion per pass.

2) The liquid flows as a film, thus offering smaller diffusion resistance.

3) Simplicity of operation and maintenance.

Some of the disadvantages associated with using trickle-bed reactors are their thermal instability and plugging tendency. High recycle rates and interstage quenching have been recommended to control the temperature.

The scaleup of a trickle-bed reactor is difficult due to the complex fluid mechanics of trickle-bed reactors.

Gas and Liquid Distribution

Three types of flows have been observed in trickle-bed reactors:

1) gas continuous flow

2) rippling and slugging flow

3) dispersed bubble flow.

In the laboratory scale units, gas continuous flow is observed, where a thin liquid film trickles down the packing and the gas phase is continuous. Satterfield (1975) observed that the liquid tends to migrate to the reactor wall, the steady state fraction corresponding to as much as 30 to 60% of the total, at a reactor-to-particle diameter ratio of 10. Determination of flow patterns and liquid holdup is important for modelling, design, and scaleup of trickle-bed reactors. The present state of knowledge about liquid holdup is rather inadequate; most of the available information is on integral values of holdup and very little is known about holdup profiles and transient changes of liquid holdup. This is probably due to the difficulty of obtaining local values of holdup. Techniques requiring the use of X-rays, electrical conductivity, and radioactive tracers have been employed (Achwal and Stepanek, 1976). Ramachandran and Smith (1979)

gave an analysis for the transient behavior of a trickle-bed reactor in which gas and liquid stream flow downward through a bed of catalyst particles. Concentration disturbances (step or pulse) of reactant were introduced into the feed and the response was observed in liquid effluent. Equations were presented for the zero and first moment responses, and procedures were discussed for evaluating equilibrium, mass transfer, and reaction rate constants from the moment equations.

Herskowitz and Smith (1978) obtained liquid distribution data for fourteen catalyst particles of different sizes (0.26 to 1.1 cm), shapes (granular, spherical, cylinderical), and porosity as a function of feed distribution, gas and liquid flow rates, and catalyst bed depths, using deionized water and air in two columns (4.08 and 11.4 cm I.D.). Equations for predicting the flow distribution include two parameters: a spreading factor "S" which accounts for the fraction of liquid moving in the radial direction, and a wall factor "f" which accounts for the flow at the wall, which is directed back into the bed. From this the packed-bed depth to attain equilibrium distribution can be predicted.

The liquid holdup is defined as the volume occupied by liquid as a proportion either of the total volume or of the free volume in a packed bed. The liquid holdup is conventionally divided into two parts: static holdup and dynamic holdup. Dynamic holdup arises from that part of the liquid which moves continuously through the bed and is continuously replaced by a fresh phase. This liquid drains freely when the flow of phases is discontinued. Dynamic holdup depends on the conditions of flow of the liquid and gas phases, and on the geometry of the packing. The static part of the holdup arises from the liquid which is

more or less stationary and is replaced only very slowly, if at all, by

the fresh phase. The liquid does not drain after the flow of the

phases is stopped. The value of the static holdup depends on the

nature and dimensions of the packing and on the physical properties of

the liquid phase. The gas holdup can also be similarly defined and it

too is divided into static and dynamic holdup. The static holdup in

this case occurs due to the gas bubbles trapped in the cavities or held

in place by surface tension. Satterfield (1975) proposed a maximum

internal holdup corresponding to the total pore volume of the catalyst,

typical range being from 0.15 to 0.40.

Satterfield and Way (1972) represented external holdup as a func-

tion of the superficial liquid velocity and liquid viscosity as follows:

$$H = A \ U_L^{1/3} \ M_L^{1/4} + B$$

where

H = external holdup (liquid)

U_L = superficial liquid velocity

M_L = liquid viscosity

A and B are constants depending upon the characteristics of the par-

ticle, its shape and size.

Goto and Smith (1975) in their studies with glass beads (0.431 cm)

and porous CuO-ZnO catalyst particles (0.291 cm) observed Satterfield

and Way's correlation to be adequate for particle diameter less than

0.3 - 0.4 cm. Achwal and Stepanek (1976) used electrical conduc-

tivity to investigate the holdup and holdup profiles in concurrent

packed columns. They observed a steady increase of gas holdup in the

direction of flow that could be related to the change in pressure. Schwartz et al. (1976) obtained data on liquid holdup in a trickle-bed reactor (1.35 cm I·D, 30.5 cm height) packed with either porous or nonporous alumina of equal size (0.06 cm) and compared it with data obtained by other investigators. They confirmed the independence of liquid holdup over a moderate range of gas flow rates.

Morsi et al. (1978) reported data obtained on experiments carried out in a 5 cm I·D column, packed to a length of 120 cm with spherical porous Co-Mo alumina catalyst particles (d = 2.4 mm) operating at atmospheric pressure over the range of $18^{\circ}C$ ($65^{\circ}F$) to $20^{\circ}C$ ($77^{\circ}F$) for gas and liquid flow rates representative of those employed in commercial reactors. A correction factor was proposed to take into consideration the liquid viscosity effect when viscosity is lower than 20 centipoise.

Henry and Gilbert (1973) attributed lower performance of pilot scale reactors to their low value of dynamic liquid holdup. For a reactor which carries out a first order reaction they proposed the following relation:

$$\log \frac{C_{in}}{C_{out}} \; \alpha \; \frac{(h)^{1/3} \, d^{-2/3} \, \nu^{1/3}}{(LHSV)^{2/3}}$$

where

C_{in}, C_{out} = initial and final concentration of the reactants gm-moles/cc

d = characteristic diameter of catalyst particle, cm

h = catalyst bed height, cm

LHSV = liquid volume hourly space velocity

ν = kinematic viscosity, cm^2/sec

This equation predicts that at fixed reaction temperatures and catalytic activity, the degree of reaction will be enhanced by increasing the catalyst bed length and be decreased by increasing the system space velocity, other factors remaining unchanged. The higher liquid holdups, according to Henry and Gilbert, may be the key to increased catalyst utilization.

Catalyst Wetting

Two types of wetting can be defined:

a) Internal wetting (pore filling): This is the measure of the amount of internal (active) surface potentially available for the reaction.

b) External effective wetting, i.e., the amount of the outside area of the catalyst effectively contacted by the flowing liquid. Almost all of the mass transfer between the internal liquid and the flowing liquid occurs through this area.

Satterfield and Ozel (1973) observed for hydrogenation of benzene over Pt-on-alumina pellets, the liquid flows downward in rivulets, which tend to maintain their position with time. Some of the catalyst pellets were covered with a trickling liquid film while others, although wet, were without a liquid film on the surface. This observation was made visually through a glass-walled reactor, where measures were taken for excellent initial liquid distribution. The authors further observed that the incomplete wetting in trickle-bed reactors gives rise to an increase of the evaluated kinetic rate constant,

"k_{app}", with an increase of liquid superficial velocity.

Mears (1974) proposed the reaction rate to be proportional to the effectively wetted fraction of the outside catalyst surface. Colombo et al. (1976) argued that in ordinary cases, wetting plays a more complex part in trickle-bed reactor performance than stressed by Mears. The external effective wetting was interpreted in terms of an apparent internal diffusivity $(D_i)_{app}$, determined on the basis of a model assuming total external wetting of the catalyst.

Sylvester and Pitayagulsarn (1974) considered under two separate cases the effect of catalyst wetting on conversion in a countercurrent trickle-bed reactor. They observed that for non-volatile liquids, when reaction occurs only on a wetted catalyst, the reaction rate is lower than the volatile liquid phase because the reaction can occur at both wetted and non-wetted catalyst. This the authors attributed to the considerably greater pore diffusion limitation of the wetted catalyst. Crine et al. (1980) presented an empirical equation which can be solved to determine the fraction of the catalyst surface which is wetted:

$$G = 1.961 \frac{L}{L_m} - 1.275 \left(\frac{L}{L_m}\right)^2 - 1.598 \left(\frac{L}{L_m}\right)^3 + 3.326 \left(\frac{L}{L_m}\right)^4 - 1.417 \left(\frac{L}{L_m}\right)^5$$

for $0 < L/L_m < 1$

$G = 1$

for $L/L_m > 1$

where

L_m = minimum liquid flow rate ensuring the existence of the liquid film and rivulets, Kg/m^2 - sec

L = superifcial liquid velocity, Kg/m^2 - sec

G = irrigated fraction

Klinken et al. (1980) observed that the dilution of a catalyst bed with small inert particles greatly improves the laboratory trickle flow reactor performance. This they attributed to the increase in liquid holdup, resulting in more effective catalyst wetting and an increase in the number of mixing stages to a level where plug-flow is closely approximated.

Crynes (1980) conducted experiments to determine the advantage of using a diluted catalyst-bed. No advantage of the larger inert particles (0.83 - 1 mm) over smaller inert particles (0.25 - 0.595 mm) was reported for hydrotreatment of Rasyn oil over 1/16 inch Ni-Mo-alumina catalyst at 700^oF (371^oC) and 1500 psig pressure.

Satterfield (1973) advocated an upflow operation as an alternative to trickle-bed processing, as it ensures the contact of all catalyst pellets with the liquid; the relative volatility of liquid reactants being an important factor.

Axial Dispersion and Mass Transfer Effects

Numerous models have been proposed to account for axial dispersion in trickle-bed reactors which can have a significant effect on the performance of the catalytic reactors.

Mears (1971, 1974) presented the following criterion for minimum h/d_p ratio required to hold the reactor length (h) within 5% of that

needed for plug flow for first-order reactions:

$$h/dp > \frac{20n}{Bo} \, \ln \frac{C_{in}}{C_{out}}$$

where

Bodenstein number, Bo, is the pecklet number based on the

particle diameter $(\bar{V}_L \, d_p/D_L)$

$\bar{V}_L$ is the superficial liquid velocity

d_p is the particle diameter

D_L is the liquid axial dispersion coefficient, and

C_{in} and C_{out} are the inlet and outlet concentrations.

Mears calculated, at Reynolds number equal to eight, the minimum

h/d_p ratio to be 350. Mears (1976) extended the axial dispersion model

for non-isothermal reactions, cooled or heated at the wall. He pro-

posed for minimum axial dispersion in non-isothermal reactors with low

conversion

$$\frac{D_{aI}}{Pe_{mz}} < \frac{0.05}{n}$$

where

D_{aI} = Damkohler number for bulk mass flow $(R \, d_p/\bar{U}D_o)$

R = reaction rate per unit bulk volume of catalyst

$\bar{U}$ = superficial liquid velocity

C_o = concentration of the limiting reactant

Pe_{mz} = axial pecklet number for mass based on catalyst diameter

$(\bar{U} \, d_p/D_z)$

d_p = particle diameter

D_z = axial dispersion coefficient for mass

n = order of the reaction

Satterfield (1975) reported that mass transfer through the liquid film is not a significant resistance under typical hydrodesulfurization conditions. The average film thickness is so much less than the radius of the usual catalyst particles that it will not ordinarily be a significant resistance, unless the effectiveness factor of the catalyst is quite low. He further observed that if gas-liquid mass transfer is an appreciable resistance, as would tend to occur at high reaction rates, and correspondingly high liquid flow rates, a higher reaction rate per unit quantity of the catalyst pellets can be obtained by mixing an inert material with the catalyst. Goto and Smith (1975) reported through experimental studies on the oxidation of formic acid in water with $CuO \cdot ZnO$ catalysts that the performance of trickle-bed reactor depends on four transfer resistances: gas-to-liquid, liquid-to-particle, intraparticle and axial dispersion.

Shah and Paraskos (1975) using an approximate solution technique, concluded at high conversion an adiabatic operation produces a larger axial dispersion effect than isothermal operation, the opposite being true for low conversions. Colombo et al. (1976) reported total pore filling of the catalyst pellets even at low liquid flow rates. According to them, $(D_i)_{app}/D_i$, where $(D_i)_{app}$ is the internal diffusivity at total wetting and D_i is the actual internal diffusivity, tends to 1 as the flow rate increases. They further observed $(D_i)_{app}/D_i$ to depend upon the packing size and the molecular diffusivity of the reactant.

Schwartz et al. (1976) reported the liquid phase pecklet number to be four to ten times smaller than in the single phase flow, indicating larger axial dispersion in trickle-bed reactors.

Wakao and Smith (1962) proposed a theory for predicting diffusion rates at constant pressure through bi-dispersed porous media. Experimental results showed for five high-area alumina pellets of different densities made from boehmite powder, that for the least dense pellets macropore diffusion is dominant; in contrast, micropore diffusion controls the diffusion rate in the dense pellets.

Montagna et al. (1977) reported data on the hydrodesulfurization of reduced Kuwait crudes. The authors used liquid holdup and an effective wetting model to show the dependence of conversion on particle diameter. Their model is as follows:

$$\ln \frac{C_i}{C_o} \; \alpha \; (L)^{1/3} \; (LHSV)^{-2/3} (d_p)^{-2/3} (M_L)^{1/3}$$

where

C_i and C_o = concentration of the reactant entering and leaving the reactor

L = catalyst bed length, cm

LHSV = liquid hourly space velocity of feed at reactor inlet conditions

d_p = particle diameter, cm

M_L = viscosity of liquid, gm/cm sec

Marangozis (1980) questioned the effect of the catalyst particle diameter on the conversion. He used equivalent spherical diameter of

the catalyst particle and showed the conversion to be proportional to $(d_s^{-4/3})$ instead of $(d_p^{-2/3})$ as proposed by Montagna (1977).

The mass transfer resistance within the catalyst can be significant; it is accounted for by means of a variable called the "effectiveness factor" η, defined as the ratio of observed rate of reaction to that which would occur if the pellet interior were exposed to the reactants at the same temperature and concentration as exist at the pellet exterior.

Smith and Ramachandran (1979) defined an overall effectiveness factor, η_o, based upon bulk stream concentration, which accounted for partial liquid coverage. Smith et al. (1979) measured rates of hydrogenation of alpha-methyl styrene at $40.6^{o}C$ and 1 atm in a recycle, trickle-bed reactor, using palladium-aluminum oxide catalyst. They concluded that except at high liquid flow rates, mass transfer limitation is very small, indicating gas covered type surface. A procedure was developed for evaluating effectiveness factor for non-uniform boundary conditions, with part of the liquid surface covered by gas. Dudukovic (1977) demonstrated the catalyst effectiveness factor for the first order reactions to be a function of the ratio of the characteristic internal diffusion, reaction time, external contacting efficiency and internal pore fillup. The following performance equation was reported for the first order reaction:

$$\ln \frac{1}{1-x} = \frac{V(1-\varepsilon)}{QL} k_{tc} \eta_{TR}$$

where

x = fractional conversion, dimensionless

ϵ = bed porosity, dimensionless

V = reactor volume, cm^3

Q_L = liquid flow rate, cm^3/sec

k_{tc} = true reaction rate, sec

n_{TB} = catalyst effectiveness factor in trickle-bed reactor, dimensionless

Studies by Satchell (1974) on denitrogenation of raw anthracene oil (a coal liquid) with Co-Mo-alumina catalyst showed the effectiveness factor to be one at 650^oF (343^oC) and 0.95 at 700^oF (317^oC). The reactor operating pressure was 1000 psig. Sooter (1975) found that a decrease in the particle size from 0.079 inch (0.2 cm) to 0.0127 inch (0.03 cm) to have no effect on hydrodesulfurization of raw anthracene oil, using Co-Mo-alumina catalyst. Van Deemter (1964) observed the effectiveness factor to increase from 0.37 to 0.97 when particle size was reduced from 0.196 inch (0.5 cm) to 0.137 inch (0.348 cm) for HDS studies with straight-run gasoline. Van Zoonen and Douwes (1963) found the effectiveness factor to be one for hydro-denitrogenation of straight-run gasoline at 707^oF (375^oC) for 3 x 3 mm Co-Mo-alumina catalyst pellets.

This section on trickle-bed reactors can be summarized as follows: Although trickle-bed reactors are used extensively in the petroleum industry, very little literature has been published about the influence of the operating variables on the reactor performance under the actual hydrotreating reaction conditions. Attempts have been made to interpret the effect of liquid maldistribution, deviation from the plug-flow and incomplete catalyst wetting on the performance of trickle-bed

reactors. Most of the studies have been made visually with air-water systems in glass-walled reactors. Many investigators have attributed the poor performance of the trickle-bed units to low liquid-holdup and incomplete catalyst wetting. Effectiveness factors in the range of 0.3 to 1.0 have been reported for hydrodenitrogenation and hydrodesulfurization reactions with commercial catalysts.

Hydrodesulfurization and Hydrodenitrogenation

Reaction Kinetics

In catalytic hydrodesulfurization processes, sulfur is removed in the form of hydrogen sulfide according to the following non-stoichiometric reaction:

organic sulfur compound + $H_2 \rightarrow H_2S$ + desulfurized organic compound
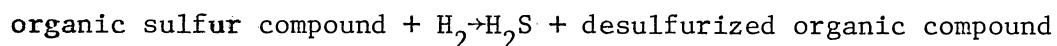
These classes of reactions have been studied extensively. An excellent review of hydrodesulfurization chemistry and technology has been given by Schuit and Gates (1973). The hydrodesulfurization technology for light petroleum feeds is well established; new technology is being evolved for residuum and coal-derived liquids. Hydrodesulfurization reactions are hydrogenolysis reactions which result in C-S bond cleavage. Hydrocracking, hydrogenation, demetallization, hydrodenitorgenation and hydrodeoxygenation reactions also occur. Relative rates of S, N, and O removal from heavy gas oil have been seen to be in qualitative agreement with C-S, C-N, and C-O bond strengths. The rate of hydrodesulfurization (HDS) is the highest, followed by hydrodenitrogenation (HDN) and hydrodeoxygenation (HDO).

Considerable literature is devoted to the study of

hydrosulfurization of pure compounds; a list of sulfur-containing compounds found in coal liquids is given in Table II. Thiophene and benzothiophene have been the most studied compounds. Houalla et al. (1978) experimentally determined the reaction network in the hydrodesulfurization of dibenzothiophene catalyzed by sulfided Co-Mo-alumina at $572^{\circ}F$ ($300^{\circ}C$) and 1500 psig. Sulfur removal is the predominant reaction, giving biphenyls and hydrogen sulfide, subsequent hydrogenation of biphenyl to cyclohexylbenzene and then to bicyclohexyl takes place slowly. Dibenzothiophene was also found to undergo primary hydrogenation prior to the sulfur removal, but it is one thousand times slower than the sulfur extrusion. Dibenzothiophene is one of the least reactive compounds and is found significantly in petroleum and especially in the coal-derived liquids. Kilanowski and Gates (1980) studied the kinetics of benzothiophene (BT) in a differential flow reactor containing sulfided Co-Mo-alumina catalyst at $486^{\circ}F$ ($252^{\circ}C$) - $630^{\circ}F$ ($332^{\circ}C$). The partial pressure of reactants was varied in the following range: Benzothiophene, 0.015 - 0.23; H_2, 0.20 - 2.0; H_2S, 0.02 - 0.14 atm. They concluded that adsorbtion of BT and H_2S occurs on one kind of catalytic sites and H_2 on another.

Kawaguchi et al. (1978) studied HDS of thiophene over a Ni-Mo-alumina catalyst at about atmospheric pressure and a temperature range of $518^{\circ}F$ ($270^{\circ}C$) to $662^{\circ}F$ ($350^{\circ}C$). They confirmed using other catalysts, that the degree of conversion increased in the sequence, Ni-W-alumina < Ni-Mo-alumina < Co-Mo-alumina.

Gates et al. (1978) reported from their studies of HDS of multi-ring sulfur compounds that the reactivity decreases from 1-ring to 3-ring compounds and then increases for 4-ring compounds. The first

TABLE II

REPRESENTATIVE SULFUR COMPOUNDS FOUND IN COAL LIQUIDS

Name	Formula
Thiophene	C_4H_4S
Benzothiophene	C_8H_6S
Dibenzothiophene	$C_{12}H_8S$
3-Methylthiophene	C_5H_6S
7-Methylbenzothiophene	C_9H_8S
7,8,9,10-tetrahydrobenzonapthothiophene	$C_{16}H_{14}S$
Thiacyclopentane	C_4H_8S
Benzonaphthothiophene	$C_{16}H_{10}S$
Dihydrobenzothiophene	C_8H_8S
4-6, 3-7, 2-8, - Dimethyldibenzothiophenes	$C_{14}H_{12}S$

order rate constants reported by them are:

Reactant	Pseudo first-order rate constant $cm^3/gm \cdot hr$
Thiophene	5000
Benzothiophene	2900
Dibenzothiophene	200
Benzonapthothiophene	600
7,8,9,10-tetrahydrobenzonapthothiophene	280

They reported the catalytic activity of the catalyst for HDS to
increase as follows: Ni-W-alumina < Ni-Mo-alumina < Co-Mo-alumina.

Hargreaves and Ross (1979) investigated the mechanism of HDS of
thiophene over sulfided Co-Mo-alumina catalysts at a temperature of
482^oF (250^oC) over relatively low pressures. They concluded that ring
hydrogenation of thiophenes occurs prior to C-S bond cleavage. Owens
and Amberg (1961) concluded that hydrogenolysis of the C-S bond in
thiophene precedes hydrogenation of the aromatic ring.

Ahmed (1975) studied the HDS of FMC oil over two commercial Co-Mo-
alumina catalysts at temperatures of 700^oF (371^oC), 800^oF (427^oC),
850^oF (427^oC) and pressure of 1500 psig, employing a liquid volume
hourly space time of 2.99 hours. More than 94% sulfur removal was
reported. Sooter (1974) and Mehta (1978) observed more than 95% removal
for raw anthracene oil at 700^oF (371^oC). Soni (1977) in his studies
with a Synthoil process liquid, observed a sudden increase in sulfur
removal when temperature was increased from 700^oF (317^oC) to 800^oF
(427^oC) at space times above 1.5 hours.

In the hydrodenitrogenation (HDN) process, nitrogen is removed in
the form of ammonia. In general, coal liquids contain more nitrogen

compared to petroleum crudes; hence the need for a special hydrodenitrogenation catalyst. Most of the nitrogen present in the synthetic fuels and petroleum is in the form of heterocyclic compounds. Nonheterocyclic nitrogen-containing compounds include aliphatic amines and nitriles, which are relatively more reactive for hydrodenitrogenation than the heterocyclic nitrogen-containing compounds. The heterocyclic nitrogen-containing compounds in petroleum and synthetic liquids can be divided into basic and nonbasic fractions. Table III lists some of these compounds. Nonbasic compounds are generally converted to basic upon hydrogenation.

Pyridine is a good model compound for study. McIlvried (1971) studied pyridine hydrodenitrogenation over sulfided Co-Ni-Mo-alumina catalyst. Hydrodenitrogenation proceeds via saturation of the heterocyclic ring, followed by ring fracture and subsequent removal of nitrogen as ammonia. He reported the principal steps in hydrodenitrogenation of pyridine as:

Pyridine → Piperdine → Pentyl amine → Pentane + Ammonia
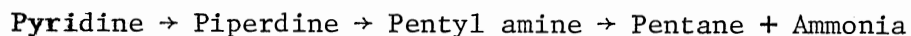
Sonnemans et al. (1974) reported the same reaction network when unsulfided Mo-alumina is used. Satterfield and Cocchetto (1975) studied hydrodenitrogenation of pyride at a pressure of 160 psi over a commercial Ni-Mo-alumina catalyst. They reported that maximum HDN of pyridine occurs at $400^{o}C$ ($750^{o}F$). Ni-Mo-alumina appears to have greater hydrogenation-dehydrogenation activity than Co-Mo-alumina, but Co-Mo-alumina appears to have greater hydrogenolysis activity than Ni-Mo-alumina below and at about $300^{o}C$ ($572^{o}F$).

Satterfield et al. (1980) studied mixtures of pyridine and

TABLE III

REPRESENTATIVE NITROGEN-CONTAINING COMPOUNDS FOUND IN
PETROLEUM CRUDE, SHALE OIL, AND COAL-DERIVED LIQUIDS

Compound	Formula
Nonheterocyclic compounds	
Aniline	$C_6H_5NH_2$
Pentylamine	$C_5H_{11}NH_2$
Heterocyclic compounds	
Pyrrole	C_4H_5N
Indole	C_8H_7N
Carbazole	$C_{12}H_9N$
O-Ethylamiline	C_8H_4N
Pyridine	C_5H_5N
Quinoline and Isoquinoline	C_9H_7N
Indoline	C_8H_9N
Acridine	$C_{13}H_9N$
Benz(a) acridine	$C_{17}H_{11}N$
Benz(c) acridine	$C_{17}H_{11}N$
Dibenz (c,h) acridine	$C_{21}H_{13}N$
1,2,3,4-Tetrahydroisoquinoline	$C_9H_{11}N$
1,2,3,4-Tetrahydroquinoline	$C_9H_{11}N$
Propylaniline	$C_9H_{13}N$
9,10 Dihydroacridine	$C_{13}H_{11}N$

thiophene as model compounds for two groups of reactions, hydrosulfurization and hydrodenitrogenation, occurring simultaneously. At temperatures of 392°F (200°C) to 752°F (400°C), thiophene and pyridine partial pressure of 1.80 psig each, and total pressures of 166, 520, or 1020 psig, over Ni-Mo-alumina catalyst, pyridine inhibited hydrodesulfurization of thiophene. They further reported that the overall conversion of pyridine and piperidine as a pair is enhanced by thiophene at temperatures greater than 572° (300°C) and pressures of 520 and 1020 psig.

An excellent review of the hydrodenitrogenation chemistry has been recently presented by Katzer and Sivasubramanian (1979). Gates et al. (1978) presented the reaction network of quinoline hydrodenitrogenation. Complete ring saturation was observed before C-N bond is broken. They also presented the reaction network of acridine over Ni-Mo-alumina and Co-Mo-alumina catalysts. Co-Mo-alumina catalyst was seen to favor heteroaromatic ring hydrogenation, whereas Ni-Mo-alumina favored aromatic ring hydrogenation. For both acridine and quinoline, little effect of replacing Co with Ni could be detected in nitrogen removal reaction. For competing hydroprocessing reactions catalyzed by Ni-Mo-alumina and involving quinoline, indole and naphthalene in white oil, marked interaction was reported.

Sivasubramanian and Crynes (1980) reported an increase of nitrogen concentration to have a detrimental effect on sulfur removal; the percent sulfur removal varying linearly with percent nitrogen removal. Three laboratory prepared Co-Mo-alumina catalysts were used to hydrotreat a coal-derived liquid (raw anthracene oil), both plain and doctored with quinoline.

Satterfield (1975) reported that thiophene and H_2S inhibit the hydrogenation of pyridine to piperidine, but H_2S enhances hydrogenolysis of piperdine, thereby accelerating the overall series of reactions.

Effect of Temperature, Pressure, Space Time
and Hydrogen Rate

Hydrodesulfurization and hydrodenitrogenation have been found to be a function of several operational variables such as temperature, pressure, space time and hydrogen flow rate. Qader and Hill (1969) observed 62% sulfur removal at $662^{\circ}F$ ($350^{\circ}C$) and 100% removal between $841^{\circ}F$ ($450^{\circ}C$) and $1022^{\circ}F$ ($550^{\circ}C$) in a batch autoclave reactor study of hydrogenation of a coal tar at 1500 psig. Johns, Jones and McMunn (1972) in a pilot plant study of a coal-derived liquid from FMC process reported an increase in sulfur removal with an increase of space time in the range of 1.3 to 5 hours (weight basis). White et al. (1968) reported a sharp break at $752^{\circ}F$ ($400^{\circ}C$) in the Arrhenius plot of the nitrogen removal.

Jones and Friedman (1970) reported first order kinetics for denitrogenation of a COED oil at 3000 psig and $725^{\circ}F$ ($385^{\circ}C$) over a Ni-Co-Mo-alumina catalyst. Wan (1974) and Satchell (1974) observed an increase in denitrogenation with an increase in space time in the range of 0.216 to 1.802 hours. Wan (1974) and Sooter (1975) in their studies of hydrodesulfurization of raw anthracene oil observed that an increase of volume hourly space over the range of 0.216 - 1.802 hours to increase the sulfur removal.

In typical laboratory scale reactors, hydrogen is supplied at high rates and high pressures, ensuring that hydrogen is present in excess

of the stoichiometric requirement. In commercial reactors, hydrogen is recycled after removing the impurities. Scotti et al. (1974) in their pilot plant studies with a coal-derived liquid from the COED process reported hydrogenation at 1800 - 2400 psig with more than 96% sulfur removal. They observed no significant effect on desulfurization by changing the hydrogen purity from 97 to 80%. For Western Kentucky syncrude, they found that the hydrogen consumption leveled off at a constant value of 3200 scf/bbl. Qader and Hill (1969b) reported an increase in nitrogen removal with pressure increase for coal tars. They found that increasing the pressure from 1000 psig to 3000 psig resulted in an increase in nitrogen removal from 50% to 80%, temperature remaining constant at $842^{\circ}F$ ($450^{\circ}C$).

Wan (1974) in his study of raw anthracene oil, varied the hydrogen flow rate from 3980 to 39,800 scf/bbl for sulfur removal and no significant effect was found; but nitrogen removal improved from 61.2 to 69.2% with increase in hydrogen flow rate. The reactor was the trickle-bed type, operating at 1000 psig, $800^{\circ}F$ ($427^{\circ}C$) and 0.901 hour volume-hourly space time. He further observed that hydrodesulfurization increased as pressure increased from 500 psig to 1000 psig. No increase in hydrodesulfurization activity was observed in the 1000 psig to 2000 psig pressure range. Sooter (1975) in his study of the same feedstock observed no significant effect on hydrodesulfurization ability when the hydrogen flow rate was varied from 1500 to 20,000 scf/bbl. The operating conditions in this study were 1000 psig, $650^{\circ}F$ ($343^{\circ}C$) and 1.5 hours volume hourly space time. He further observed no increase in hydrodesulfurization ability when operating pressure was increased above 1000 psig. Satchell (1974) observed an increase in

hydrodenitrogenation as pressure increased from 500 psig to 1500 psig.
Changing the hydrogen flow rate from 1500 to 20,000 scf/bbl had a neg-
ligible effect on nitrogen removal from raw anthracene oil. Various
models have been reported for hydrodesulfurization and hydrodenitro-
genation of coal-derived liquids in trickle-bed reactors. An excel-
lent review of the hydrodesulfurization and hydrodenitrogenation
reactors has been provided by Ahmed (1979).

The section on hydrodesulfurization and hydrodenitrogenation can
be summarized as follows: Both in catalytic hydrodenitrogenation and
hydrodesulfurization reactions, the S and N atoms are removed by
reaction with hydrogen as H_2S and NH_3, respectively. Sulfur removal
is relatively easier compared to the nitrogen atom removal. The sulfur
atom removal from the heterocyclic ring occurs prior to ring hydro-
genation, whereas nitrogen removal always occurs after ring hydrogen-
ation. Highly hydrogenating catalysts have been recommended for HDN
operation; Co-Mo-alumina is preferred for HDS operations. HDS and HDN
reaction rates increase with temperature. Pressure increase above 1500
psig has a negligible effect on the HDN and HDS reaction rates. Much
of the information on HDS and HDN available in the literature origin-
ates from model compound studies. The experimental conditions applied
in such studies are often different from those encountered in indus-
trial operations.

Catalysts

The oxides and sulfides of molybdenum, tungsten, promoted by
cobalt, nickel, zinc, or manganese have been found to be effective
hydrotreating catalysts. The most frequently used metal combinations

are Co-Mo, Ni-Mo, Ni-Co-Mo, and Ni-W, with Co-Mo combination gener-
ally being preferred for hydrodesulfurization and the Ni-Mo combina-
tion being used when hydrodenitrogenation is required.

Support Properties

High purity alumina and alumino-sillicates have been widely
employed as catalysts or catalyst supports in the petroleum industry.
The alumina support typically has surface areas of the order of 200 -
300 m^2/gm, pore volumes of 0.4 - 0.5 cm^3/gm, and an average pore
diameter of 50 - 100 A^o. Alumina can be obtained in eight phases,
gamma and eta phases being most popular for catalytic application.
It is well known that alumina when sufficiently pure is acidic, and
its activity is generally characterized as being of the Lewis type.
Silica-alumina, also, has been shown to be acidic. Both eta and
gamma alumina have been found to have tetragonally deformed spinel
lattices; eta alumina tetragonal structure being much weaker than
gamma alumina structure.

Micininch (1964) explained the cracking activity of pure alumina
above 400^oC by assuming the presence of a Lewis acid site and a
passive Bronsted acid site. Misserov (1969) attributed the cata-
lytic activity of alumino-silicates in the presence of trace amounts of
moisture to the appearance of an acid site of Bronsted type through the
formation of exchangeable alumina-water complex. Muha (1979) reported
the electron acceptor and electron donor properties of gamma-alumina;
some of the active sites on the gamma-alumina act as electron acceptors
while others behave as electron donors.

Gamma-alumina has found widespread use as a support for the active

metals in the hydrodesulfurization of petroleum feedstocks. Gamma-alumina (only support) is used as a catlyst for olefin isomerization, olefin saturation, hydrocarbon cracking, and polymerization. Silica stabilized gamma-alumina has been observed to have more hydro-cracking ability than alumina support alone.

Among the various models proposed for hydrodesulfurization cata-lyst systems, the role assigned to the support differs widely. In both the "intercalation model" and "synergy model" the carrier plays no role in the HDS reaction. However, in the "monolayer model," the moly-bdenum species are supposed to be present in a monolayer chemically bonded to the surface of the gamma-alumina support. DeBeer et al. (1976) reported that any support with high specific surface area (e.g., gamma-alumina, silicon dioxide, carbon) is good for hydrodesulfuriza-tion catalyst system, the alumina being preferred because it inhibits the formation of $CoMoO_4$.

The effect of physical properties of the catalyst support on the catalyst activity has been the subject of many investigations. Siva-subramanian and Crynes (1979) found for the hydrodenitrogenation of raw anthracene oil with essentially no ash content, that changes in the pore-size distribution did not affect nitrogen removal and that bimodal pore-size distribution did not offer any advantage over a monodispersed pore-size distribution. However, they did find that the reduction in the surface area resulted in the reduction of nitrogen removal. Sooter (1974) reported that increasing the pore size tends to increase sulfur removal in his hydrodesulfurization study with anthracene oil. Satchell (1974) found that increasing pore radius from 25 to 33 A^o had no effect on nitrogen removal from raw anthracene oil.

Van Zoonen and Douwes (1963) showed that volume average pore radius in the range of 33 to 232 A^O had a negligible effect on hydrodenitrogenation of a Middle East gas oil. Their study showed that for two catalysts with similar surface areas (190 and 240 m^2/gm) but with different average pure radii (33 and 73 A^O), the average pore radius had a negligible effect on the rate of denitrogenation. However, for desulfurization, they found that pore size influenced converaion.

Catalyst Properties

Co-Mo-alumina catalyst is used extensively in the hydrotreatment of heavy petroleum fractions. The preferred industrial catalysts contain 2 - 4% Co as CoO and 8 - 15% Mo as MoO_3. McKinley (1959) reported the maximum activity to occur at cobalt molybdenum atomic ratios around 0.3:1.0. Commercial preparations use metal ratios in the range of 0.1:1.0 to 1.0:1.0. Hagenbach (1973) showed cobalt molybdate catalysts to be most active at Co to (Co - Mo) ratio of 0.3 - 0.4.

Nickel with tungsten or molybdenum is frequently used for hydrodenitrogenation; Ni-Mo combination is more favored. Laine et al. (1979) found the optimum composition for maximum activity to be 3% NiO:35% MoO_3. The surface areas of the catalysts were found to decrease with increasing MoO_3 loading.

Ratnasamy et al. (1974) reported that cobalt, present in the subsurface layer of alumina, prevents the sintering and phase transformation of the support; which process would otherwise have been facilitated by molybdenum oxide, especially during the calcination of the oxide prior to sulfidation. They further observed that in Co-Mo-alumina systems, not only the structural interaction between the cobalt and

molybdenum constituents, but the nature of this interaction itself is a function of the structural features of the support (such as sodium concentration, surface vacancies, etc.). Even though the active centers of the desulfurization reaction involve only Mo, Co exerts a promotion effect in the creation of these sites and keeping the surface "clean" by hydrogenating the diolefins and other coke precursors. All three constitutents (Co, Mo, and alumina) form an interacting system.

There is uncertainty regarding the structure of the active hydro-treating catalysts. In general, three different models have been pre-sented to explain the hydrotreating activity of the catalyst. These models are described as follows:

1) The monolayer model was originally proposed by Lipsch and Schuit (1969) and later modified by Schuit and Gates (1973). This model assumes the presence of a monolayer of molybdenum oxide on the support. The Mo cations are present in the octahedral position. Alumina is assumed to consist of particles formed by alternate stack-ing of two different layers in the direction of the (110) crystalo-graphic plane. The molybdenum monolayer is supposed to be chemically bonded to the surface of the support; the monolayer being epitaxial to the surface in such a manner that the alternate stacking is continued at the surface. Charge effects due to the Mo^{6+} ions are assumed to be compensated by O^{2-} ions situated in the so-called capping layer on top of the monolayer. The maximum number of these O^{2-} ions per unit mesh is four. The primary effect of Co promotion is the incorporation of tetrahedrally coordinated Al^{3+} ions on the monolayer, their presence increasing the stability of this layer because part of the task of bind-ing the monolayer to the surface layer is taken by the nonreducible

Al^{3+} ion. All of the oxygen present in the monolayer is engaged in completing the surrounding of the Al ions in the surface layer. The cobalt ion is tetrahedrally located below the boundary layer. The accompanying oxygen ions in CoO can find no position in the support and therefore remain in the capping layer. The actual catalyst operated in a reduced and sulfided state; that is, O^{2-} ions are removed from the boundary layer; as in case of reduction with hydrogen, or exchanged by S^{2-} ions, as in the case of treatment with H_2S. The exchange is assumed to occur only in the surface layer. Four O^{2-} ions are replaced by only two sulfur ions, because of the much larger size of sulfur ions. The Co present increases the reduction of Mo while significantly stabilizing the monolayer.

2) Intercalation model was presented by Voorhoeve and Stuiver (1971) and Farragher and Cossee (1972). They based their studies on Ni-W-alumina catalysts. (Intercalation is defined as the accommodation of atoms in the empty sites between double layers.) The interaction of Co or Ni in an ideal crystal of MoS_2 or WS_2 is energetically unfavorable, but it does occur at the layer edges of the sulfide crystals. The authors postulated that intercalation can occur to a certain extent provided the crystals are small. This model stresses the preference of the promoter for an octahedral site. The intercalated Co^{2+} or Ni^{2+} cations are octrahedrally surrounded and their special promoter function is to increase the number of exposed Mo^{3+} or W^{3+} ions, which are believed to be the active sites.

3) The synergy model was presented by Habenbach, Courty and Delmon (1973). The model is based on a study with pure MoS_2 and Co_9S_8. The presence of two completely separate phases in cobalt-molybdenum catalyst

is proposed; one pure MoS_2 and the other pure Co_9S_8. The presence of small amounts of Co_9S_8 causes the MoS_2 to form ideal crystals which as such are very disorderly crystals. Transfer of electrons occurs across the interface between MoS_2 and Co_9S_8 phases; this transfer of electrons results in the MoS_2 phase to become more catalytically active.

Interaction may occur between the catalyst precursors (MoO_3 or WO_3) and the promoters (CoO or NiO) during preparation when the catalyst is still in the oxide form. Richardson (1964) applying magnetic measurement to commercial hydrodesulfurization catalysts, reported that most of the Co^{2+} was present as $CoAl_2O_4$ but that a small fraction might be present as $CoMoO_4$.

Wentrcek and Wise (1978) related catalytic activity with semiconductivity rather than structure. From Hall, coefficient measurements of a single crystal of MoS_2 doped with Co^{2+}, they concluded that the addition of Co^{2+} (<0.1 mol %) causes a change from n-type to p-type conducitvity on MoS_2. Since most of the sulfur or nitrogen-containing substances are electron-donating type, they suggested that the catalytic activity could be related to p-type conductivity.

The catalyst preparation has been found to affect the activity of Ni-Mo catalyst. Whether Ni is impregnated before Mo or vice-versa, affects the catalytic activity. It is not clear why the method of preparation has such a large influence on the catalyst activity. DeBeer et al. (1976) concluded the difference to be largely due to the formation of $CoMoO_4$ in the catalyst. Presulfided $CoMoO_4$ showed a very low activity even in its sulfided state. Efforts should be made to avoid the formation of $CoMoO_4$ during the catalyst preparation.

The section on the hydrotreating catalyst can be summarized as

follows: Catalysts containing Mo, W on gamma-alumina and promoted by
either Ni or Co have been widely employed in the petroleum industry for
hydrodesulfurization and hydrodenitrogenation operations. There is
uncertainty regarding the structure of the hydrotreating catalysts.
Three models, "monolayer, synergy, and intercalation," have been pre-
sented to explain their catalytic activity. The monolayer model best
describes the catalyst structure; intercalation and synergy models
best describe the catalyst during actual operation. The role the pro-
moter plays in the catalytic activity is not clearly understood. The
promoter effect of Ni and Co atoms has been related to the prevention
of the support phase transformation and hydrogenation of coke pre-
cursors. In the intercalation model, the promoter atoms (Co or Ni)
are believed to increase the number of exposed active sites, whereas in
the synergy model the promoter atoms cause the MoS_2 to form ideal
crystals.

Presulfidation

It is generally believed that sulfided species are responsible for
the HDS and HDN activities of Co-Mo-alumina, Ni-Mo-alumina, and Ni-W-
alumina catalysts. The actual involvement of sulfur in the HDS reac-
tions is not entirely understood (refer to section on catalyst proper-
ties.

Mitchell and Trifiro (1974) reported a study of both oxidic and
sulfided Co-Mo-alumina catalysts. By means of magnetic measurements,
infrared transmittance spectroscopy, and diffuse reflectance spectro-
scopy in the ultraviolet and visible spectral region, they came to the
conclusion that during sulfiding, the sulfide adds to the MoO_4

tetrahedra, present in the fresh oxidic catalyst and linked to CoO_6 octahedra. According to these investigators, not more than one or two oxide ions, probably those bridging Mo and Co, are replaced by sulfide. They found the atomic ratio of the sulfided catalyst to be Co:Mo:S = 1:1.77:4.18, which is less than required for complete sulfiding (4.43 atoms per atom of cobalt).

Richardson (1964) proposed MoS_2 to be the true catalytic agent, it being promoted by active Co in octahedral coordination, which could be neither sulfided nor reduced. Hagenbach (1973) attributed the HDS activity to a synergetic effect of strongly interacting MoS_2 and Co_9S_8 phases. Schuit and Gates (1973) in their monolayer model, assumed MoO_3 to be partially sulfided to an extent that the maximum S/Mo ratio is 1. Ahmed (1975) in his hydrodesulfurization study of a coal-derived liquid found the extent of catalyst presulfiding by H_2S/H_2 mixture to have an effect on catalyst activity.

DeBeer et al. (1976) studied the sulfur uptake of MoO_3-alumina, CoO-alumina, and $CoO-MoO_3$-alumina catalysts, using H_2S/H_2 and thiophene/H_2 as sulfiding gases, at temperatures of 752°F (400°C). They considered the formation of MoS_2 and Co_9S_8 as a result of sufiding to be the most likely process, although the presence of other small sulfur-containing compounds was not excluded. They further reported that the freshly sulfided Co-Mo-alumina reacts with oxygen even at room temperature. The sulfur content was reported to be only weakly dependent on the partial pressure of H_2S. An increase from 1/24 to as much as 1/1 in H_2S/H_2 ratio resulted in a corresponding S/Mo ratio of 2.21 and 2.44 after two hours of sulfiding. Experimental evidence of the diffusion of Co^{2+} ions from the bulk toward the surface of the

gamma-alumina support during sulfidation was reported. Ahmed (1979) reported the existence of a concentration gradient for the various catalyst elements from the outside to the inside of the pellet surface.

Tantrov et al. (1972) found from their investigation of the effects of sulfiding of Co-Mo-alumina catalyst that:

1) preliminary sulfiding is advantageous for hydro-refining of thermally-cracked gasoline.

2) The mechanical strength of Co-Mo-alumina catalysts is increased by a factor of 1.4 during sulfidation.

3) Deposition of coke on a previously sulfided catalyst is one-third that of the oxide catalyst for the same period of operation.

Van der Aalst and DeBeer (1977) recorded the ultraviolet and vis-ible reflectance spectra for oxidic and sulfided Co-Mo containing cata-lysts supported on alumina and silica. They reported the formation of MoS_2 and Co_9S_8 as a result of sulfidation with H_2S/H_2. They also strongly supported the intercalation and/or synergetic model as a viable description of the structure of HDS catalysts.

DeBeer et al (1974) reported Ni^{2+} to be more active than Co^{2+} as a promoter provided it is introduced in the presulfided MoO_3-alumina, viz., MoS_2-alumina. They postulated that the $CoO-MoO_3$-alumina starts as a monolayer system but is converted into an intercalated structure within a few hours either when in operation or during the presulfiding treatment. Reduction of S^{2-} ions by means of hydrogen results in the formation of an isolated Mo^{3+} ions or a pair of Mo^{3+} ions which are supposed to be the active sites. Ahmed (1979) observed molybdenum species with oxidation states of +4 to +6 on the crystal surface using X-ray photoelectron spectroscopic technique. Sulfur species both in

sulfide and sulfate forms were observed. Spent catalyst contained more of sulfate than the sulfide compared to the fresh catalyst.

Sulfided metal species are believed to be responsible for HDS and HDN activity of the hydrotreatment catalysts. Sulfidation of active metal species has been explained according to various models. In the monolayer model, MoO_3 is assumed to be partially sulfided to MoS_2. The formation of MoS_2 and Co_9S_8 as a result of sulfidation has been reported, and the catalyst structure explained by the intercalation or synergetic models. It is widely accepted that the hydrotreatment catalyst (CoO-MoO-alumina) starts as a monolayer system but is converted into an intercalated structure in a few hours, either during presulfiding or during actual operation.

Catalytic Deactivation

Long catalyst life is essential to hydrotreating processes; catalyst deactivation rates often determine the commercial feasibility of a process. Three cases of catalyst deactivation, namely metal deposition, basic species adsorption, and coke deposition contribute to the deactivation of hydrotreating catalysts.

Metal deposition on the catalyst causes irreversible deactivation due to the plugging of the pores and covering of the active sites on the catalyst. In contrast, coke deposition is a reversible process; the catalyst can be regenerated by controlled combustion of coke deposits. The type of metals that occur in the coal liquids are different from those that occur in petroleum feedstocks. Coal-derived liquids have high iron and titanium contents, whereas the petroleum liquids contain significantly higher levels of vanadium and nickel.

Deactivation in case of coal liquids is more pronounced than the petroleum fuels due to the higher polynuclear aromatic content of the coal liquids. In petroleum liquids, the metals are present mostly as organometallic compounds, contained primarily in the asphaltene fraction of the residuum. These organometallic compounds are believed to be associated in the form of micelles. The size of these large species is in the range of 10^{-6} to 10^{-9} m.

Lipsch and Schuit (1969) reported strong deactivation effect due to pyridine adsorption in thiophene hydrodesulfurization and in olefin hydrogenation. Basic nitrogen compounds are believed to be adsorbed on the catalyst surface and result in the decrease of the acidity of the surface. Roberts (1958) observed that nitrogen-containing heterocyclic compounds have a higher coking tendency than do their hydrocarbon analogs at temperatures of $842^{o}F$ ($450^{o}C$) and higher. Furminsky (1978) reported that aromatics containing S-, N-, and O-containing heterocyclic compounds are the precursors for the coke deposition.

Beeckman and Froment (1980) presented a mathematical model for porous catalyst deactivation by coke deposition. They described deactivation in terms of two mechanism: site coverage and pore blockage. They assumed that the coke precursor deposits on the active sites randomly, and polymerization takes place and proceeds until the growth of coke molecules is stopped by pore blockage caused by neighboring coke deposits. The coking reactions and the main reaction occur at the same active site.

Furminsky (1979) described the procedure for determining the amount of coke deposited on catalyst surfaces. According to him, the procedure should be carried out in essentially two steps. Soluble

fractions must be removed by means of any kind of extraction. The fraction heavier than asphaltenes or carbonaceous material which remains on the surface of the catalysts after extraction must be referred to as coke. This should be determined by weight change during catalyst burning, making sure to make corrections to account for chemical changes in the catalyst material. Beeckman and Froment (1979) presented a model for relating catalyst deactivation function to the coke content and the time. The model is based on the assumption that there is no diffusional limitation inside the catalyst and that the growth of a coke molecule is infintely fast compared with the rate of precursor formation on an active site.

Regeneration of deactivated catalyst by burning off the carbonaceous coke deposits in a stream of air or air diluted with inerts ia a well established industrial process. The main problem is to limit the temperature rise during the exothermic oxidation to a level below that at which the hydrotreatment catalyst becomes deactivated by sintering. Various mechanistic models have been presented to predict the maximum temperature rise theoretically. Ramachandram et al. (1975) presented a model to predict the transient temperatures during the period of regeneration of coked catalyst. This model considers the reaction of both hydrogen and carbon in coke. Massoth (1967) postulated a double interference process for coke removal, which allows specifically for the hydrogen content of the coke.

Kovach et al. (1978) found that K, Na, Mg, Co, P, Ti, Fe, and Si poison the HDS catalyst permanently. The depositon of carbonaceous matter within the catalyst pores suppresses the deposition of metals insoluble in coal-derived liquids. They further observed

that organometallic compounds like titanium-containing species, gain access to the interior catalyst surface and are deposited there in high concentration because of their solubility in coal-derived liquids. Chang and Silverti (1974) determined the rate of demetallation to be first order with respect to the metal concentration for demetallation of topped petroleum crudes by naturally occurring manganese nodules.

Newson (1975) developed a model for predicting the life of demetallation catalysts for hydrotreating residuum oil, assuming uniform pore plugging. Rajagopalan and Luss (1979) presented a model for predicting the influence of pore size on the rate of demetallation; it takes into account the influence of restricted diffusion of large reactant species in the pores. They observed that for various catalysts with the same surface area and porosity, the largest initial activity is attained for pellets with a uniform pore size.

Stanulonis et al. (1976) analyzed aged $CoO/MoO/SiO_2/Al_2O_3$ catalyst pellets from the Synthoil process using Electron Microprobe and Scanning Electron Microscope. They found that the catalyst accumulated inorganic and organic contaminants both on the interior and the exterior surfaces and in the pore mouth. Relatively higher inorganic deposits were found in the upstream end of the fixed bed reactor. The inorganic deposits were identified as $Fe_{14}S_{15}$ and these covered 50 to 70% of the catalyst peripheral surface and penetrated into the catalyst pores to a depth of about 100 micrometers.

The iron concentration is approximately proportional to the sulfur concentration in the exterior surface (crust); the sulfur/iron ratio is higher on the interior of the catalyst because of the presence of Co-Mo sulfides. Titanium is deposited primarily in the interior of

the catalyst. Mainly silicon and aluminum were found in the downstream end of the reactor. Ahmed (1979) found that there is more deposition of carbonaceous deposits on the Co-Mo-alumina catalysts relative to the Ni-Mo-alumina catalysts during the hydrotreatment of a mixture of a Synthoil liquid and raw anthracene oil. When deactivated, Co-Mo-alumina lost more surface area than Ni-Mo-alumina catalyst; most of the surface area was recovered upon regeneration. Significantly low concentrations of molybdenum and cobatlt/nickel were reported on the spent catalyst using the Scanning Auger Microprobe (SAM). More molybdenum was detected on the insider surface of the catalyst pellet than on the outside surface.

Ahmed (1979) presented a quantitative model to account for the activity decay of hydrotreating catalysts based upon changes in catalyst physical properties.

$$\frac{k_t}{k_o} = \left(\frac{r^{-5}}{r_o^{-5}} \cdot \frac{(1-\alpha)^3 \, e^{-4.6 r_1/\bar{r}}}{e^{-4.6 r_1/r_o}} \right)^{1/2} \quad \frac{\tanh [h(1-\alpha)]}{[1+\alpha-\tanh\langle h(1-\alpha)\rangle - \tanh(h)]}$$

where

k_o = rate constant, first order, fresh catalyst, per unit surface area of fresh catalyst

k_t = rate constant, first order, after t hours of operation, per unit surface area of fresh catalyst

$\bar{r}$ = pore radius of used catalyst, average

r_1 = radius of reactant molecule

r_o = pore radius of fresh catalyst, average

h – thiele modulus

α = fraction of pore poisoning, related to carbon deposition

The literature section on catalyst deactivation can be summarized as follows:

Metal, mineral, and coke deposition contribute to the deactivation of the hydrotreating catalysts. Metal deposition on the catalyst causes irreversible deactivation, whereas coke deposition is reversible; the catalyst can be regenerated by controlled combustion of the coke deposits. Coke depositions accounts for the short-term deactivation of the catalyst. The long-term deactivation of catalyst is caused by metal deposition. Various theoretical models have been presented to account for the activity decay of the hydrotreating catalysts. None of the models presented can predict the deactivation of the catalyst from coke buildup and metal deposition adequately. Greater carbonaceous deposition has been reported for the Co-Mo-alumina compared to the Ni-Mo-alumina catalyst.

Guard Chambers and Zonal-Catalyst Beds

Various techniques have been developed to prolong the life of catalyst used for resid and coal-derived liquid hydrotreatment. Guard beds containing cheap, disposable material to take out the metals, particulate matter, and rapid coking components are very desirable to extend the catalyst life in the main reactor. Two guard beds may be included so that one can be used alternately while the catalyst in the other is replaced.

Union Oil Company of California developed a commercially proven process for resid catalytic cracking and desulfurization (Murphy and

Treese, 1979). In this process, guard chambers are used ahead of the main reactor. These guard beds remove metals simultaneously and partially hydrogenate the resids. A special catalyst was developed for use in guard chambers; it has substantially different pore size distribution than the Co-Mo-alumina catalyst employed in the main reactor.

Lister (1965) recommended mesh baskets at the top end of the fixed bed reactor to remove the solids and feed contaminant such as sodium chloride. These should contain loosely packed solids providing high interstitial capacity for deposited materials. Kubica et al. (1968) demonstrated the usefulness of a guard chamber in the pilot scale, fixed bed hydrodesulfurization of Ramashkino residuum. The solid deposits (especially iron and scales) were concentrated near the bed entrance; vanadium was more strongly concentrated near the bed entrance than nickel, corresponding to greater reactivity of organovanadium compounds. Lundberg (1979) reported the use of guard chambers for extending the life of low temperature shift catalysts. A guard vessel containing one-third the volume of catalyst in the main reactor improved the catalyst life considerably. The guard vessels could be replaced with little loss of production. Catalyst discharged from the main reactor or a mixture of new and old catalyst was used in the guard chamber.

The FMC Corporation demonstrated use of the guard chamber as a technique for removing metals and solids from the raw COED oils. A 30-barrel/day unit was operated successfully, using Koch stainless steel flexi-rings, alumina tablets, spheres and pellets, and Co-Mo-alumina catalysts. The use of catalyst in the guard chamber resulted in better performance than the use of alumina and flexi-rings. Guard

chambers employing alternating sections of catalyst and alumina layers followed by a Co-Mo-alumina catalyst resulted in better temperature control and slower catalyst deactivation (Jones et al., 1975).

Arey et al. (1966) described a two-stage residuum hydrocracking process: in the first stage, metals and other contaminants were partially removed by reaction catalyzed by cobalt-molybdate having an average pore diameter of 80 A^o; paladium loaded zeolite with a pore diameter of 13 A^o was used in the second stage. The second stage catalyzed selectively further reaction of the smaller molecules. Schuit and Gates (1973) suggested the use of catalyst with molecular seiving properties which could sieve the metal-containing asphaltenes while the sulfur-containing molecules could enter the catalyst pores. Small pore diameters (40 A^o or lower) were recommended.

The present generation catalysts were developed for petroleum hydrodesulfurization; they are not optimum for processing coal liquids. The catalysts which have been developed for hydrodenitrogenation achieve nitrogen removal by first hydrogenating the aromatic ring, followed by carbon-nitrogen bond scission. Optimization may be carried out in developing a catalyst for the carbon-nitrogen bond scission without hydrogenation of the ring. Suggested materials of particular interest are transition metal nitrides possibly promoted by other metals. Mixed transition metal oxides and oxysulfides in addition to materials such as borides and carbides or mixed systems such as Mo_2BC and $M_3Mo_2O_8$ where M can be Mg, Zn, Co, Mn, or other transition metals may be used for selective hydrodenitrogenation (Katzer, 1979). A process for upgrading heavy hydrocarbon oils using an ammonia activated catalyst containing a mixture of Ni and W on a crystaline

zeolite base has been patented by Hammer et al. (1973). The catalyst selectively favors the hydrodenitrogenation reaction. Zeolites have been used to catalyze hydrodesulfurization reactions. Use of alumina-silicate zeolite has been reported in a patent by Arey et al. (1966). Morkooka and Hamrin (1979) used a continuous flow reactor to obtain reaction rates of benzothiophene and hydrogen over mineral matter from Western Kentucky No. 11 coal. Mineral matter was prepared by low temperature ashing of the coal. They reported benzothiophene to be more readily hydrodesulfurized than the thiophene over the low-temperature ash, with no hydrogen sulfide in the feed gas.

Wells (1977) observed a maximum of 51% sulfur removal and 29% nitrogen removal, using pure gamma-alumina to hydrotreat raw anthracene oil at 750°F and 1500 psig. Chikrakaparambil (1974) observed negligible hydrodesulfurization in the presence of porcelain chips.

The section on guard chambers and zonal catalyst beds can be summarized as follows: Various techniques have been developed to improve the life of hydrotreating catalyst. Guard chambers containing cheap, disposable material have been used with commercial success in the petroleum industry. Zonal-catalyst beds employing two different catalysts have been recommended by some investigators. The attention is presently being focussed on developing highly selective catalysts.

Literature Summary

The following are the conclusions that can be drawn from this literature review:

1) Trickle-bed reactors have been widely employed in industry for the hydrotreatment of petroleum feedstocks.

2) Most of the gas and liquid distribution data for trickle-bed reactors has been determined under atmospheric conditions employing air-water systems. Conflicting evidence is presented regarding the dependence of conversion on liquid holdup, catalyst size, and catalyst wettability.

3) The choice of operating conditions is markedly affected by the nature of the feedstock. Pressures and temperatures in the range of 500 psig – 3000 psig and $500^{\circ}F$ ($260^{\circ}C$) – $850^{\circ}F$ ($455^{\circ}C$), respectively, have been employed in coal liquid hydroprocessing. In most of the literature studied, an increase in space velocity results in higher hydrodesulfurization (HDS) and hydrodenitrogenation (HDN).

4) Co-Mo-alumina is the most favored catalyst for HDS, whereas Ni-Mo-alumina is used mostly for HDN and hydrogenation of petroleum feedstocks and coal-derived liquids.

5) Gamma alumina and silica-alumina have been widely used as support for the hydrotreatment catalysts.

6) The catalytic promoting effect of Co /Ni is not well understood. Molybdenum has been reported to be present in oxidation states of +4, +5, and +6. Molybdenum in +4 oxidation state is generally believed to be responsible for the HDS and HDN activity of the hydrotreatment catalyst.

7) Presulfiding of the catalyst improves the activity of the catalyst. MoS_2 is believed to be the active species.

8) Metal deposition, mineral deposition, and coke deposition severely decrease the catalytic activity of the hydrotreating catalyst. Metal deposition is irreversible and results in permanent loss of catalytic activity.

9) The use of guard chambers improves the catalyst life in the reaction bed.

CHAPTER III

EXPERIMENTAL SETUP AND PROCEDURE

A trickle-bed reactor system was designed and constructed to conduct the present study. This new system was constructed to fulfill the following requirements:

1) The reactor should be capable of nearly isothermal operation up to a temperature of $850^{\circ}F \pm 3^{\circ}F$ ($455^{\circ}C \pm 1.5^{\circ}C$).

2) The reactor should operate with lower catalyst loading compared to the reactors used in previous studies in the School of Chemical Engineering, Oklahoma State University.

3) The reactor should be able to operate up to 1800 psig with minimum pressure fluctuations.

4) No voids for liquid accumulation should be present in the system feed and exit lines.

5) Flow rates of oil and gas must be measured and controlled accurately.

6) The feed pump and all of the oil lines should be kept heated to facilitate pumping of heavier feedstocks.

7) Sampling of liquid products should be possible without disturbing normal operation.

8) Provisions should be made to read the temperature along the reactor length.

9) The feed oil pump should be capable of delivering very low

flow rates (2 cc/hr upwards) accurately.

10) Adequate safety procedures should be incorporated into the system.

A simplified diagram of the experimental setup employed in this study is given in Figure 1. Hydrogen and feed oil were allowed to combine at the top of the reactor before passing concurrently down the catalyst bed. Hydrogen was used directly from the bottles on a once-through basis. The feed oil was pumped at a constant preset rate by the Ruska feed pump. The gases and liquids leaving the reactor were separated in the sample bombs and the liquid samples were collected by isolating the lower bomb from the rest of the system. The flow rate of the exit gases was monitored using a bubble flowmeter.

The trickle-bed reactor used in this study was made of 1/2-inch (1.27 cm) OD stainless steel tubing with 1/8-inch (0.32 cm) OD, centrally located thermocouple tubing. The reactor was heated by means of beaded electrical heating wires wound around aluminum blocks. The reactor temperature was measured by means of a thermocouple which could traverse axially along the thermowell from the top to the bottom of the catalyst bed. The reactor pressure was measured on a Heise gauge which was located upstream of the reactor.

The catalyst pretreatment consisted of calcination and presulfiding steps. The catalyst bed was heated gradually and the temperature stabilized at $900^\circ F$ ($482^\circ C$) and this temperature was maintained for one hour. Nitrogen gas was allowed to flow through the reactor at the rate of 200 cc/min. The temperature was reduced to $500^\circ F$ ($260^\circ C$) and maintained at this temperature for 12 hours. The catalyst was then presulfided at $500^\circ F$ ($260^\circ C$) with a 5% H_2S/H_2 mixture for 90
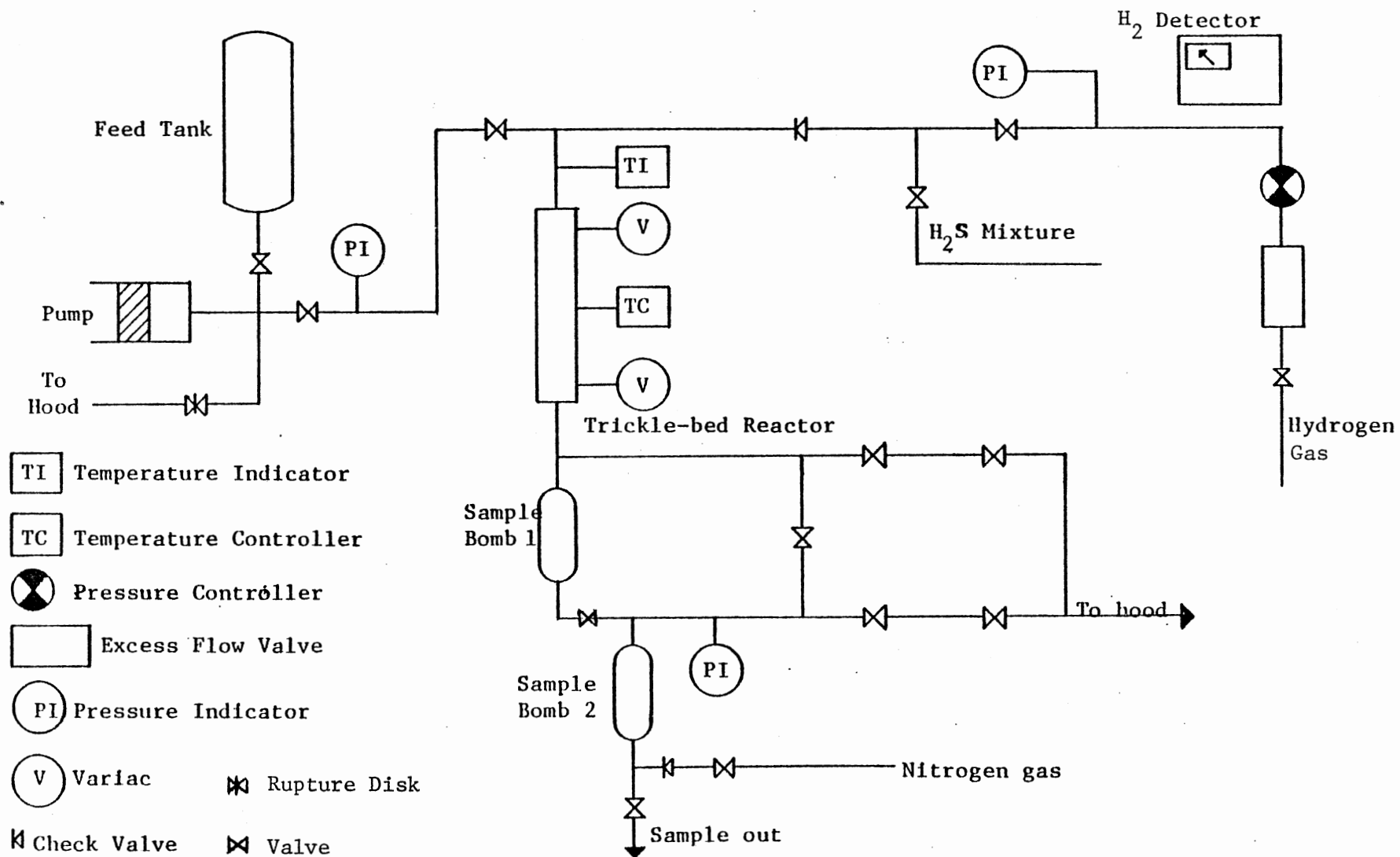
Figure 1. Experimental System

Legend:

TI — Temperature Indicator

TC — Temperature Controller

Pressure Controller

Excess Flow Valve

PI — Pressure Indicator

V — Variac

Rupture Disk

Check Valve

Valve

Diagram labels: Feed Tank, Pump, To Hood, PI, TI, V, TC, V, Trickle-bed Reactor, Sample Bomb 1, Sample Bomb 2, PI, Sample out, Nitrogen gas, To hood, H_2S Mixture, PI, H_2 Detector, Hydrogen Gas

minutes. Care was taken to isolate the Hiese gauge and the pressure

regulator from the system during presulfidation. The system was

flushed with nitrogen gas at a flow rate of 20 cc/min for 20 minutes.

Next, the reactor was heated to within 10^OF (5.6^OC) of the desired oper-

ating temperature and the temperature was stabilized before bringing

the hydrogen feed oil on stream.

The experiment setup and procedures are described in much greater

detail in Appendix A.

Sample Analyses

The product liquid samples were analyzed for their sulfur, nitro-

gen, and hydrogen contents. Some samples were subjected to ASTM dis-

tillation. The analytical procedures are described in brief below.

Appendix B contains the complete details.

Sulfur Analysis

The sulfur content was determined by means of a Leco Automatic

Sulfur Analyzer, consisting of a Model 532-000 Automatic Titrator, a

Model 521-500 Induction Furnace, and an oxygen purifying train. The

general procedure for operation of these instruments is given in the

Leco Bulletin. In this system, the induction furnace is used to burn

the sample in an atmosphere of purified oxygen. The SO_2 and other

combustion products are passed to an automatic titrator, where they

are titrated against standard KIO_3 solution, using starch as indicator.

Nitrogen and Hydrogen Analyses

The complete analytical system consisted of a Model 240 Perkin-

Elmer Elemental Analyzer, a Model AD-2 Perkin-Elmer Autobalance, a Model 56 Perkin-Elmer one millivolt Range Recorder, and a Model 04-1280 Perkin-Elmer Sealer. This system could analyze for three elements--carbon, hydrogen, and nitrogen, simultaneously. The Perkin-Elmer instruction manual describes the general procedures for analyses with this equipment.

A combustion tube, a reduction tube, and a detector system are the major components of the analyzer. The combustion tube is maintained at a temperature of $650 - 700^{\circ}C$, and the reduction temperature is $950 - 1000^{\circ}C$. The weighed sample, contained in a special aluminum capsule, burns in an atmosphere of oxygen in the combustion zone. The gases so produced are carried by high purity helium through packings of the combustion tube, which remove sulfur oxides and halogens from the gases. The gases then pass through a reduction tube, where nitrogen oxides are reduced to molecular nitrogen. The exit gases from the combustion tube consist of water vapor, carbon dioxide, nitrogen and helium diluent. These collect in a 300-ml capacity glass vessel. The pressure in the glass vessel is allowed to rise to two atmospheres and the temperature is held constant. After equilibrium, the gas mixture is expanded into an elongated sampling system and then passed through a series of thermal conductivity cells. Before entering the first cell, the sample mixture passes through a trap containing magnesium perchlorate. This removes water from the gas stream. The difference in thermal conductivities of the sample before and after the trap gives the concentration of water and hence the hydrogen concentration in the sample. The gases are then allowed to pass through a CO_2 trap and a similar thermal conductivity difference gives the carbon

content in the sample. The remaining gases contain nitrogen and helium and are passed through a conductivity cell, the output of which is compared with that from another cell through which only pure helium is flowing. The difference in the thermal conductivities gives the nitrogen concentration in the sample.

ASTM Distillation of Oil Samples

The feed oil and selected product oil samples were subject to ASTM D-1160 distillation (Annual Book of ASTM Standards, Part 23, 1979). The fractionation was carried out at 50 mm Hg pressure. One hundred cc of the sample to be distilled were taken in a distillation flask and heated by a mantle controlled by a powerstat. The vapor and the pot temperatures were recorded against the volume distilled.

Ash Content in Oil Samples

The feed oil was tested for ash content. The procedure was the same as Standard ASTM D-482 (Annual Book of ASTM Standards, Part 23, 1979), except for some modifications established by Ahmed (1979).

Feedstock

The feedstock used in the present study, Pamco Process Solvent, was obtained from the Pittsburg and Midway Coal Mining Company, a subsidiary of Gulf Energy and Minerals Company. This coal liquid was produced by the SRC process in a 50 ton/day plant at Fort Lewis, Washington.

The properties of the coal liquid used in this study are given in Table IV. This liquid has a typical nitrogen and sulfur content

TABLE IV

ANALYSIS OF THE PAMCO PROCESS SOLVENT

Composition	Wt %
Carbon	89.08
Hydrogen	7.11
Nitrogen	0.97
Sulfur	0.43
Oxygen	2.41 (by difference)
Ash	nil

Boiling Point Data (50 mm and 760 mm Hg)

Determined by ASTM D1160 Distillation

	50 mm Hg	760 mm Hg [**]
Initial	318°F (159°C)	487°F (253°C)
10 Vol %	331°F (166°C)	500°F (260°C)
20%	338°F (170°C)	510°F (266°C)
30%	358°F (181°C)	532°F (278°C)
40%	378°F (192°C)	557°F (292°C)
50%	415°F (213°C)	597°F (314°C)
60%	446°F (230°C)	635°F (335°C)
70%	480°F (249°C)	670°F (354°C)
80%	509°F (265°C)	705°F (374°C)
End point	509°F (265°C)	
Specific gravity	1.067[*](1.044)	

[*] Vendor's data.

[**] Conversion carried out using Chart 53-12, ASTM D2892 (Annual Book of ASTM Standards, Part 24, 1979).

of 0.97 and 0.43 wt %, respectively, and no detectible ash. The typical distillation range at 50 mm Hg is 318°F (159°C) to 509°F (265°C).

Two different catalysts were used in this study. The commercial Ni-Mo-alumina catalyst was obtained from the American Cyanamid Corporation. The Co-Mo-alumina laboratory test catalyst was obtained from Akzo Chemical Company. These catalysts differed in metal content, composition, surface area, pore volume, and most frequent pore diameter. The most frequent pore diameter is obtained from the pore size distribution data. The physical properties of the two catalysts were similar; both were 1/16-inch extrudes.

The pore size distribution was obtained from mercury penetration data at 50,000 psi. Figure 2 is a plot of the pore volume versus the penetration pressure. Figure 3 gives the pore size distribution, HDN-30 (Ni-Mo-alumina) has a most frequent pore diamater of 84 A°, compared to the Ketjenfine-124 (Co-Mo-alumina) catalyst, most frequent pore diameter of 51 A°. The catalyst properties are given in Table V.
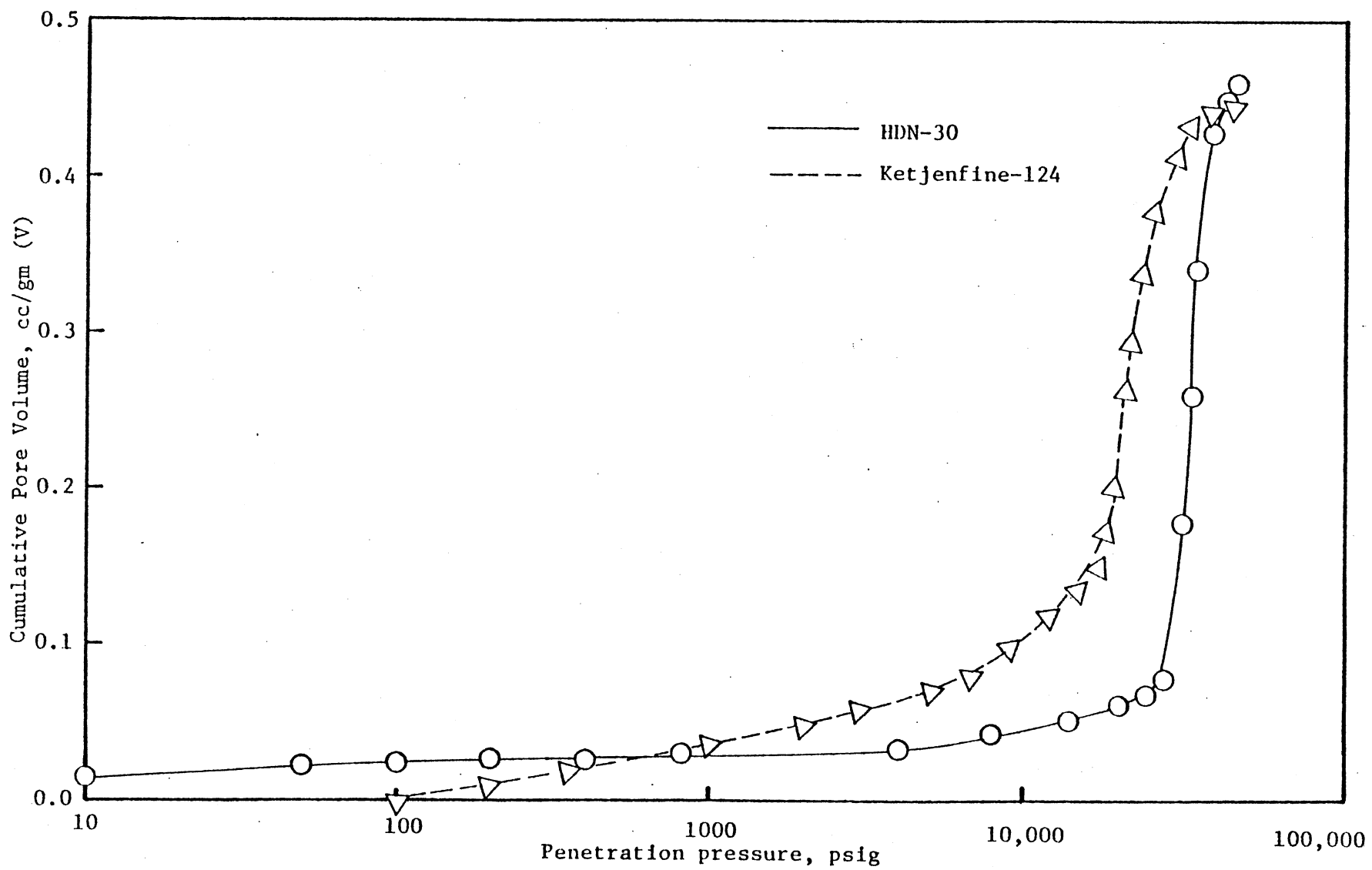
Figure 2. Dependence of Catalyst Pore Volume on Hg Penetration Pressure
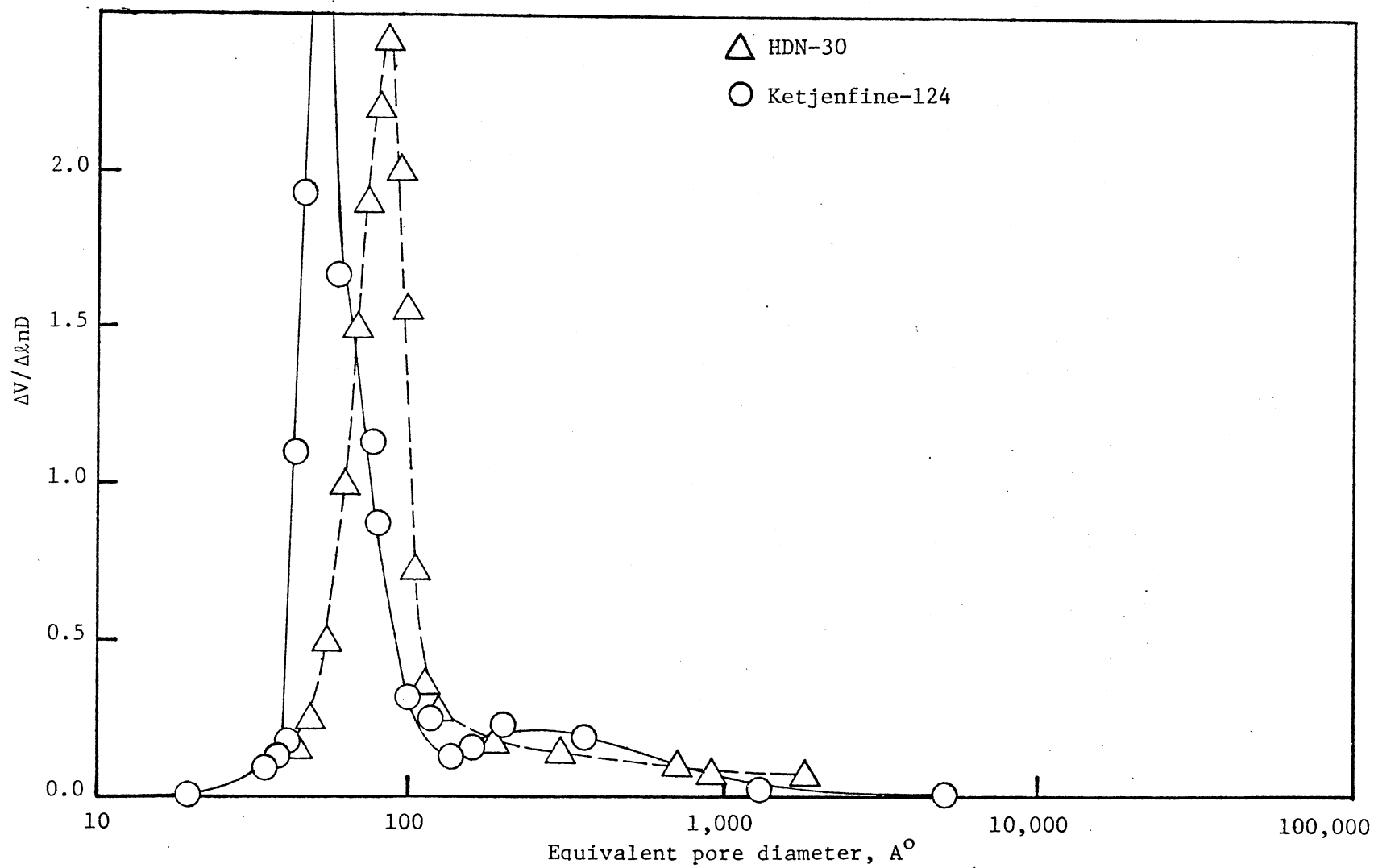
Figure 3. Pore Size Distribution

TABLE V

CATALYST PROPERTIES

Catalyst	Ketjenfine 124	HDN-30
Chemical Analysis*		
Wt % - Dry Basis		
MoO_3	11.8	20.5
Ni O	–	5.0
Co O	3.93	–
Na_2 O	0.09	0.03
Si O_2	1.22	–
SO_4	1.60	0.30
Alumina	Balance	Balance
Physical Properties (extrudes)	1/16"	1/16"
Surface Area, m^2/gm 238	238 (251*)	122 (160*)
Pore volume, cc/gm 0.46	0.46 (0.52)	0.45(0.44*)
Most frequent pore diameter (A^o)	51	84

*Vendor's data.

CHAPTER IV

EXPERIMENTAL RESULTS

In experiments conducted to study the hydrodesulfurization and
hydrodenitrogenation ability of a Co–Mo–alumina and a Ni–Mo–alumina
catalyst, separately and in combination as a zonal catalyst, a total
of five experimental runs was made. Since the design and con-
struction of the reactor system was an objective of this study, the
system performance will be mentioned first.

Uniformity in temperature, pressure, catalyst loading, and liquid
space velocity were maintained in all five experimental runs conducted.
Temperatures of $815^{O}F$ ($435^{O}C$) and $615^{O}F$ ($324^{O}C$) were employed. The
pressure was maintained at 1500 psig for all experimental runs. Liquid
volume hourly space times in the range of 0.512 to 2.56 hours were
employed. The catalyst bed height was maintained constant at 10.0
inches (25.4 cm).

In this chapter, the hydrodesulfurization (HDS), hydrodenitro-
genation (HDN), and hydrogenation results of all experimental runs will
be presented. Detailed discussion follows in subsequent sections.
Liquid volume hourly space time is used, which is defined as the ratio
of the catalyst bed volume to the liquid volume hourly flow rate. The
reactor bed pre- and post-inert sections are not included.

61

Run ZBA

This run was conducted to evaluate the HDS and HDN ability of a Ni-Mo-alumina catalyst and to fully test the systems. The results from this run served as reference for further zonal-bed studies. A malfunction in the temperature indicator resulted in a lower operating temperature than planned ($615^{o}F$ ($324^{o}C$) obtained vs $750^{o}F$ ($400^{o}C$) desired.

This experiment was the first ever conducted in the newly constructed trickle-bed reactor system. This run was also meant to familiarize the personnel in the operation of the new equipment and to check any shortcomings of the new setup. The lower operating temperature afforded an opportunity to study the HDS, HDN, and hydrogenation activity at a relatively lower temperature than that employed in most previous studies.

The pressure was maintained constant at 1500 psig $\pm$ 20 through the duration of the run. Liquid volume hourly space times of 0.512, 1.024, and 2.048 hours were employed. The hydrogen flow rate in the range of 2525 to 6730 SFC/bbl was maintained. The gas flow rate could not be controlled accurately due to a malfunction in the micrometer metering valve, resulting in variation in the hydrogen flow rate. The reactor was operated continuously for a period of 96 hours, and the reactor process conditions in the startup were repeated before shutdown to check for loss of activity. Ni-Mo-alumina catalyst was used; its properties are given in Table V. The Ni-Mo-alumina was sulfided with a 5% H_2S in H_2 mixture at $360^{o}F$ ($182^{o}C$) for a period of $1\frac{1}{2}$ hours. The startup procedure given in Appendix A was followed.

Only some of the samples were analyzed for sulfur, nitrogen, and

hydrogen content. (These samples were taken after the reactor was considered to have stabilized at a particular space time [three hours for stabilization]). The data obtained from this run are given in Figures 4 and 5. Figure 4 presents the weight percent sulfur and nitrogen present in the product oil as a function of the liquid volume hourly space time (LVHST). Tabulated data from this run along with all other runs are given in Appendix D. Almost half of the sulfur present in the feed oil was removed at the temperature of $615^{\circ}F$ ($324^{\circ}C$). Within the first fifteen hours of operation, the sulfur content in the product oil was reduced to 0.255, corresponding to 43% removal at a space time of 1.024 hrs. The sulfur content in the product oil stabilized at around 47% removal after 40 hours of oil-catalyst contact. As is evident from Figure 4, the sulfur content remained almost constant when the space time was increased from 1.024 hrs to 2.048 hrs. At lower temperatures, the space time effects were less pronounced for the sulfur removal. The nitrogen removal also reduced appreciably within the 15 hours of operation; 37% nitrogen removal was obtained at a space time of 1.024 hrs. The nitrogen content of the product oil stabilized at 0.829 wt % after 40 hours of operation, corresponding to 15 wt % removal.

As is apparent from Figure 4, space time change has a negligible effect on the nitrogen removal above the space time of 1.024 hrs. Removal within the range of 5% to 37% was obtained for the 96 hours of operation. Figure 5 presents the weight percent sulfur or nitrogen present in the product oil as a function of total hours of oil-catalyst contact time. The time was measured from the instant the oil and gas contacted the catalyst bed until the last sample was withdrawn.

The response of the weight % nitrogen in the product oil was
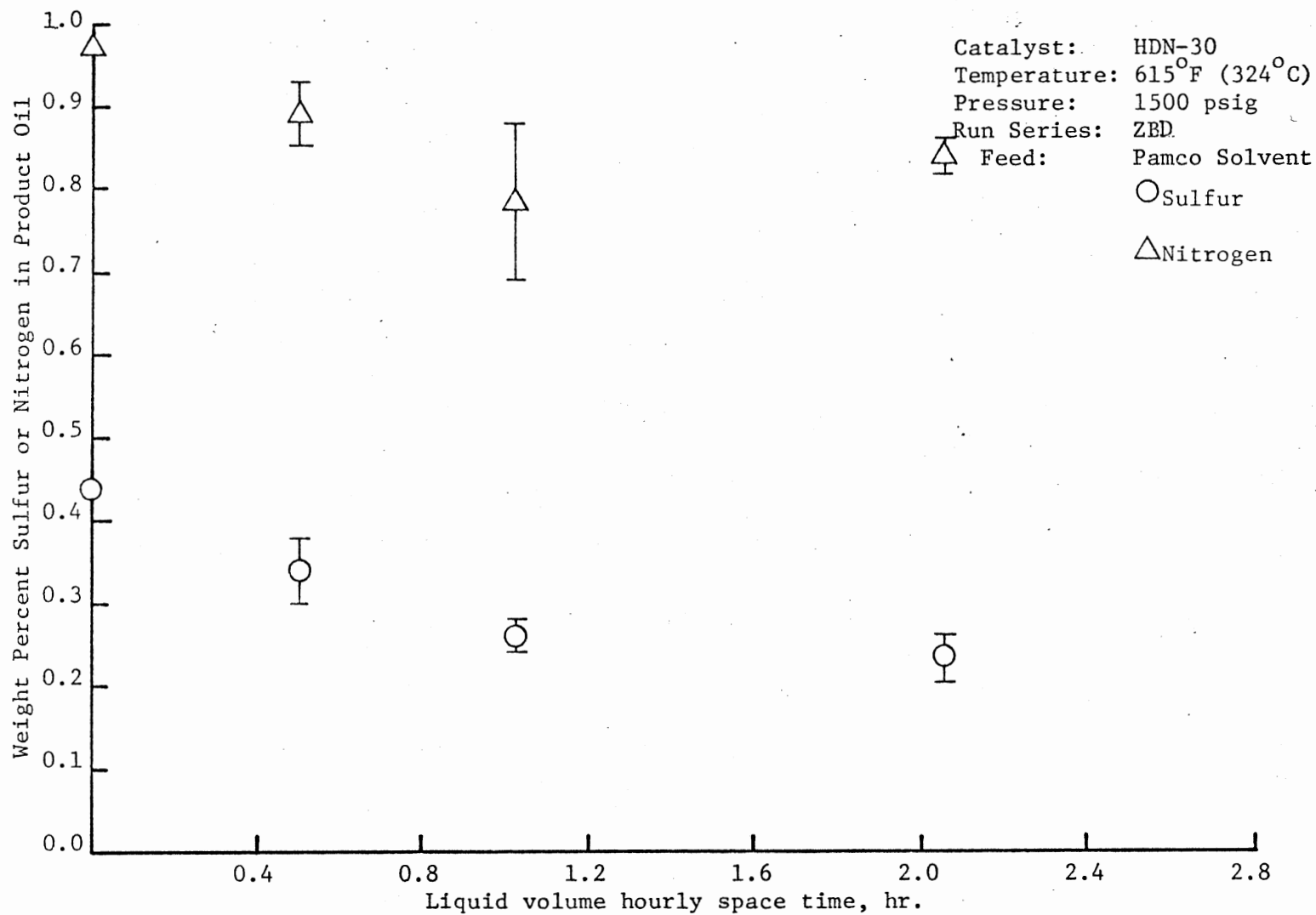
Figure 4.   HDS, HDN Activity Response, Run ZBA
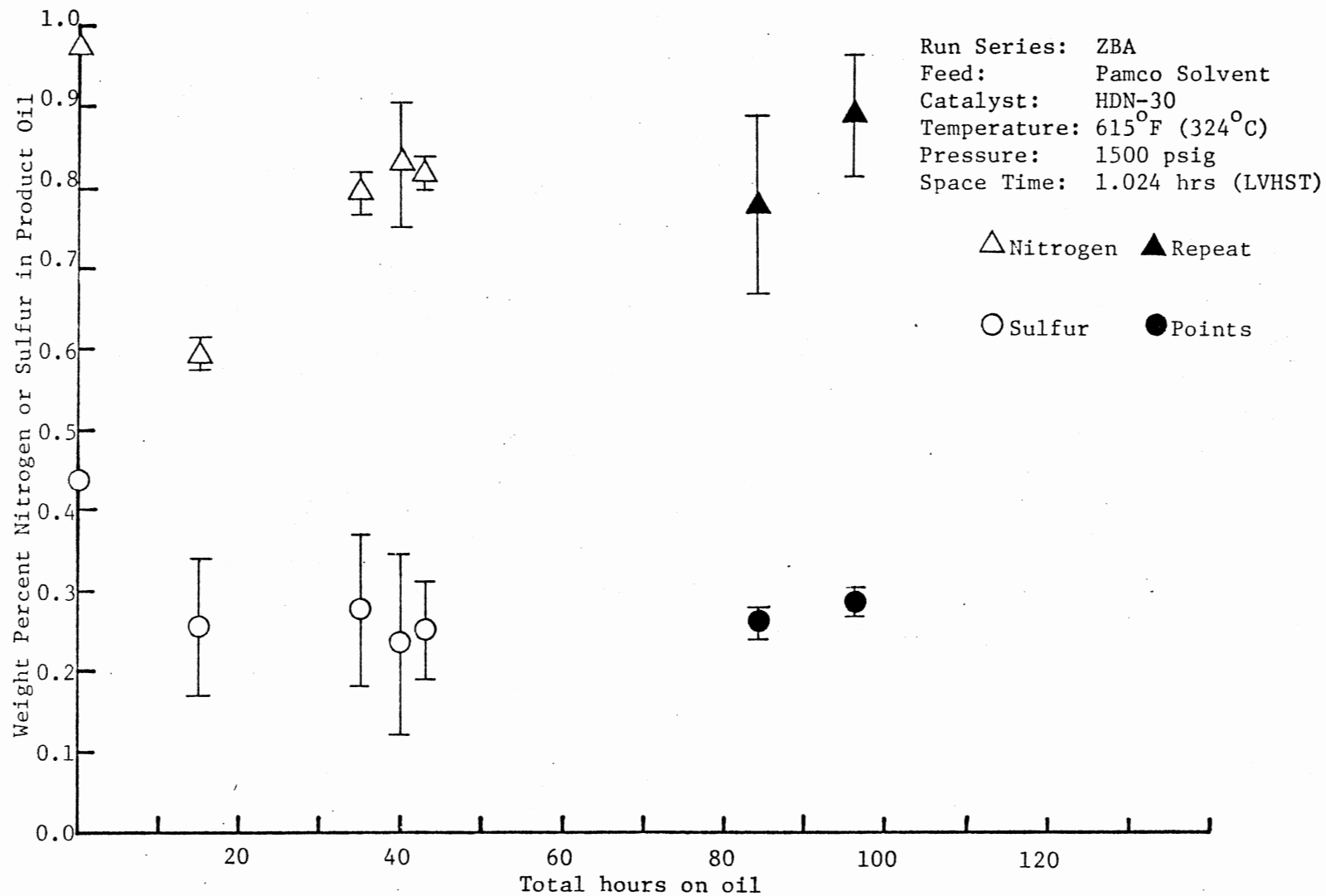
Figure 5. HDS, HDN Activity Response, Run ZBA

typical. The catalyst was very active in the first 15 hours of oper-
ation, resulting in 37% nitrogen removal. The catalyst stabilized
within 35 hours of operation. The product oil nitrogen content of
0.793 wt % was reported after 35 hours of oil catalyst contact. Only
9% nitrogen removal was reported after 96 hours of operation when the
initial conditions were duplicated.

Very little deactivation of the sulfur removal activity was noted
during the entire duration of the run. The shutdown was scheduled
after 96 hours of operation.

Run ZBB

This run was conducted to assess the HDN and HDS ability of a com-
mercial Co-Mo-alumina catalyst. This catalyst was selected because of
its silica content and high surface area. The silica-alumina support
is believed to have more hydrocracking activity. The hydrocracking and
hydrogenation ability of this and other runs are assessed in the latter
part of this chapter.

This run was conducted for a period of 104 hours before planned
shutdown. The temperature, pressure, and hydrogen flow rates employed
were $815^{\circ}F$ ($435^{\circ}C$), 1500 psig $\pm$ 20, and 6730 SCF/bbl, respectively.
These same process conditions were employed for runs ZBB through ZBE.
By keeping the process conditions constant through the runs, deactiva-
tion, HDS and HDN activity of various catalysts, individually and in
combination as zonal beds could be investigated. Unfortunately, HDN-
30 and Ketjenfine-124 catalysts and Pamco Process Solvent were never
used in our laboratory previously; hence comparisons with previous
studies were not possible.

Figure 6 shows the effect of space time on HDS and HDN for this run. The effect of space time on the sulfur removal was very marginal above 1.024 hours, LVHST. The sulfur removal is almost complete at relatively low space times. The lower limit of Leco Sulfur analyzer is 0.02 wt % sulfur, and as such, concentrations below this limit could not be measured. In fact, the concentrations lower than 0.05 wt % can be considered to be the lower limit for the Leco Sulfur analyzer. The reliability of the sulfur analyzer is discussed more thoroughly in Chapter V.

The weight % nitrogen content of the product oil showed substantial decrease with an increase in the LVHST. The weight % nitrogen content was reduced from 0.977 wt % originally present in the feed oil to 0.405 wt % at the space time of 1.024 hrs. Increase in space time to 2.048 hrs reduced the final nitrogen content to 0.121 wt %, which corresponds to 88% nitrogen removal. Figure 7 presents the HDN and HDS activity as a function of hours of total catalyst-liquid contact. The sulfur content of the product oil reduced to 0.048 wt % within 20 hours of operation. The activity of the catalyst increased during the next ten hours, and 95% sulfur removal was achieved. When the initial conditions were duplicated, some deactivation in the catalyst was observed; 82% sulfur removal was observed for the product liquid sample taken after 104 hours of operation.

The nitrogen removal activity of Co-Mo-alumina catalyst was reduced considerably after about 94 hours of continuous operation. The nitrogen concentration in the product oil sample after 20 hours of operation was 0.161 wt %, corresponding to 84% nitrogen removal.
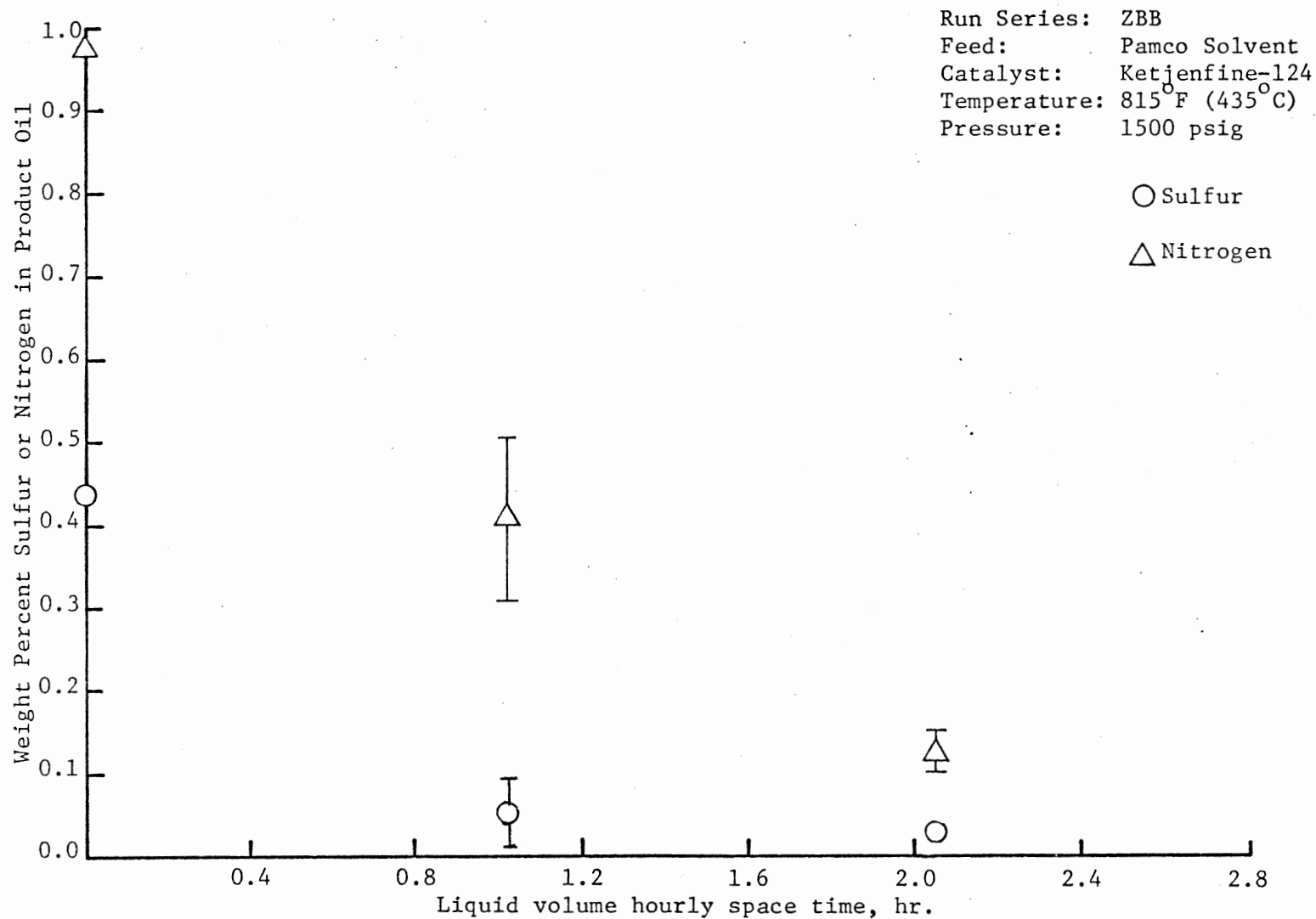
Figure 6. HDS, HDN Activity Response, Run ZBB
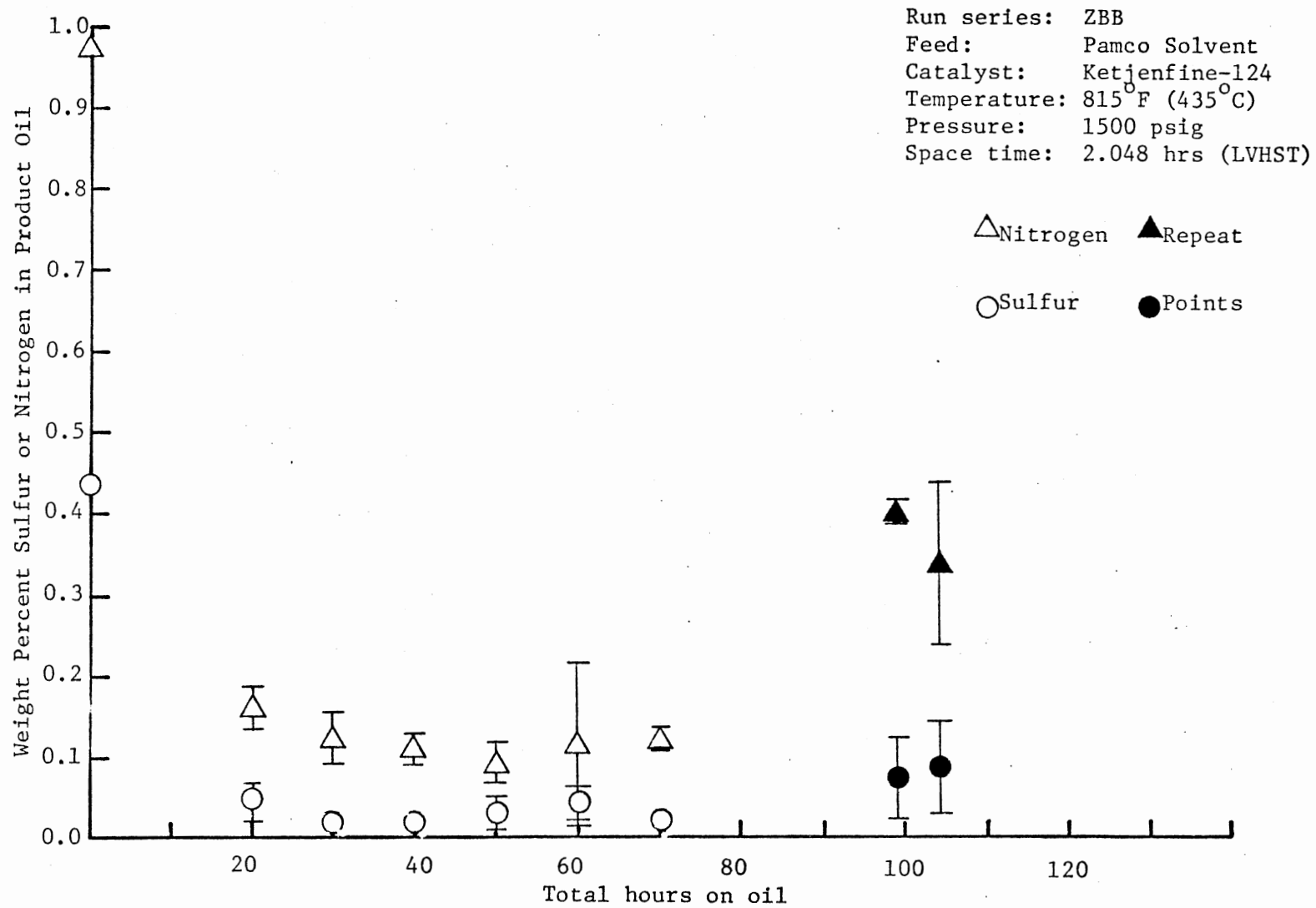
Figure 7. HDS, HDN Activity Response, Run ZBB

However, after 104 hours of operation, the nitrogen level in the product oil increased to 0.336 wt % (66% removal). The nitrogen removal was significant during the first 50 hours of operation, during which the nitrogen weight % in the product oil decreased to 0.090 wt % (91% removal). A gradual increase in the nitrogen content was noted in the subsequent liquid samples.

Run ZBC

The objective of this run series was to assess the HDS and HDN activity of the Ni-Mo-alumina catalyst. This run was also meant to serve as a reference run for further zonal-bed studies. HDN-30, Ni-Mo-alumina catalyst employed in this experimental run had a small surface area (122 m^2/gm) and a large most frequent pore diameter (84 A^o). Ketjenfine-124, Co-Mo-alumina catalyst employed in Run ZBB had a much higher surface area (238 m^2/gm) and a smaller most frequent pore diameter (51 A^o) compared to the HDN-30 catalyst.

This experimental run was conducted for a period of 117 hours with planned shutdown. The initial catalyst activity for the first 20 hours was lower compared to Run ZBB employing the Co-Mo-alumina catalyst. The catalyst gained its maximum activity within 30 hours of liquid-catalyst contact. The product oil nitrogen concentration was reduced to 0.02 wt % at a space time of 2.048 hours. No significant loss of sulfur activity was noted during the 117 hours of operation. The HDN and HDS activities for this run are plotted in Figure 8 in terms of weight % sulfur and nitrogen in the product oil as a function of time of operation. Note that the nitrogen content of the product oil reduced to 0.129 wt % (87% removal) after 20 hours of operation.
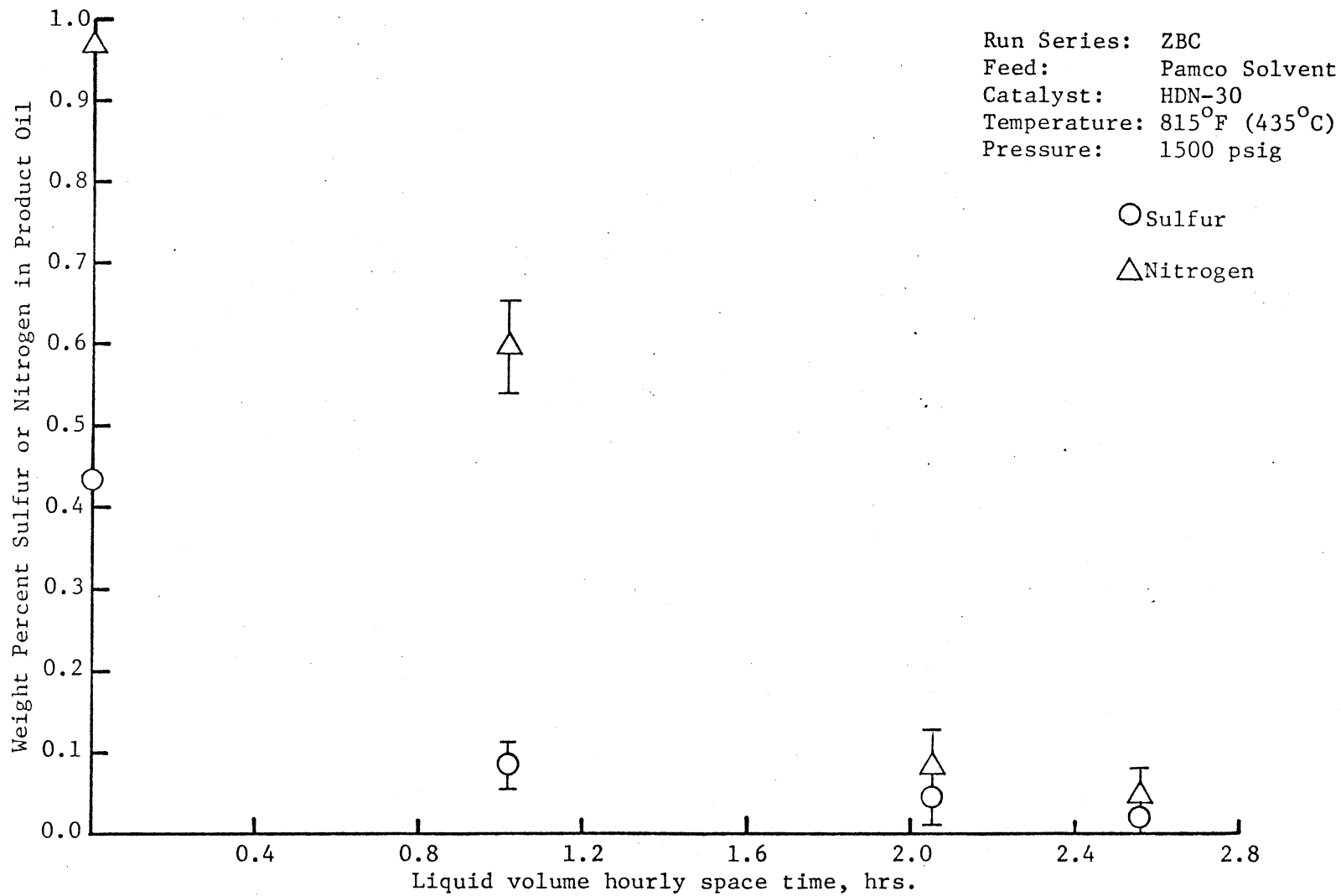
Figure 8. HDS, HDN Activity Response, Run ZBC

The nitrogen content of the product oil further dropped to 0.031 wt %
corresponding to 96% removal in 40 hours of operation. Figure 9 pre-
sents a plot of HDS and HDN activity as a function of time of oper-
ation.

A significant loss of hydrogenitrogenation activity occurred dur-
ing 117 hours of catalyst-oil contact. This is in contrast to the
negligible loss of activity for sulfur removal capacity of the Ni-Mo-
alumina catalyst.

As shown in Figure 8, increasing the space time beyond 1.024
hours resulted in a significant increase in the nitrogen removal. At
a space time of 2.048 hours, the product nitrogen content was reduced
to 0.084 wt % (92% removal). Note that for all experimental runs only
the active catalyst data were used for calculating the average product
nitrogen content at a certain space time.

The sulfur content of the product oil was reduced to 0.085 wt %
(81% removal) at a liquid volume hourly space time of 1.024 hours.
Further increase in the space time decreased the sulfur content to
0.042 wt %, corresponding to 85% removal. The subsequent sulfur con-
tent in the product oil was lower than the detection limit of the
Leco Sulfur analyzer (0.02 wt % sulfur) for a space time of 2.56 hours.
Note that a negligible loss in sulfur removal activity occurred during
the 117 hours of catalyst-liquid contact. This is in contrast to the
significant deactivation observed for nitrogen removal activity.
Nitrogen removal ability of the Ni-Mo-alumina catalyst dropped from a
maximum of 97% removal to 61% removal during the 117 hours of oper-
ation. The deactivation was less severe compared to the Co-Mo-alumina
catalyst used in Run ZBB, where product oil nitrogen content dropped
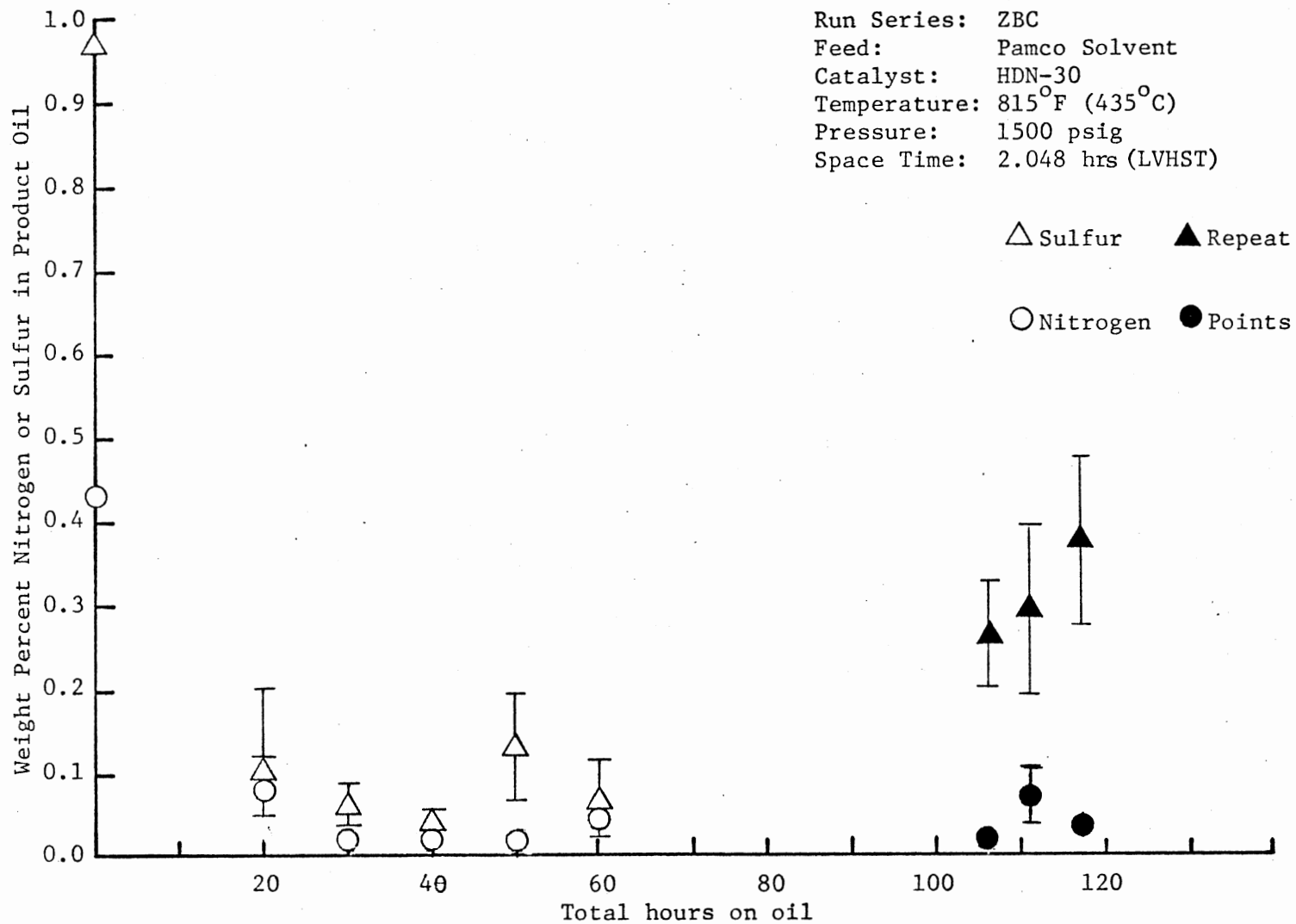
Figure 9.   HDS, HDN Activity Response, Run ZBC

to 0.336 (66% removal) in only 104 hours of operation. Nitrogen removal of 73% was observed after 106 hours of operation for this Ni-Mo-alumina catalyst.

Run ZBD

The objective of this experimental run was to assess the hydrodesulfurization and hydrodenitrogenation ability of a combination of Ketjenfine-124 and HDN-30. The catalyst bed was made of two half-sections, one imposed over the other. The Ketjenfine-124 (Co-Mo-alumina) encountered the coal-liquid first. The zonal catalyst bed contained 50% by volume of Ketjenfine-124, the balance being HDN-30 (Ni-Mo-alumina). The bed was packed according to the procedures outlined in Appendix A. The total bed height was 10 inches.

The catalyst bed consisted of 48.0 wt % of Co-Mo-alumina and 52.0 wt % of Ni-Mo-alumina. The Co-Mo-alumina constituted 57.8% and Ni-Mo-alumina 42.2% of the total surface area of the catalyst bed.

The Ketjenfine-124 was used in the upper layer for the following two reasons:

First, the SiO_2 in the Ketjenfine-124 would possibly promote hydrocracking and cracking of the multi-ring compounds present in the coal-derived liquids. The oil then encountering the HDN-30 would be relatively lighter, which could be readily hydrotreated by the Ni-Mo-alumina catalyst present in the second catalyst zone.

Second, the removal of most of the sulfur present in the feed oil would occur in the Co-Mo-alumina catalyst bed. The partially treated coal liquid, relatively lower in sulfur content, would encounter the Ni-Mo-alumina catalyst bed. The removal of nitrogen by the

Ni-Mo-alumina bed would be higher in the absence of sulfur compounds.

Experimental Run ZBD was conducted for a period of 120 hours with scheduled shutdown. The run conditions were the same as in experimental run series ZBB and ZBC.

The weight % nitrogen and sulfur in the product oil are plotted as a function of liquid volume hourly space time in Figure 10. The product oil nitrogen concentration was 0.464 wt % at the space time of 1.024 hours. An increase in space time over 2.048 hours had a negligible effect increase on the hydrodenitrogenation. Note that this phenomenon was noticed for experimental runs ZBB and ZBC also.

As can be seen from Figure 11, the nitrogen content in the product oil was reduced to 0.116 wt % during the first 20 hours of oil-catalyst contact, at a space time of 2.048 hours. During the 120 hours of operation, deactivation comparable to experimental runs ZBB and ZBC was observed. Initial nitrogen removal of around 88% fell to 68% in 120 hours of oil-catalyst contact; 80% nitrogen removal was observed in the liquid sample after 109 hours of operation. From comparison of the nitrogen removal of experimental runs ZBB, ZBC, and ZBD, one can conclude that the nitrogen and sulfur removal capacity of the zonal catalyst bed is the same as that of the individual catalyst beds. 52.5% nitrogen removal was noted at a space time of 1.024 hours for the zonal catalyst bed. This falls between the range of 59% and 52% nitrogen removal observed for experimental runs ZBB and ZBC. Similarly at a space time of 2.048 hours, nitrogen removal for the zonal catalyst bed was 88%, and for runs ZBB and ZBC, it was 88% and 91%, respectively. The sulfur removal capacity of all three experimental runs was similar; the sulfur content of product oil reducing below 0.02 wt %.
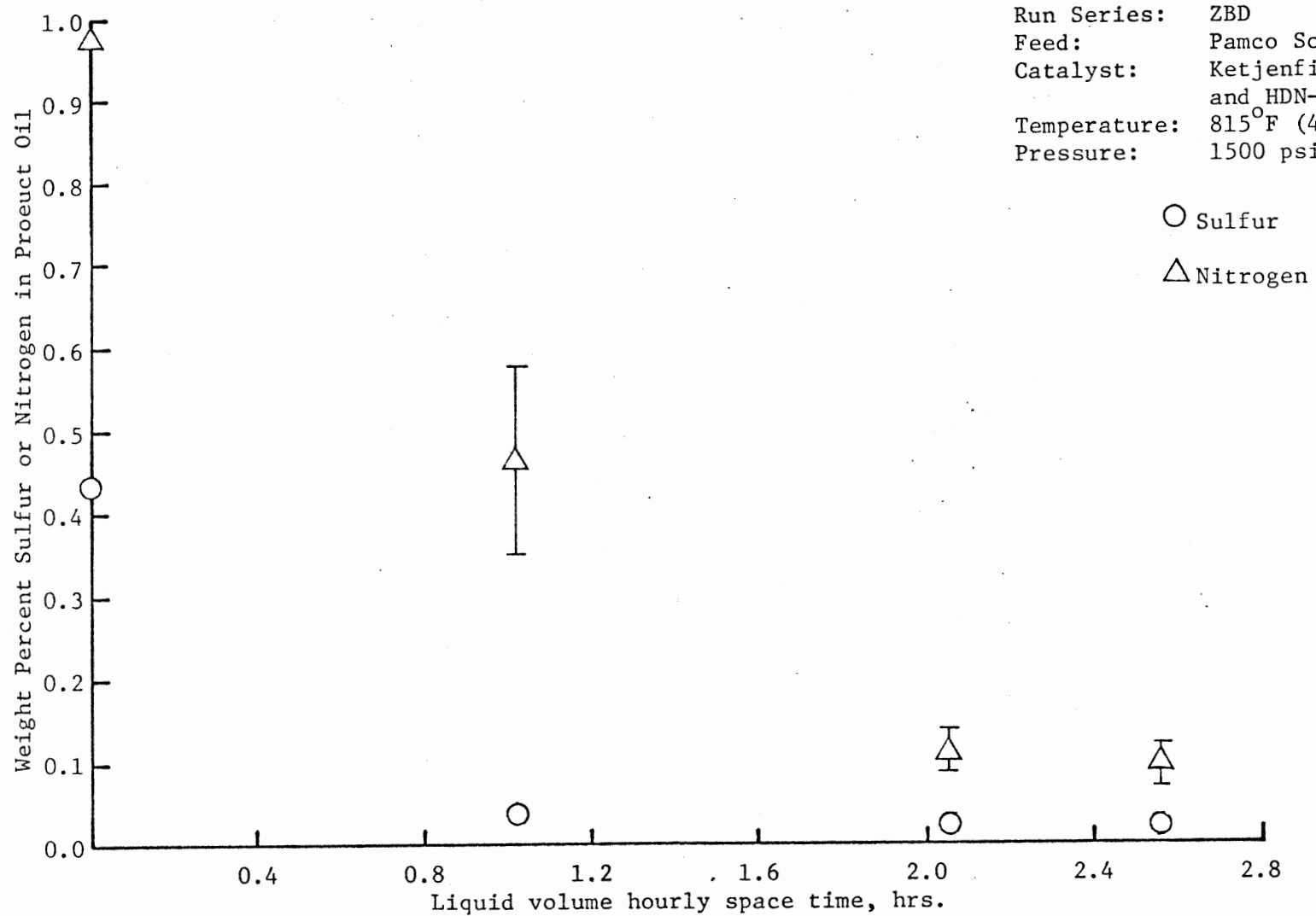
Figure 10. HDS, HDN Activity Response, Run ZBD
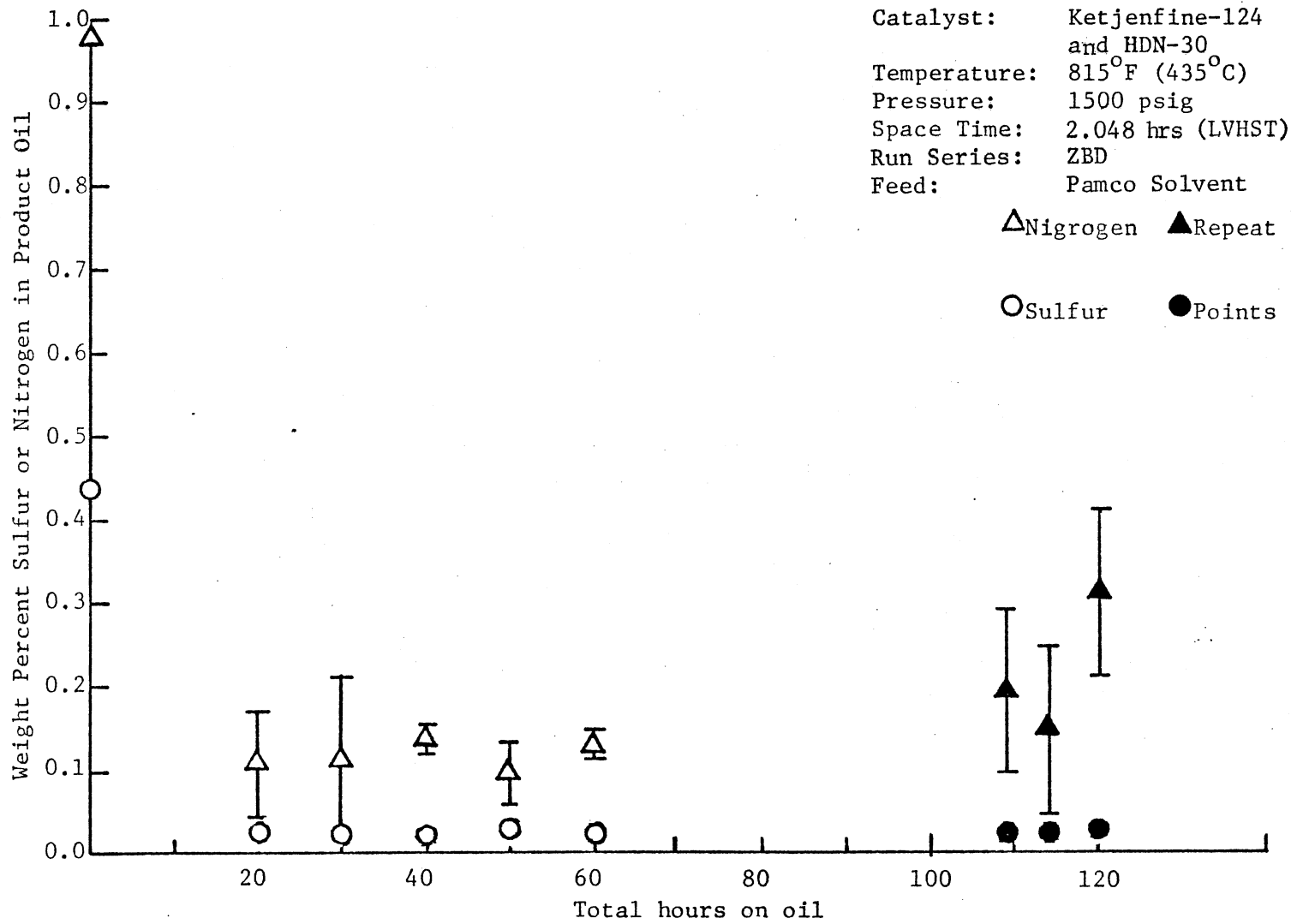
Figure 11. HDS and HDN Activity Response, Run ZBD

Run ZBE

This particular experimental run was conducted to assess the reproducibility of the experimental procedure and reactor operation. Space time was maintained constant at 2.048 hours, the pressure, temperature, and flow rates employed were the same as in experimental run ZBC. HDN-30 (Ni-Mo-alumina) catalyst was used for this run (note that the same catalyst was used for experimental run ZBC).

The weight % sulfur and nitrogen in the product oil for both experimental runs ZBC and ZBE are plotted in Figure 12 as a function of hours of oil catalyst contact. Nitrogen concentration in the product oil was reduced to 0.125 wt % in 20 hours of oil-catalyst contact. This is comparable to the product oil concentration obtained in experimental run ZBC under the same operating conditions. The sulfur content of the product oil was reduced to 0.02 wt % within 20 hours of operation. The nitrogen content of the product oil dropped to 0.063 wt % (93% removal) during the first 30 hours of catalyst-liquid contact. The catalyst showed steady decrease in HDN activity during the 125 hours of operation. The product oil nitrogen concentration increased to 0.281 wt % (71% removal) during the 125 hours of catalyst-liquid contact. Only 61% nitrogen removal was noticed for experimental run ZBC during 117 hours of continuous operation. No deactivation in the sulfur removal activity of the Ni-Mo-alumina catalyst occurred during the entire duration of the run.

ASTM Distillation and Hydrogenation Results

In order to assess the cracking, hydrocracking and hydrogenation
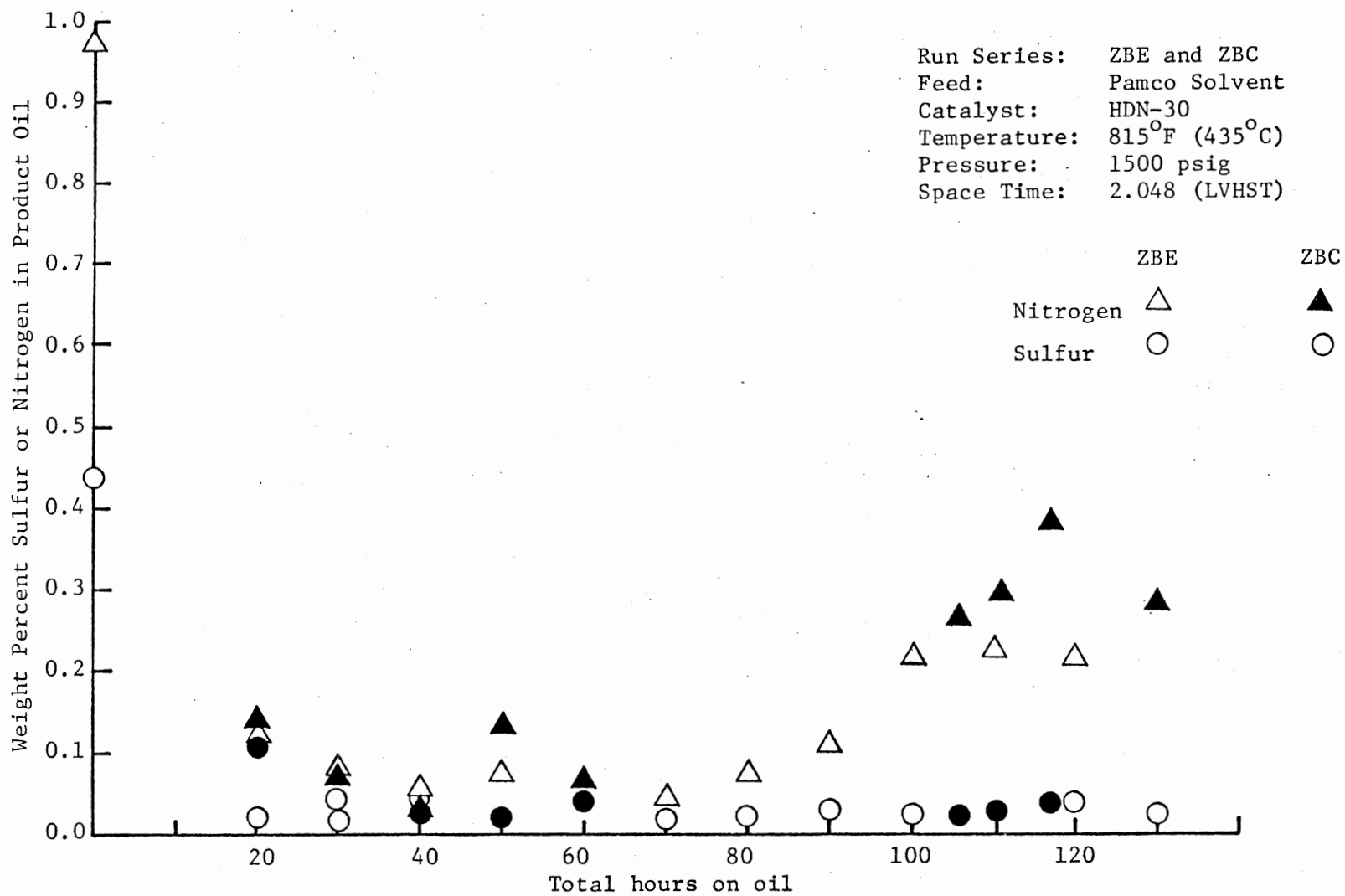
Figure 12. Comparison of Run Series ZBE and ZBC

activity of the various catalysts studied, the feed oil and selected product oil samples were fractionated following the ASTM D-1160 procedure. All product samples were analyzed for hydrogen content by the Perkin-Elmer 240 Elemental Analyzer. The hydrogen content of the product oil is a good indicator of the extent of hydrogenation of the feed oil. The ASTM D-1160 data can indicate the shift in the boiling ranges which, in turn, can be indicative of the hydrogenation, cracking and hydrocracking reactions.

ASTM D-2892 charts are used in the petroleum industry for converting petroleum hydrocarbons' boiling ranges from any subatmospheric pressure to 760 mm of Hg (details follow in the Appendices). Assuming their applicability, the coal liquid fraction (at 760 mm of Hg) boiling up to $422^{o}F$ ($216.6^{o}C$) can be considered to be a light oil. Liquid boiling in the range of $422^{o}F$ ($216.6^{o}C$) and $650^{o}F$ ($343.3^{o}C$) can be considered to be the middle distillate fraction and the fraction boiling higher to be the heavy ends.

Table II presents the ASTM D-1160 results (translated to 760 mm Hg pressure) for the Pamco feedstock and some of the product oil samples, representative of each experimental run conducted. The product oil samples selected for ASTM D-1160 distillation were those taken during the 40 to 60 hours of oil-catalyst contact at a space time of 2.048 hours. The temperature of all runs except experimental run ZBA ($615^{o}F$) was $815^{o}F$ ($435^{o}C$).

The volume distribution of the various fractions in the Pamco feed and selected product oil samples is summarized in Table VI. Note that the Pamco Process Solvent oil is 65.8% middle distillates and 34.2% heavy distillates. No light fractions are present. The cracking,

TABLE VI

DISTRIBUTION OF PAMCO OIL AND PRODUCT LIQUID SAMPLES
AS A FUNCTION OF BOILING RANGE

	Feed* Oil	Product Oil				
		Experimental Run Series				
		ZBA	ZBB	ZBC	ZBD	ZBE
Wt % Removal						
Sulfur		43	91.5	96	95	92.5
Nitrogen		13.5	89.5	91	89	93.5
Temperature (^{o}F)	–	615	815	815	815	815
Hours of Oil on Catalyst	–	55–65	50–60	40–50	40–50	40–50
Space Time, hrs (LVHST)	–	2.048	2.048	2.048	2.048	2.048
Catalyst	–	HDN–30	Ketjenfine –124	HDN–30	Ketjenfine –124 and HDN–30	HDN–30
Light Oil, Vol % [T**<422°F (216.6^{o}C]	–	2.70	17.0	15.5	17.8	14.0
Middle Distillate Vol % [422°F < T**<650°F]	65.8	63.30	60.5	60.0	62.5	60.5
Heavy Ends, Vol % [T**>650°F (343.3^{o}C)]	34.2	34.0	22.5	24.5	19.7	25.5

*Mixture of two liquid product samples was used.

**Boiling point at 760 mm Hg.

hydrocracking and hydrogenation increases the light oil fraction, while the percentage of middle distillates and heavy ends decrease. As is evident from Table VI, negligible hydrogenation of the feedstock occurred in Run ZBA (615°F).

CHAPTER V

DISCUSSION OF RESULTS

The objective of the present study was to design and construct a trickle-bed reactor system and to run a set of experiments on the new system to assess the hydrodesulfurization (HDS) and hydrodenitrogenation (HDN) activity of two different catalysts, separately and in combination as zonal-catalyst beds.

Sulfur and nitrogen concentrations in the product oil were taken as a measure of HDS and HDN activity of the catalysts. The variations in the performance of the trickle-bed reactor system and the precision of the liquid sample analyses were assessed by conducting two experimental runs under similar process conditions.

Reactor Operation

In trickle-bed reactors, temperature control can be an operational problem because of the exothermic reactions occurring on the catalyst; hot spots can result which can deactivate the catalyst. The temperature control problem is very acute in industrial scale reactors where hydrogen or an inert gas is introduced at different stages in the reactor to control the temperature. Aluminum block heaters were used in the present study to provide isothermal temperature profile. Their heating was controlled by means of an automatic temperature controller and a set of powerstats. For both low and high

temperatures, 615°F (324°C) and 815°F (435°C), excellent temperature control was observed, but at the high temperatures (815°F), slightly higher temperatures were encountered in the first two inches of the catalyst bed. Figure 13 presents a typical temperature profile taken during the low temperature (615°F) and high temperature (815°F) experimental runs. The maximum temperature deviation of $\pm 3^{\circ}$F ($+ 1.6^{\circ}$C) was observed for the entire duration of the low temperature (615°F) experimental run. Note the relatively lower hydrodenitrogenation and hydrodesulfurization activity for this run. For the experimental runs conducted at the higher temperature (815°F), a maximum deviation of $\pm 10^{\circ}$F (5.5°C) was observed during the first two inches of the catalyst bed length. The maximum deviation of temperature for the rest of the bed was $\pm 4^{\circ}$F (2.2°C). The higher temperatures for the first two inches of the catalyst-bed were observed for the entire duration of the high temperature (815°F) experimental runs. The cause for the higher temperatures is that the oil and hydrogen hit the highly active catalyst at their highest concentrations. This is when inhibiting gases such as ammonia are present in relatively low concentration, resulting in high reaction rates and hence high heat releases. In order to maintain the reproducibility of the results, the aluminum heater block configuration was not altered during the entire series of experimental runs.

In previous studies conducted with a similar experimental setups, a maximum radial temperature difference of 3°F (1.6°C) was observed between the temperature measured at the reactor wall and the temperature measured at the center of the reactor. The reactor used in the present study was of the same diameter and approximately the same wall thickness as the reactor used in the previous studies; one can conclude
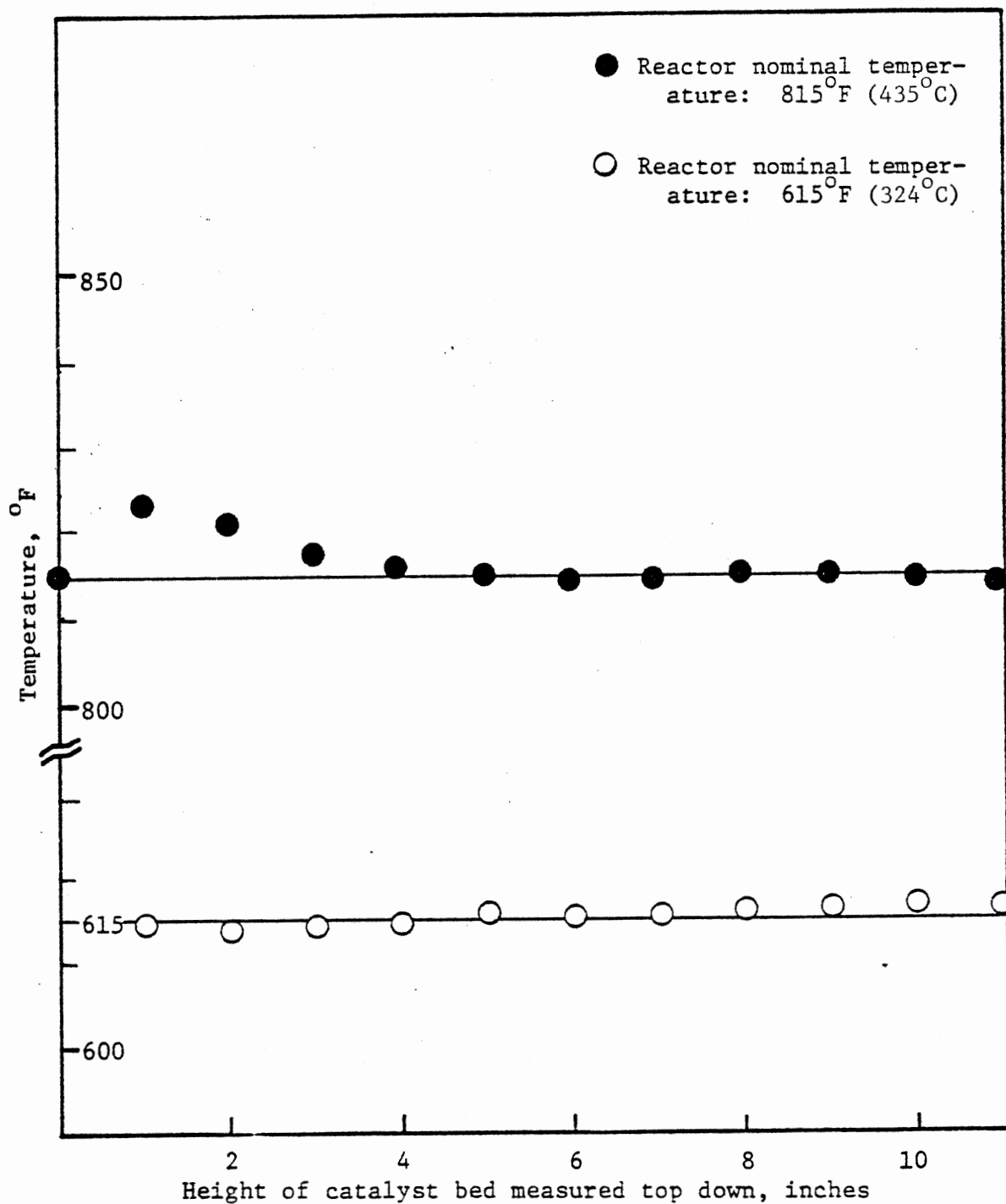
Figure 13. Typical Temperature Profile at Nominal Reactor Temperature of 615°F and 815°F

that the radial bed temperature in this study was also less than 3°F (1.5°C). In fact. the temperature difference between the temperature of the aluminum heating block and the temperature measured at the center of the reactor was always less than 3°F (1.5°C). This strengthens our assumption of minimum radial temperature variation.

All of the experimental runs in this study were conducted at a pressure of 1500 psig. A maximum pressure variation of $\pm$ 20 psig was observed in the present study. This corresponds to a deviation of 1.32% based on absolute pressure from the desired value of 1500 psig. As discussed in the literature section, an increase in pressure above 1000 psig has negligible effect on the heteroatom removal from some coal-derived liquids. Thus, a $\pm$ 20 psig variation is considered to have a negligible effect on the reproducibility of the results.

A positive displacement pump was used for metering the feed oil to the reactor. The pump could feed at a preset constant rate with little or no variations in liquid flow rate. Hence, variations in the liquid flow rates were either absent or negligible in the present study.

In all experimental runs in this study the catalyst bed height was maintained at 10 inches (25.4 cm). The bed height was maintained within $\pm$ 0.1 inch (0.254 cm). At the highest flow rate, 40 cc/hr, this could cause the liquid volume hourly space time to change by $\pm$ 0.005 hour. For the lowest flow rate, 8 cc/hr, these fluctuations would be within $\pm$ 0.02 hour. The volume hourly space time in this study is defined as the ratio of the reactor volume based on catalyst bed height to the liquid volumetric flow rate. Thus the variations in the liquid volume hourly space time can be neglected in this study. Variations in mass of the catalyst used in the various experimental runs occurred due to

the different packing densities of the catalysts used. The variations

in the catalyst mass are taken into account while calculating the

first order reaction rate constants based on the mass of the catalyst.

For the duplicate runs ZBC and ZBE, where the same type of catalyst

was used (HDN-30), a variation of $\pm$ 0.02 gm was noted—corresponding

to 1% of the total catalyst mass charged in the reactor.

In the present study, the hydrogen flow was maintained at 6730 $\pm$

600 standard cubic feet/barrel (SFC/bbl) for the experimental run ser-

ies ZBB, ZBC, ZBD, and ZBE. Hydrogen flow rates at 2500 to 6570 SFC/

bbl were maintained for experimental run ZBA. As discussed in the

literature review section, changing the hydrogen flow rate above 1500

SCF/bbl has a negligible effect on the heteroatom removal. The vari-

ations in this ratio affected the results insignificantly.

The reproducibility of the catalyst loading, activation, and

presulfidation was assessed from the duplicate experimental run. This

will be discussed later in this chapter. An estimate of the precision

of nitrogen analysis can be had from the analysis of Pamco Process

Solvent, given in Table VII. The table presents an estimate of 24 dif-

ferent feed and product samples, chosen randomly, for their nitrogen,

sulfur, and hydrogen contents and their standard deviations. These

standard deviations have been calculated from the data obtained after

analyzing each sample at least three times. In the case of Pamco feed

oil, 16 samples were analyzed for sulfur, 10 samples of each were anal-

yzed for hydrogen and nitrogen contents. The average sulfur concentra-

tion was 0.438 wt % with a standard deviation of $\pm$ 0.040 wt %; the

average nitrogen and hydrogen contents were 0.977 wt % and 7.1110 wt %

with standard deviations of $\pm$ 0.33 and $\pm$ 0.156 wt %, respectively.

TABLE VII

PRECISION OF THE ANALYTICAL TECHNIQUE

% Nitrogen	Standard Deviation	# of Samples	% Sulfur	Standard Deviation	# of Samples	% Hydrogen	Standard Deviation	# of Samples
0.977	± 0.033	10	0.438	± 0.040	16	7.110	± 0.158	10
0.712	± 0.056	3	0.371	± 0.097	4	7.638	± 0.177	3
0.557	± 0.037	4	0.251	± 0.059	3	8.543	± 0.372	4
0.446	± 0.094	3	0.206	± 0.049	3	9.349	± 0.652	3
0.161	± 0.029	4	0.107	± 0.085	4	9.481	± 0.387	3
0.089	± 0.021	4	0.048	± 0.023	3	10.070	± 0.543	4
0.056	± 0.043	3	0.032	± 0.026	4	10.493	± 0.702	4
0.031	± 0.023	3	0.029	± 0.021	3	10.747	± 1.219	3

An estimate of the standard deviation was obtained from sample variance; the following equations were used:

$$\text{Variance} = \frac{1}{n - 1} \Sigma \ (X_i - \bar{X})^2$$

where n = number of independent observations; $\bar{X}$ = mean of the X_i; standard deviation = $(\text{variance})^{\frac{1}{2}}$

As can be seen from Table VII, the accuracy of determining the amounts of nitrogen and sulfur in the samples deteriorates as the percent nitrogen and sulfur are below 0.05 wt %. Sivasubramanian (1979) also established the same conclusion in his hydrodenitrogenation study with raw anthracene oil. Only four liquid samples with nitrogen content lower than 0.05 wt % were observed in the present study. The lower limit of our analytical capabilities for sulfur analysis has been set at 0.02 wt %. Sulfur concentrations in the range of 0.05 to 0.02 wt % have been observed in this study, indicating a highly active catalyst. Sulfur concentrations around 0.05 wt % and below did not allow a distinction between various catalysts. Sooter (1974) in his thesis work on the HDS of raw anthracene oil, observed that the precision of analytical results using the same type of instrument were seriously affected below 0.02 wt % sulfur in the oil. The average hydrogen content of Pamco oil was 7.110 wt % with a standard deviation of $\pm$ 0.108 wt % obtained by Wells (1977) for raw anthracene oil with an average content of 5.570 wt %. As can be seen from TAble VII, the standard deviation varies from + 0.158 to $\pm$ 1.219 wt % as the average hydrogen content varies from 7.110 to 10.747 wt %; the analysis precision deteriorates above 10.070 wt % hydrogen content.

Figure 14 presents a comparison between the boiling point data of runs ZBC and ZBE, conducted under similar conditions, using Ni-Mo-alumina catalyst. The boiling point curves overlap for the two experimental runs, indicating excellent reproducibility of the results. Figure 12 presents a comparison between the weight % nitrogen and sulfur present in the product oil as a function of the total hours of oil catalyst contact for runs ZBC and ZBE. By conducting duplicate
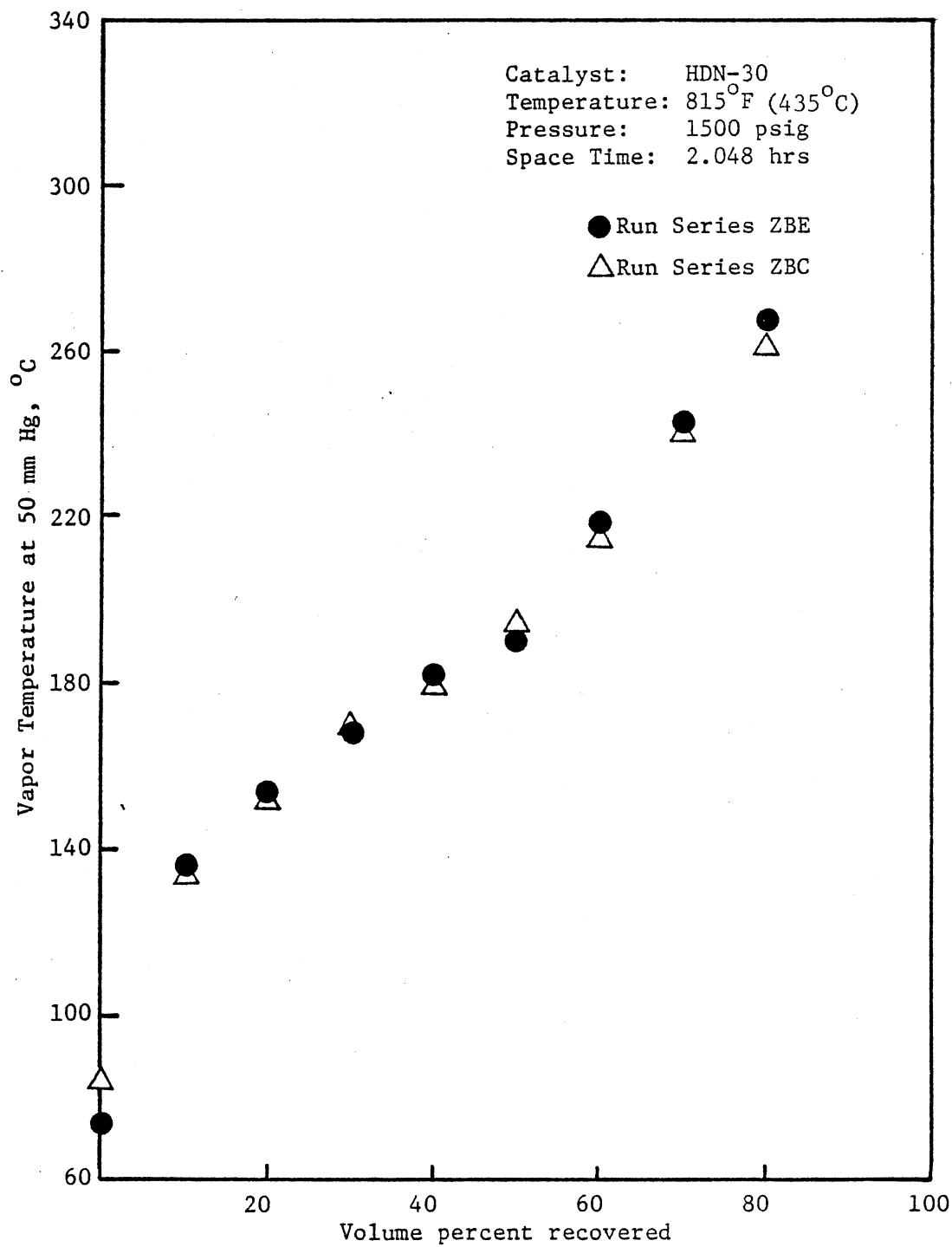
Figure 14. Comparison of Distillation Data for Run
Series ZBC and ZBE

experimental runs, the reproducibility of catalyst loading, catalyst activation and presulfidation, reactor operation and sample analyses can be ascertained. Note that the maximum variation in the nitrogen and sulfur content of the product oil from runs ZBC and ZBE is 0.06 and 0.08 wt %, respectively. This is within the range of the standard deviation noted for the sulfur and nitrogen analyses. Thus we can conclude that the reproducibility of the experimental procedure and sample analyses in this study is excellent.

Performance of Trickle-bed Reactors

This study was not intended to measure the effect of fluid dynamic parameters on the performance of trickle-bed reactors. However, an attempt will be made to analyze the extent in which these factors affect the reactor performance. As has been discussed earlier in the literature section of this study, catalyst liquid holdup, effective catalyst wetting, mass transfer and axial dispersion have been cited by various authors to affect the reactor performance.

In packed bed reactors, liquid flows in a gas continous phase as a thin liquid film over the catalyst. The liquid flow rates in the present study ranged from 8 to 40 cm^3/hr. This corresponds to a liquid flow in the range of 0.003 to 0.015 gm/cm^2/sec. At these low flow rates, the liquid mass transfer resistance can be negligible because of the high ratio of the particle diameter to the thickness of the liquid film. Consideration of the tube diameter to particle diameter ratio (D_t/D_p) can provide an insight into the flow distribution effects. In this study, the D_t/D_p ratio was 6.4.

Sooter (1974) and Satchell (1974) in their hydrotreatment studies

with raw anthracene oil on a similar reactor used a D_t/D_p ratio of
3.45 and varied the liquid flux in the range of 0.009 - 0.038 gm/cm^2/
sec and observed no significant effects on heteroatom removal. The
liquid flux used in the present study is in the range of 0.003 - 0.015
gm/cm^2/sec. Conflicting evidence is present in the literature regard-
ing the effect of liquid hydrodynamics on the performance of trickle-
bed reactors. Most of the data present has been determined from air-
water systems under non-reaction conditions. Thus the criterion for
reactor performance present in the literature cannot be used in the
present study.

The evaluation of kinetic data from fixed bed catalytic reactors
is usually based on the assumption of plug flow; that is, all react-
ants reside in the reactor for a definite period of time determined by
bed volume and flow rate. Mears (1971) reported substantial deviation
from plug flow model for shallow bed experimental reactors due to
axial dispersion effects (details present in the literature section).

$$h/D_p > \frac{2on}{Bo} \ln \frac{C_{in}}{C_{out}}$$

Mears' criterion is seriously questionable because empirical equations
presented in the literature to calculate Bodenstein number involve
substantial error. Moreover, determination of liquid physical prop-
erties at process conditions can result in substantial error.
Sivasubramanian (1977) in his hydrodenitrogenation study with raw
anthracene oil concluded that axial dispersion effects were absent at
a reactor bed height of 83.82 cm and catalyst particle diameter of
0.219 cm. He calculated for a first order reaction, the right-hand

side of Mears' inequality to be 275 for no axial dispersion effects to be present.

Kinetic Modelling

The LVHST and LVHSV have been used extensively in the literature to represent the HDS and HDN kinetics. In this study, liquid volume hourly space time (LVHST) has been used as a parameter for kinetic modelling.

The first- and second-order models were fitted to the HDN data from the various experimental runs. A linear regression technique was employed and the models were compared on the basis of the "F-test." The HDN data fit was excellent for the first-order model; considerable lack of fit existed for the second-order model. The lack of fit was determined by computing the value of "F" and comparing it with the standard statistical F tables for 95% confidence. The results from the first- and second-order linear regression model are assumed in Tables VIII and IX, respectively. Note the high "F" values (compared to the tabulated "F" values), indicating a lack of fit. The sulfur content of the product oil being lower than 0.02 wt % (the lowest limit of sulfur determinator), the HDS data from this study could not be used for mathematical modelling.

The reaction rate constant (volume basis), k_v, obtained from the first-order kinetic fit, can be used as a good indicator of the catalyst activity. The value of k_v, obtained for experimental run ZBA $(615^{\circ}F)$ was $0.0419 \ hr^{-1}$. With the same catalyst, at a temperature of $815^{\circ}F \ (435^{\circ}C)$, the value of k_v increased to $1.564 \ hr^{-1}$. The value of k_v obtained for experimental runs ZBB and ZBD were similar--1.0742

TABLE VIII

RESULTS OF FIRST ORDER FIT

Model: $\ln \dfrac{C_{Ai}}{C_{Ao}} = k_v \tau$ A = nitrogen species

Run Series	Catalyst	Temperature ^oF	k_v hr^{-1}	Est. St. Error k_v	Calculated "F"	Tabulated "F" 95% Confidence
ZBA	Ni–Mo–alumina (HDN–30)	615	0.0419	$\pm$ 0.0534	0.615	4.96
ZBB	Co–Mo–alumina (Ketjenfine–124)	816	1.0742	$\pm$ 0.125	73.599	4.84
ZBC	Ni–Mo–alumina (HDN–30)	815	1.564	$\pm$ 0.215	52.056	4.84
ZBD	Ni–Mo–alumina (HDN–30) and Co–Mo–alumina (Ketjenfine–124) combination	815	1.0374	$\pm$ 0.0957	117.397	4.84
ZBE	Ni–Mo–alumina	815	1.584	$\pm$ 0.200	62.726	4.84

Est. St. Error $= \dfrac{s}{\left(\Sigma(X_i - \bar{X})^2\right)^{\frac{1}{2}}}$ $\bar{X}$ = Mean of X_i

Mean Square Residual = s^2 τ = LVHST

$F = \dfrac{\text{Mean Square Regression}}{\text{Mean Square Residual}}$

TABLE IX

RESULTS OF SECOND ORDER FIT

Model $\dfrac{1}{CAo} - \dfrac{1}{CAi} = k_v \tau$ A = nitrogen species

Run Series	Catalyst	Temperature °F	k_v hr^{-1}	Est. St Error k_v	Calculated "F"	Tabulated "F" 95% Confidence
ZBA	Ni-Mo-alumina (HDN-30)	615	0.0634	$\pm$ 0.0849	0.556	4.96
ZBB	Co-Mo-alumina (Ketjenfine-124)	815	9.541	$\pm$ 3.884	0.165	4.84
ZBC	Ni-Mo-alumina (HDN-30)	815	11.250	$\pm$ 3.905	0.121	4.84
ZBD	Ni-Mo-alumina (HDN-30) and Co-Mo-alumina (Ketjenfine-124) combination	815	9.732	$\pm$ 3.762	0.149	4.84
ZBE	Ni-Mo-alumina (duplicate run)	815	10.975	$\pm$ 3.832	0.125	4.84

Est. St. Error $= \dfrac{s}{\left(\Sigma (X_i - \bar{X})^2\right)^{1/2}}$ $\bar{X}$ = Mean of X_i

τ = LVHST

Mean Residual $= s^2$

$F = \dfrac{\text{Mean Square Regression}}{\text{Mean Square Residual}}$

hr^{-1} and 1.0374 hr^{-1}, respectively. This shows that zonal catalyst beds behave more like the Co-Mo-alumina, which constituted the first half of the reactor volume. The reaction rate constant for the Ni-Mo-alumina catalyst is higher than that of the Co-Mo-alumina catalyst. For the reproducibility run conducted at 815°F (435°C) with Ni-Mo-alumina catalyst, the reaction rate constant was found to be 1.584 hr^{-1}. This compares very well with 1.564 hr^{-1} obtained for the similar experimental run, ZBC.

To obtain further comparisons, the first order rate constants based on the total surface area of the catalyst (k_s) and catalyst mass (k_w) were determined from the reaction rate constant based on the catalyst volume (k_v) using the following relations:

$$k_s = k_v \cdot v/s$$

$$k_w = k_v \cdot v/w$$

where v, s, and w are the total catalyst volume, total surface area of the catalyst bed, and weight of the catalyst bed, respectively. Table X lists the reaction rate constants k_v, k_s, and k_w, based on a first-order reaction model. It is evident that the reaction rate constant based on surface area (k_s) is the highest for the Ni-Mo-alumina catalyst used in experimental runs ZBC and ZBE. The reaction rate constant, k_s, for the mixed catalyst bed (6.666 x 10^{-7} cm $\cdot$ hr^{-1}) falls between the range observed for the Ni-Mo-alumina catalyst (14.759 x 10^{-7} cm $\cdot$ hr^{-1}) and the Co-Mo-alumina catalyst (5.590 x 10^{-7} cm $\cdot$ $hr^{-1)}$ at the temperature of 815°F (435°C). The reaction rate constant, k_s, is significantly lower (0.395 x 10^{-7} cm $\cdot$ hr^{-1}) at 615°F (435°C) for

TABLE X

COMPARISON OF CATALYSTS USED IN THIS STUDY

| Run Series | Temperature | | First Order Rate Constants | | |
	$^{\circ}F$	$^{\circ}C$	k_v hr^{-1}	k_s x 10^{-7} $cm.hr^{-1}$	k_w $cm^3.gm^{-1}.hr^{-1}$
ZBA (Ni-Mo-alumina)	615	(324)	0.0419	0.395	0.0481
ZBB (Co-Mo-alumina)	815	(435)	1.0742	5.590	1.330
ZBC (Ni-Mo-alumina)	815	(435)	1.564	14.759	1.801
ZBD (Co-Mo-alimina and Ni-Mo-alumina combination)	815	(435)	1.0374	6.666	1.214
ZBE (Ni-Mo-alumina)	815	(435)	1.584	14.619	1.725

the same Ni-Mo-alumina catalyst. For the reproducibility run ZBE, the

reaction rate constant (k_s) is 14.619 x 10^{-7} cm . hr^{-1}, which is close

to the k_s value of 14.759 x 10^{-7} cm . hr^{-1} determined for run ZBC.

On the weight basis, the first order reaction rate constant (k_w)

behaves exactly like the reaction rate constant (k_v) based on the cata-

lyst volume. Since almost equal masses of catalysts were used in all

of the runs, the similarity of k_v and k_w is not unexpected. On the

weight basis also, the Ni-Mo-alumina catalyst showed the highest acti-

vity. The reaction rate constant (k_w) for run ZBC is 1.080 . $cm^3/$

gm/hr (Ni-Mo-alumina), which is higher than the value of 1.330 $cm^3/gm/$

hr observed for run ZBB (Co-Mo-alumina). On the weight basis, the

reaction rate constant (k_w) for the mixed catalyst bed (1.214 $cm^3/gm/$

hr) is lower than the value of k_w for individual catalyst beds.

Hydrogenation and Distillation

As is evident from TAble VI, negligible hydrogenation of the feed-

stock occurred during the run ZBA conducted at $615^{\circ}F$ $(324^{\circ}C)$. Figure 15

presents a comparison of the ASTM D-1160 distillation results for

liquid samples from run series ZBA and the Pamco Process Solvent oil.

The shift in the boiling ranges is negligible, signifying very little

or no cracking, hydrocracking and hydrogenation of the feedstock at

this temperature.

Figure 16 presents the ASTM D-1160 distillation results for the

liquid samples from run series ZBB, ZBC and ZBD. Note that the experi-

mental runs ZBB and ZBC were conducted using Co-Mo-alumina and Ni-Mo-

alumina catalyst, respectively. Experimental run ZBD used a combi-

nation of a Co-Mo-alumina and a Ni-Mo-alumina catalyst in a zonal bed
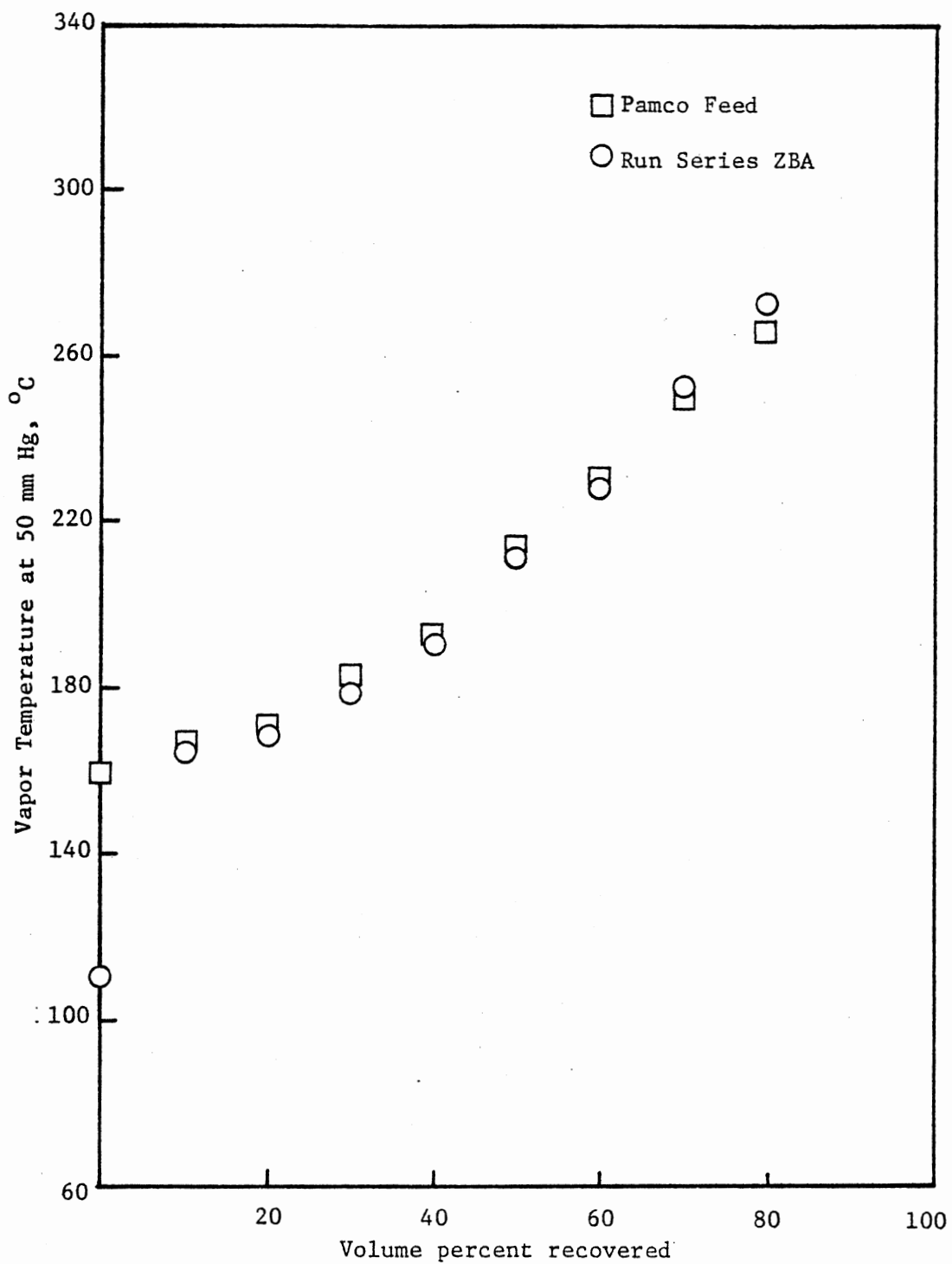
Figure 15. Comparison of Distillation Data for Run Series
ZBA and Pamco Feedstock
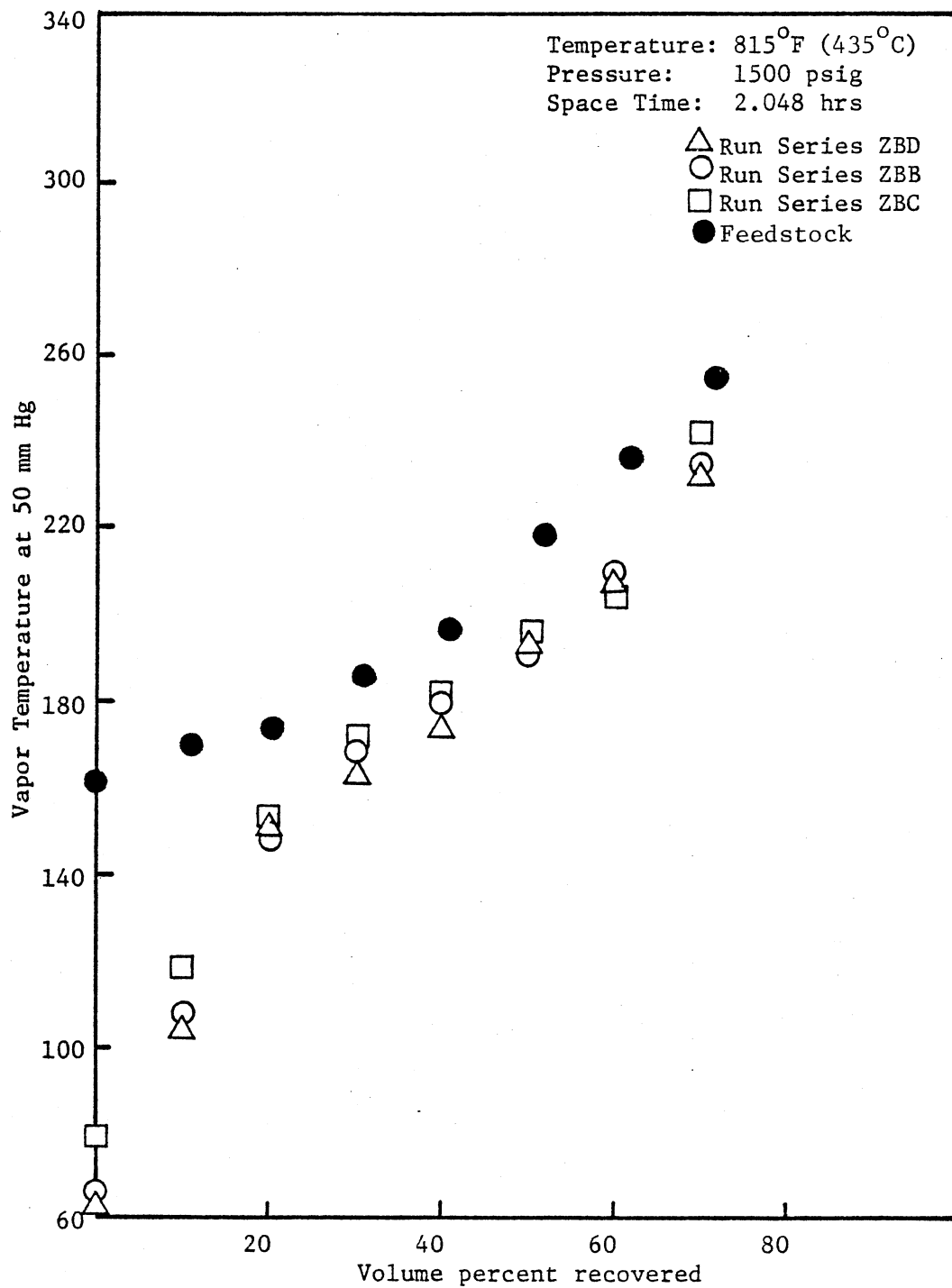
Figure 16.   Comparison of Distillation Data for Run
Series ZBB, ZBC and ZBD

configuration. As can be seen from Figure 16, the boiling curves over-
lap, indicating similar hydrocracking, cracking, and hydrogenation
activity of the Co-Mo-alumina, Ni-Mo-alumina and their zonal bed com-
bination.

As is clear from Table VI (page 81), a substantial fraction of
the heavy ends is converted into middle and light fractions. The vol
% of the feedstock heavy fraction is reduced from 34.2 vol % to a
minimum of 19.7 vol %. Middle fractions also suffer considerable hydro-
treatment; the volume percentage of middle fractions is reduced from
65.8 in the feedstock to a minimum of 60.0 vol %.

Very little hydrogenation occurred at the low temperature of 615°F
(324°C) for run ZBA. The hydrogen content of the product oil was 7.38
wt % for 0.512 hrs liquid volume hourly space time. The hydrogenation
activity improved only slightly as the space time was increased to 2.048
hrs. The hydrogenation activity increases substantially with increase
in temperature. For the space time of 1.024 hrs, the product oil
hydrogen content for run ZBB was 9.82 wt %. The hydrogenation acti-
vity of the Co-Mo-alumina increased only slightly with an increase in
space time. Lower hydrogenation was observed for lower space time
(1.024 hrs) for the Ni-Mo-alumina catalyst (run ZBC). The hydrogenation
activity increased substantially with the increase in space time (2.048
hrs). The product oil hydrogen content for space time of 1.024 hrs
was 8.4 wt %, which increased to 10.42 wt % for space time of 2.56 hrs.
The hydrogenation activity of run ZBD (zonal catalyst bed) was similar
to experimental run ZBB (Co-Mo-alumina) at lower space times. The
hydrogen content of the product oil was 9.67 wt % for the space time
of 1.024 hrs, which is comparable to 9.81 wt % observed for experimental

run ZBB. Product oil hydrogen concentration of 10.1 wt % was observed at a space time of 2.048 hrs. This falls between the hydrogen contents of 10.37 wt % and 9.84 wt % observed for experimental runs ZBC and ZBB, respectively.

Figure 17 presents a plot of the wt % hydrogen in the product oil as a function of the time of operation for experimental runs ZBA, ZBB, ZBC, ZBD and ZBE. Note that the hydrogen content of the product oil reduced from 10.493 wt % to 8.543 wt % during the 120 hours of catalyst operation for the experimental run series ZBD. Similar loss of hydrogenation activity was noticed for experimental runs ZBB and ZBC. The hydrogen weight percentage in the product oil was reduced from 10.439 wt % at 20 hours to 9.960 wt % after 104 hours of oil-catalyst contact. 9.243 wt % hydrogen was reported for experimental run series ZBC after 106 hours of operation. Steady loss of hydrogenation activity can be observed for run ZBE, where product oil hydrogen content is reduced to 9.03 wt % after 125 hours of operation; 10.624 wt % hydrogen was reported after 20 hours of operation.

A linear model $Y = \beta_o + \beta_1 t$, where Y is the product oil hydrogen content and t is the time of oil-catalyst contact (hrs) was fitted to the hydrogenation data from experimental runs ZBB, ZBC, ZBD and ZBE using linear regression technique. A steady decrease in the product oil hydrogen content (Y) was noted with the increase in oil-catalyst contact time (t). The least square estimate of the slope (β_1) for the linear model was equal to -0.00827 wt % hydrogen/hr, representing steady decrease in the hydrogenation activity of the catalysts (Co-Mo-alumina, Ni-Mo-alumina).

This decrease of hydrogenation activity can be explained as
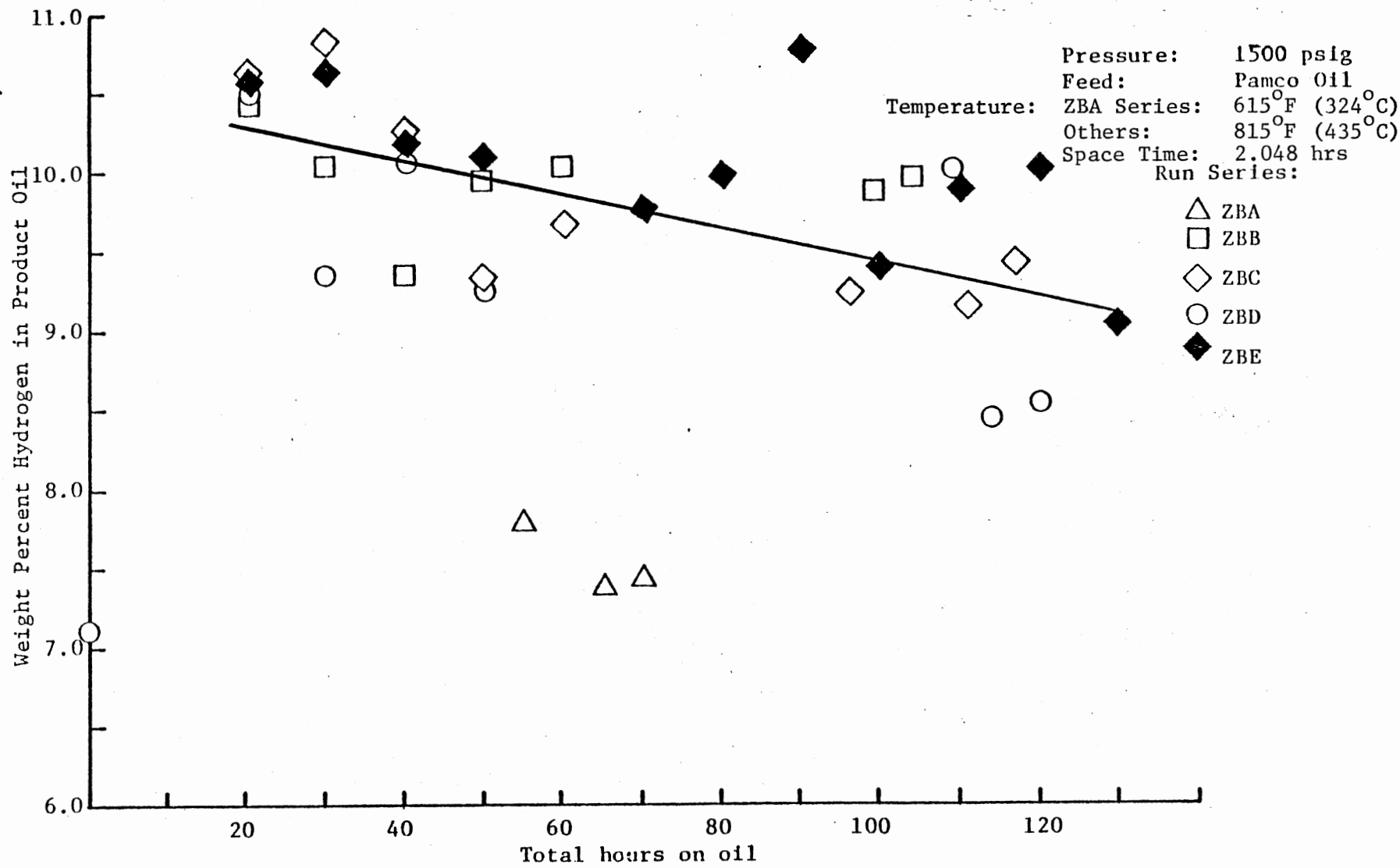
Figure 17. Hydrogenation Activity Response

follows: The hydrotreatment catalysts used in this study, Co-Mo-alumina

and Ni-Mo-alumina, both are bi-functional catalysts, where both support

material and the impregnated metals are responsible for the hydro-

treatment activity. The hydrocracking reactions occur on the support

material, whereas the hydrogenation reactions occur on the sulphided

metal species (MoS_2 in this case). The bulk surface for the reaction

to occur is present within the micropores in the catalyst.

The deposition on the catalyst surface occurs due to the side

reactions (polymerization, condensation) occurring on the catalyst sur-

face. The coke deposition is higher for the low hydrogen containing

fraction present (asphaltenes and pre-asphaltenes). Coke deposition is

accelerated by the heteroatoms (S, N. O) contained in coal liquids

which, when deposited on the catalyst surface, act as precursors for

coke desposition. The coke deposition makes the bulk of the catalyst

surface inaccessible to the coal liquid molecules because of the par-

tial or complete blockage of the pores, which results in loss of cata-

lytic activity with increase in oil-catalyst contact time. Metal

deposition and adsorption of basic species also play an important role

in catalyst deactivation. The metal deposition causes long-term

deactivation of catalyst, whereas the coke laydown is responsible for

the initial loss of catalytic activity. The basic species adsorption

on the acidic catalyst support reduces the hydrocracking activity of

the catalyst, which also results in reducing the hydrogen content of

the product oil.

Hydrodesulfurization and Hydrodenitrogenation

Figure 18 presents a comparison of the weight percent nitrogen in
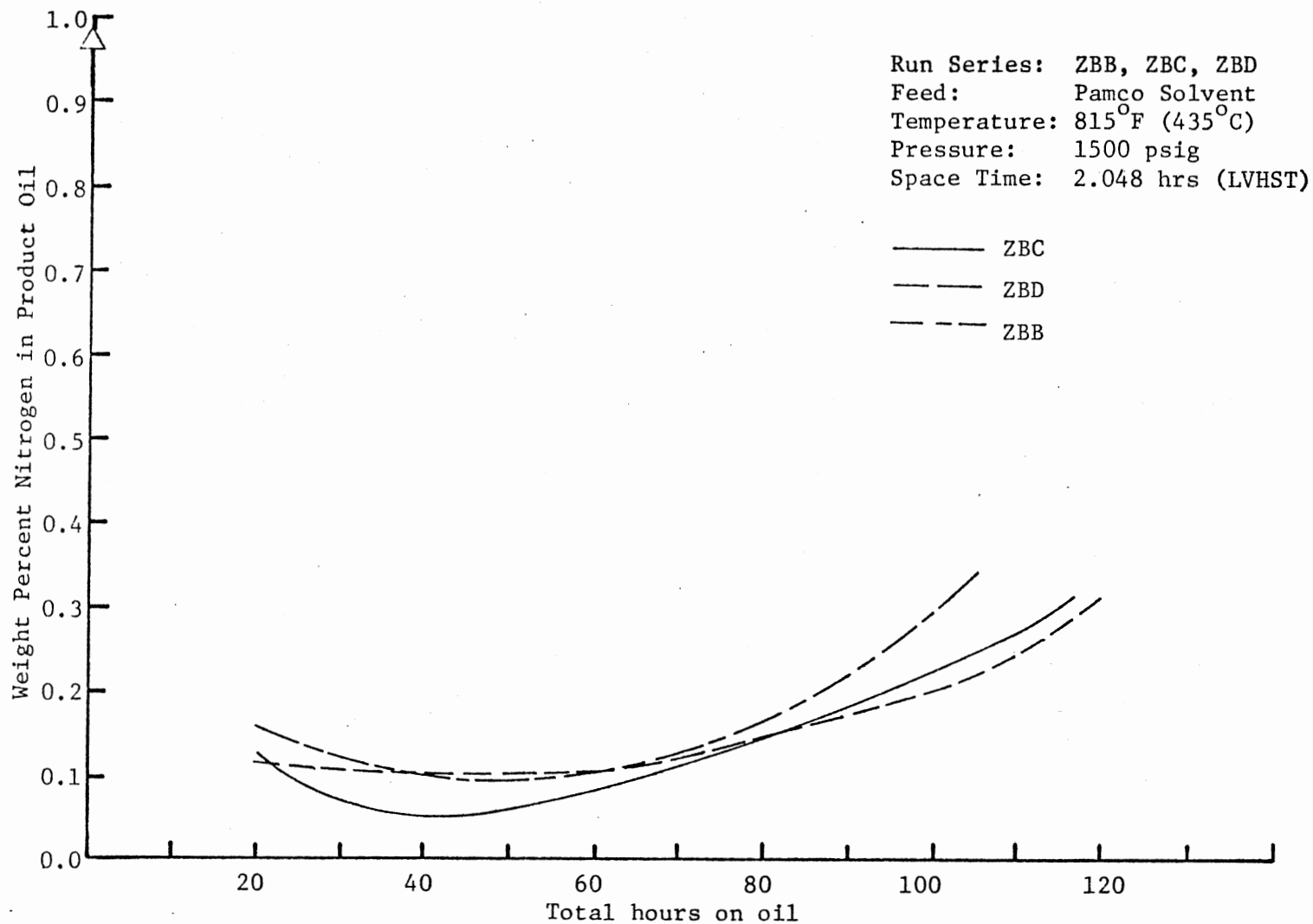
Figure 18. Comparison of HDN of Run Series ZBB, ZBC, ZBD

the product oil as a function of hours of oil-catalyst contact time for experimental run series ZBB, ZBC and ZBD. (These lines are simply smoothed curves from the data of Figures 7, 9 and 11 and are meant to reveal only the general trends in activity loss.) As can be seen from the figure, the nitrogen content of the product oil increases with the oil-catalyst contact time. This loss of activity is observed for all runs. Approximately 85% nitrogen removal was noted within 30 hours of oil-catalyst contact for all three runs. The Co-Mo-alumina showed greater loss of nitrogen removal capacity compared to the Ni-Mo-alumina and the Co-Mo-alumina, Ni-Mo-alumina combination. Approximately 70 wt % removal was observed for run ZBB (Co-Mo-alumina) compared to approximately 80 wt % removal for run ZBC (Ni-Mo-alumina) after 100 hours of oil-catalyst contact.

Only slight loss of sufur removal activity was observed compared to the nitrogen removal ability for runs ZBB, ZBC and ZBD. Here also the Co-Mo-alumina showed higher loss of sulfur removal ability compared to the Ni-Mo-alumina catalyst. Only 82 wt % sulfur removal occurred after 94 hours of oil-catalyst for run ZBB (Co-Mo-alumina) compared to 94 wt % sulfur removal for the ZBC run (Ni-Mo-alumina).

The loss of sulfur and nitrogen removal activity of run ZBD (Ni-Mo-alumina, Co-Mo-alumina combination) was similar to run ZBC. Negligible loss in sulfur removal activity occurred for run ZBD. 75 wt % nitrogen removal was observed for run ZBD after 100 hours of operation, which is comparable to 73 wt % removal for run ZBC.

Ahmed (1979) conducted various experimental runs to assess the hydrotreating performance of a Ni-Mo-alumina catalyst (Nalco NM-502) using different coal liquids. Using Synthoil II liquid at $700^{o}F$

(371°C), 1500 psig and 1.5 LVHST, he observed no appreciable decay for sulfur removal. However, nitrogen removal of around 46 wt % fell to only 27 wt % in 100 hours of oil-catalyst contact. Note that the Synthoil II contained 2.1 wt % ash. Appreciable HDN activity decay was reported for a similar experimental run conducted for 176 hours. He also observed significant loss of nitrogen removal activity during a 674-hour experimental run, using Rasyn oil. The product oil nitrogen content approached the feed oil nitrogen content only after 180 hours of catalyst-oil contact. Significant loss in catalyst HDS activity was reported during the 674-hour operation. The product oil sulfur concentration levelled off around 0.38 wt %. The Rasyn liquid feedstock used in this experimental run contained 0.54 wt % sulfur.

Ahmed (1975) reported sulfur levels below 0.02 wt % throughout 100 hours of operation at 800°F, 1500 psig, using FMC oil, A space time of 2.99 hours was employed using commercially available Co-Mo-alumina catalyst (Nalcomo-474). Similar high removal of sulfur was reported at 850°F (455°C), other conditions being the same.

The HDS and HDN activity of a catalyst is highly dependent upon the type of coal liquid processed. In earlier studies with raw-anthracene oil, no appreciable decay was observed for HDN activity. The HDN activity is lower for a feedstock with higher sulfur concentration. The sulfur compounds inhibit the HDN reactions, and vice-versa.

The catalyst deactivation during this study can be explained to have occurred due to coke deposition on the surface of the catalyst. This is the main mechanism of catalyst deactivation, as discussed in the literature review section. The coke deposition is promoted at high temperature due to the undesirable side reactions (polymerization,

condensation, etc.) occurring on the active sites. The catalyst can lose activity due to either pore blockage, which renders a substantial fraction of catalyst inaccessible to the catalyst surface, or loss of active sites by depositions (inorganic, metal, etc.).

The higher loss in sulfur and nitrogen removal activity of the Co-Mo-alumina can be explained to have occurred due to the greater coke deposition on the surface of the Co-Mo-alumina catalyst. Severe pore blockage can result due to the relatively small pore diameter of the Co-Mo-alumina catalyst (51 A^o - most frequent diameter) compared to the Ni-Mo-alumina catalyst (84 A^o - most frequent diameter). This results in most of the active catalytic sites being inaccessible to the coal liquid molecules. Due to the negligible ash present in the feedstock (Table IV), the inorganic desposition cannot seriously affect the catalyst activity. The metal deposition causes long-term catalyst deactivation and it too can be neglected for the short experimental runs conducted during this study (less than 125 hrs of oil-catalyst contact). The hydrodesulfurization and hydrodenitrogenation differ considerably in the mechanism of heteroatom removal (refer to the literature section). Sulfur removal occurs prior to ring hydrogenation, whereas nitrogen removal occurs after ring hydrogenation. The rapid loss in hydrodenitrogenation activity occurs due to loss of active hydrogenation sites. The alumina catalyst being bifunctional, the hydrogenation and heteroatom removal occurs at different active sites, the hydrogenation being favored at the Lewis sites of the alumina catalyst and heteroatom removal occurring at the active metal species. The Lewis sites are more susceptible to poisoning by the basic nitrogen compounds present in the coal-derived liquids. This could result in

a rapid loss of hydrogenation activity, resulting in loss of hydrode-
nitrogenation activity, whereas the catalyst is still active for sulfur
removal (Furminsky, 1979; Ahmed, 1979).

CHAPTER VI

CONCLUSIONS AND RECOMMENDATIONS

Conclusions

1. The experimental system designed and constructed in this study operated satisfactorily. Nitrogen and sulfur product oil concentrations of some product liquid samples were below 0.05 wt % (95% removal) and 0.02 wt % (96% removal, respectively at 2.048 hrs LVHST), signifying excellent trickle-bed reactor operation.

2. Successful operation was conducted using Co-Mo-alumina, Ni-Mo-alumina and their zonal bed combination for hydrotreating Pamco Process solvent oil at temperatures as high as 815°F (435°C), pressure of 1500 psig, and a space time in the range of 0.5 to 2.5 hrs for up to 125 hrs of continuous operation.

3. The zonal bed combination of Co-Mo-alumina and Ni-Mo-alumina offered no advantage for HDN and HDS of Pamco Process Solvent oil over the single catalyst beds for the operating conditions employed.

4. On volume, mass and surface area basis, the HDN activity of Ni-Mo-alumina catalyst was higher than the activity of the Co-Mo-alumina catalyst and the zonal catalyst beds.

5. The sulfur removal activities of the Ni-Mo-alumina, Co-Mo-alumina and the zonal bed combination were high; in fact, the product oil sulfur concentration was below 0.02 wt % even at a low space time of 1.024 hrs.

110

6. Ni—Mo—alumina and Co—Mo—alumina and their zonal bed combination (835°F) indicated steady loss of hydrogenation activity. This loss of activity could be represented by a linear relationship with a least square slope of -0.0083 wt % hydrogen per hour.

7. HDN, HDS and hydrogenation activity of Ni—Mo—alumina catalyst increased substantially with an increase in temperature from 615°F (324°C) to 815°F (435°C).

8. Ni—Mo—alumina, Co—Mo—alumina and their zonal bed combination indicated some loss in the activity for nitrogen removal.

9. Co—Mo—alumina showed 14% loss in sulfur removal activity over the hundred hours of continuous operation. This loss of HDS activity was not noted for the Ni—Mo—alumina catalyst nor the zonal catalyst bed combination.

10. The HDN activity of Ni—Mo—alumina, Co—Mo—alumina and zonal catalyst bed showed dependence on volume hourly space time. First order kinetic model correlated the data better than a second order kinetic model.

Recommendations

1. The zonal catalyst bed concept should be tested for heavier feedstocks.

2. The zonal catalyst beds employing the following catalyst combinations should be tested:

a) Catalyst with uniform pore size of 20-30°A followed by a catalyst with very high pore size (150-300 A^{o}). This combination is very suitable for liquid feeds containing high concentration of organo-metallic compounds (Arey et al., 1967). The

large organo-metallic molecules would be screened in the first
part of the bed, thus increasing the active life of the cata-
lyst in the following bed. The large pore diameter in the
second bed can withstand greater coking.

    b) A highly hydrogenating catalyst (Ni-W-Zeolite) followed by
a hydrotreating catalyst with high hydrocracking activity (Co-
Mo-alumina or silica stabilized alumina).

    3. The concept of guard-bed chambers containing cheap or dispos-
able catalysts should be investigated. The present experimental setup
should be modified to accommodate a guard-bed in series with the cata-
lyst bed. The guard-bed should be capable of being operated at a
different temperature than the main catalyst bed. The following
materials should be tested in the guard-bed chambers:

    a) Loosely packed, high strength, preferrably spherical, large
particle size (1/8") hydrotreating catalyst for processing
heavy feedstocks. Alumina can be substituted for the hydro-
treating catalyst.

    b) Used catalyst from the main reactor without regeneration.

    c) Reduced iron.

    d) Coal-ash, ash residue from solvent coal refining process.
They exhibit some catalytic activity due to the presence of
alumina, silica and various metals present (Guin et al., 1979).

    4. Experiments should be conducted to assess the effect of pre-
sulfidation on the catalytic activity of Ni-Mo-alumina catalyst.
Higher sulfidation temperatures should be employed; recommended sulfi-
dation temperature, $662^{\circ}F$ ($350^{\circ}C$).

BIBLIOGRAPHY

Achwal, S. K. and J. B. Stepanek, Chem. Eng. J., $\underline{12}$, 69 (1965).

Ahmed, M. M. and B. L. Crynes, Adv. Chem. Ser., $\underline{179}$, 175 (1979a).

Ahmed, M. M., M. S. Thesis, Oklahoma State University, Stillwater, Oklahoma (1975).

Ahmed, M. M., Ph.D. Dissertation, Oklahoma State University, Stillwater, Oklahoma (1979).

Ahmed, M. M. and B. L. Crynes, The Institution of Chemical Engineers Symposium Series, No. 62, Coal Chem. 2000, August/September (1980).

Alexander, B. F. and Y. T. Shah, Can. J. Chem., $\underline{54}$ (1976).

Arey, W. F., R. B. Mason and R. C. Paule, U. S. Pat. #3,254,017 (1966).

Beeckman, J. W. and G. F. Froment, Ind. Eng. Chem. Fund., $\underline{18}$, No. 3, 245 (1979).

Beeckman, J. W. and G. F. Froment, Chem. Eng. Sci., $\underline{35}$, 805 (1980).

Bertolacini, R. J., L. C. Gutberlet, D. K. Kim and K. K. Robinson, "Catalyst Development for Coal Liquefaction." Report AF-574, November, 1979, by Amoco Oil Company.

Beuther, H., R. A. Flinn and J. B. McKinely, Ind. Eng. Chem., $\underline{51}$, 1349 (1959).

Butt, J. B., Adv. Chem. Ser., $\underline{109}$, 259 (1972).

Chang, C. D. and A. J. Silvestri, Ind. Eng. Chem. Process Des. Dev., $\underline{13}$, 315 (1974).

Chirakaparambil, F. G., M. S. Thesis, Oklahoma State University, Stillwater, Oklahoma (1974).

Colombo, A. J., G. Baldi and S. Sicardi, Chem. Eng. Sci., $\underline{31}$, 1101 (1976).

Crine, M. P. Marchott and G. A. L'Homme, Chem. Eng. Sci., $\underline{35}$, 66 (1980).

Crynes, B. L. Chapter in Chemistry of Coal Utilization (to be published in Spring, 1981).

Crynes, B. L., D.O.E. Quarterly Report for the Period April 1- June 30, 1980, Contact No. DE-AC01-79ET-14876.

Dal, J. M., L. D. Holett, E. L. Fuller, H. L. Richards and R. L. Sherman, J. Catal., 61, 66 (1980).

DeBeer, V. H. J., T. H. M. Van Sint Fiet, J. F. Engelen, A. C. Van Haandel, M. W. J. Wolfs, C. H. Amberg and G. C. A. Schuit, J. Catal., 27, 357 (1972).

DeBeer, H. V. J., T. H. M. Van Sint Fiet, G. H. A. M. Van der Steen, A. C. Zwaga and G. C. A. Schuit, J. Catal., 35, 297 (1974).

DeBeer, V. H. J., M. J. M. Van der Aalst, C. J. Machibiels and G. C. A. Schuit, J. Catal., 43, 78 (1976a).

DeBeer, V. H. J., C. Bevelander, T. H. M. Van Sint Fiet, P. G. A. J. Werter and C. H. Amberg, J. Catal., 43, 68 (1976b).

Dudkovic, M. P., A.I.Ch.E. Journal, 23, 940 (1977).

Dumez, F. and G. F. Froment, Ind. Eng. Chem. Proc. Des. Dev., 15, 291 (1976).

Farragher, A. L. and P. Cossee, Proc. Fifth Int. Congr. Catal., Amsterdam, 1301 (1973).

Furmisky, E., Ind. Eng. Chem. Proc. Res. Dev., 17, 329 (1978).

Furmisky, E., Ind. Eng. Chem. Proc. Res. Dev., 18, 206 (1979).

Gates, B. C., J. R. Katzer, J. H. Olson, H. Kwart, A. B. Stiles, Energy Research and Development Administration, Eleventh Quarterly Report (1978), Contract No. E(49-18)-2028.

Goto, S. and J. M. Smith, A.I.Ch.E. Journal, 21, 706 (1975).

Goto, S., S. Watabe and M. Matsubara, Can. J. Chem., 54, 551 (1976).

Guin, J. A., A. R. Tarrer, J. M. Lee, L. Lo and C. W. Curtis, Ind. Eng. Chem. Proc. Des. Dev., 18, No. 3, 371 (1979).

Hagenbach, G., P. H. Courly and B. Delmon, J. Catal., 31, 264 (1973).

Hammer, G. P. and R. B. Mason, U. S. Pat. #3,778,365 (1973).

Hargreaves, A. E. and J. R. H. Ross, J. Catal., 56, 363 (1979).

Henry, H. C. and J. B. Gilbert, Ind. Eng. Chem. Proc. Des. Dev., 12, No. 3, 328 (1973).

Hochman, J. M. and E. E. Effron, Ind. Chem. Fund., 8, 63 (1969).

Houalla, M., N. K. Nag, A. V. Sapre, D. H. Broderick and B. C. Gates, A.I.Ch.E. Journal, 24, No. 6, 1015 (1978).

Johns, J. J., J. F. Jones and B. P. McMunn, Preprints, Div. of Fuel Chem., A. C. S., 16(1), 26 (1972).

Jones, J. F. and L. D. Friedman, "Char Oil Energy Dev. Final Report," Office of Coal Research, No. 56 (1970).

Jones, J. F., N. J. Brunsvold, H. D. Terazin, L. J. Scotti, F. H. Schoemann, R. C. Merrill, J. D. Alcantova, S. J. Romelczyk and L. Ford, "Char Oil Energy Development," Vol. I, Final Report for the Period August 18, 1971, through June 30, 1975.

Katzer, J. R. and R. Sivasubramanian, Catal. Rev., Sci. Eng., 20(2), 155 (1979).

Kawaguchi, Y., I. G. Dalla Lana and F. D. Oho, Can. J. Chem., 56, 65 (1978).

Kilanowski, D. R. and B. C. Gates, J. Catal., 62, 70 (1980).

Klinken, J. V. and R. H. Van Dongen, Chem. Engr. Sci., 35, 59 (1980).

Kovach, S. M., L. J. Castle, J. V. Bennett and J. T. Schroudt, Ind. Eng. Chem. Proc. Res. Dev., 17, 62 (1978).

Kubica, R., J. Cir, V. Novak and V. Veprek, Brennst-Chem., 49, 308 (1968).

Laine, J., K. C. Pratt and D. L. Trimm, Ind. Eng. Chem. Process Des. Dev., 18, No. 4, 329 (1979).

Lee, H. G. and J. B. Butt, J. Catal., 49, 320 (1977).

Lipsh, J. M J. G. and G. C. A. Schuit, J. Catal., 15, 163 (1969).

Lister, A., Third European Symp. Chem. Reaction Eng., pp. 225-235. Pergamon Press, Oxford (1965).

Leco Automatic Sulfur-Determinator, Instruction Manual, Laboratory Equipment Corporation, Michigan, 49085.

Lundberg, W. C., Chem. Eng. Prog., June, 81 (1979).

Madeson, J. J. and R. M. Roberts, Ind. Eng. Chem., 50, 237 (1958).

Maranguzis, J., Ind. Eng. Chem. Proc. Des. Dev., 19, 326 (1980).

Massoth, F. E., Ind. Eng. Chem. Proc. Des. Dev., 6, 200 (1967).

McKinley, J. B., Catalysis, Emmett, ed., 5, 405 (1957).

Mears, D. E., Chem. Eng. Sci., 26, 1361 (1971).

Mears, D. E., Ind. Eng. Chem. Fund., 15, No. 1 (1976).

Mears, D. E., Adv. Chem. Ser., 133, 218 (1974).

Mehta, D. C., Ph.D. Dissertation, Oklahoma State University, Still-
     water, Oklahoma (1978).

Miesserov, K. G., J. Catal., 13, 169 (1969).

Mitchell, P. C. H. and F. Trifiro, J. Catal., 33, 350 (1974).

Montagna, A. A., Y. T. Shah, and J. A. Paraskos, Ind. Eng. Chem. Proc.
     Des. Dev., 16, 152 (1977).

Morooka, S. and C. E. Hamrin, Chem. Eng. Sci., 34, 521 (1979).

Morsi, B. I., N. Midoux and J. C. Charpentier, A.I.Ch.E. Journal,
     24(2), 357 (1978).

Muha, C. M., J. Catal., 38, 470 (1979).

Murphy, J. R. and S. A. Treese, Proc. Am. Pet. Inst. Refin. Dep. Mid-
     year Meeting, 44th, San Francisco, Cal., May 14-17, 1979. Publ.
     by API, 343 (1979).

Micrometrics Instr. Corp., Georgia, Instruction Manual for Model 900/
     910 Series Mercury Penetration Porosimeter, June (1973).

Micrometrics Instr. Corp., Georgia, Instruction Manual for Model 2100D
     Orr Surface Area, Pore Volume Analyzer, September (1974).

Nelson, W. L., Oil Gas Journal, February, 126 (1977).

Newson, E. J., Ind. Eng. Chem. Proc. Des. Dev., 14, 27 (1975).

Owens, P. J. and C. H. Amberg, Adv. Chem. Ser. 33, 182 (1961).

Paraskos, J. A., J. A. Frayer and Y. T. Shah, Ind. Eng. Chem. Proc. Des.
     Dev., 14, 315 (1975).

Perkin Elmer, Norwalk, Conn., Instruction Manual for Model 240 Elemen-
     tal Analyzer.

Qader, S. A., Hydrocarbon Processing, 48 (9), 147 (1969a).

Qader, S. A. and G. R. Hill, Ind. Eng. Chem. Proc. Des. Dev., 8, No.
     4,455 (1969).

Rajagopalan, K. and D. Luss, Ind. Eng. Chem. Process Des. Dev., 18, No.
     3 (1979).

Ramachandran, P. A., M. H. Rashid and R. Huges, Chem. Eng. Sci., 30, 1391 (1975).

Ratnasamy, P., R. P. Mehrotra and A. V. Ramaswamy, J. Catal., 32, 63 (1974).

Richardson, J. T., Ind. Eng. Chem. Fund., 3, 154 (1964).

Richardson, R. L., F. C. Riddick and M. Ishikawa, API Midyear Ref. Meeting, 44th, San Francisco, Calif. (1979).

Ruska Proportioning Pumps - Instructional Manual, Ruska Instrument Corporation, Houston, Texas.

Satchell, D. P., Ph.D. Dissertation, Oklahoma State University, Still-water, Oklahoma (1974).

Satterfield, C. N., A.I.Ch.E. Journal, 21, No. 2, 209 (1976).

Satterfield, C. N. and F. Ozel, A.I.Ch.E. Journal, 19, No. 6, 1259 (1973).

Satterfield, C. N. and P. E. Way, A.I.Ch.E. Journal, 18, No. 2, 305 (1972).

Satterfield, C. N. and J. F. Cocchetto, A.I.Ch.E. Journal, 21, No. 6, 1107 (1975).

Satterfield, C. N., M. M. Modell and J. A. Wilkens, Ind. Eng. Chem. Proc. Des. Dev., 19, 154 (1980).

Schuit, G. C. A. and B. C. Gates, A.I.Ch.E. Journal, 19, No. 3, 417 (1973).

Schwartz, C. E. and J. M. Smith, Ind. Eng. Chem, 45(6), 1209 (1953).

Schwartz, J. G., E. Weger and M. P. Dudukovic, A.I.Ch.E. Journal, 22, No. 5, 953 (1976).

Scott, L. J., R. C. Merrill, B. D. McMunn, S. J. Romelczyk, D. J. Domina, L. Ford, H. D. Terzian and J. F. Jones, "Char Oil Energy Development," E.R.D.A. Interim Report No. 5, FE-1212-T-9,, September (1975).

Shah, Y. T. and G. J. Stiegal, Ind. Eng. Chem. Process Des. Dev., 16, No. 1, 37 (1977).

Shah, Y. T. and J. A. Paraskos, Chem. Eng. Sci., 30, 1169 (1975).

Silverstein, J. and R. Shinnar, Ind. Eng. Chem. Process Des. Dev., 14, No. 2, 127 (1975).

Sivasubramanian, R. and B. L. Crynes, Ind. Eng. Chem. Proc. Res. Dev., 19, 456 (1980).

Sivasubramanian, R., Ph.D. Dissertation, Oklahoma State University, Stillwater, Oklahoma (1977).

Smith, J. M. and P. A. L. Ramachandran, Chem. Eng. Sci., 34, 75 (1979).

Smith, J. M., M. Herskowitz and R. G. Carbonnell, A.I.Ch.E. Journal, 25, No. 2, 272 (1979).

Smith, J. M. and P. A. Ramachandran, A.I.Ch.E. Journal, 25, No. 3, 539 (1979).

Sonnemans, J., N. J. Neyens and P. Mars, J. Catal., 34, 230 (1974).

Soni, D. S., M. S. Thesis, Oklahoma State University, Stillwater, Oklahoma (1977).

Sooter, M. C., Ph.D. Dissertation, Oklahoma State University, Stillwater, Oklahoma (1974).

Stanulonis, J. J., B. C. Gates and J. H. Olson, A.I.Ch.E. Journal, 22, No. 3, 576 (1976).

Sylvester, D. N. and P. Pitayagulsarn, Can. J. Chem., 52, 539 (1974).

Sylvester, D. N. and P. Pitayagulsarn, A.I.Ch.E. Journal, 19, No. 3, 640 (1973).

Tantarov, M. A., R. A. Faskhvtdinov, M. E. Levinter and I. G. Akhmetov, Int. Chem. Eng., 12, No. 1, 85 (1972).

Tautster, S. J., J. Catal., 26, 487 (1972)

Tung, S. I. and E. McIninoh, J. Catal., 3, 229 (1964).

U. S. Department of Energy, Quarterly Report, Coal Liquefaction, April (1980).

Van Deemter, J. J., Third European Symposium on Chem. React. Eng., p. 215, Pergamon Press, Oxford (1964).

Van der Aalst, M. J. M., V. H. J. DeBeer, J. Catal., 49, No. 3, 247 (1977).

Van Zoonen, D. and C. T. Douwes, J. Pet., 49, 383 (1963).

Voorhoeve, R. J. H. and J. C. M. Stuiver, J. Catal., 23, 243 (1971).

Wakao, N. and J. M. Smith, Chem. Eng. Sci., 17, 825 (1962).

Wan, K. T., M. S. Thesis, Oklahoma State University, Stillwater, Oklahoma (1974).

Well, J. W., M. S. Thesis, Oklahoma State University, Stillwater, Oklahoma (1977).

Wentrcek, P. R. and H. J. Wise, J. Catal., $\underline{51}$, 80 (1978).

White, P. J., J. F. Jones and R. T. Eddinger, Hydrocarbon Processing, $\underline{47}$, No. 12, 97 (1968).

APPENDIX A

EXPERIMENTAL EQUIPMENT

A schematic diagram of the experimental setup employed in this study is given in Figure 19. Hydrogen enters the top of the reactor through valve 5. A Ruska feed pump 19 feeds oil at a predetermined rate to the top of the reactor. The oil and the hydrogen gas flow concurrently through the reactor packed with catalyst. The hydrogen pressure is maintained by a pressure regulator 41. Hydrogen flow rate is adjusted by micrometer valves 9 and 11, and measured with the help of a bubble flowmeter installed on the off-gas line. The oil and gas coming out of the reactor are separated in sample bombs 34 and 35. Gases leave the system through exit valves 8, 9, 10, and 11. Sample bomb 35 can be isolated from the system by closing valves 7 and 12. Gases present in sample bomb 35 can be released through valves 8 and 9. Liquid present in the bomb can be purged with nitrogen gas entering through valves 16 and 14 and exiting through valves 8 and 9. The liquid sample can be collected at atmospheric conditions, without disturbing normal operation. The pressure of the system is monitored on a Heise gauge 44; temperature along the length of the catalyst bed is measured by means of a thermocouple and indicated on the digital readout. A detailed description of the main components of the system is given below. A complete listing of the equipment items with relevant information is given in Table XI.

Reactor

The reactor consisted of a 20-inch (50.4 cm) long, 1/2 inch (1.27 cm) O.D., and 0.035 inches (0.089 cm) thick stainless steel tube, fitted with a half-inch swagelok cross and union at the top and bottom, respectively. The effective reactor length was 18 inches. Figure

TABLE XI

LIST OF EXPERIMENTAL EQUIPMENT

Tubing	1/8-inch OD, 316 stainless steel 1/4-inch OD, 316 stainless steel 1/2-inch OD, 316 stainless steel
Reactor 26	1/2-inch OD, 0.035-inch thickness, 316 stainless steel tubing, 20 inches in length
Thermowell	1/8-inch OD, 316 stainless steel tubing, 30 inches with one end welded
Temperature controller 45	Hewlett-Packard temperature programmer, Model 240
Powerstats	Input 120 volts, output 0-140 volts, 10 amperes, 1.4 KVA Superior Electric type 116
Insulation material	Fiberglass, McMaster-Carr
Temperature indicator 46	Doric Scientific DS-350, K-type
Thermocouple 46	Iron-Constantan, 0.04-inch OD, 304 stainless steel sheath, grounded sensor tip, 36-inch Conax, J-type
Thermocouple 27, 47	Iron-Constantan, 1/16-inch, 304 stainless steel sheath, grounded sensor tip, 12-inch Omega, J-type
Pressure gauge 44	Heise-Bourdan tube gauge, max pressure, 3000 psig
Pressure gauge 18	Crosby pressure gauge, max pressure, 3000 psig
Pressure gauge 20, 25, 36	Aschcroff pressure gauge, max pressure, 3000 psig
Sample bombs 34, 36	300 C.C., 1800 psig, 304 stainless steel, Matheson Model 6-645-232
Feed tank 17	8.5-inch OD, 7.5 inches in height, stainless steel tank
Surge bomb 23	2250 C.C, 1800 psig pressure, 304 stainless steel Matheson Model 806
Pumps 19	Ruska positive displacement pump, 500 C.C. barrel capacity, feed rates 2-240 cc/hour, 4000 psig max, Model #2242 BI

OR

TABLE XI (Continued)

	Ruska positive displacement pump, 1000 C.C. barrel capacity, feed rates 2.5-260 cc/hour, 12,000 psig max, Model 2236 SII
Pressure regulator	Whitey Model 94, Mity-Mite Type, internally loaded, inlet pressure 5000 psig, outlet pressure 3000 psig, 1/4-inch inlet and outlet connections
Rupture disks 21, 22	1/4-inch, bursting pressure 1800 and 2300 psi at $72^{O}F$. Autoclave Engineering
Valve 4	1/2-inch, extended stem type, Autoclave Engineering Model 6V71 UL8
Valves 2, 3	1/4-inch, gate valve, 316 stainless steel, Whitey Model 6VS4
Valves 1, 48, 7, 14, 15, 8, 10	1/4-inch, gate valve, 316 stainless steel, Autoclave Engineering Model 10V-4071
Valves 9, 11, 16	1/4-inch, 316 stainless steel micro metering valves, Whitey Model 22 RS4
Valve 5	1/4-inch, White Model 3TS4
Valve 13	1/8-inch, Whitey Model ORS2
Valve 6	1/8-inch, 316 stainless steel, Autoclave Engineering Model 10V 2071
Valve 42	Quarter-turn valve, White 43S4
Valve 50	Shutoff valve, Whitey PS 490
Valve 30, 31	1/8-inch, H.I.P. Model 15-11EF2
Hydrogen detector 39	Combustible gas alarm, MSA Instrument Corporation, Model I-501
Hydrogen sulfide detector	Sierra Labs Inc. concentration range, 0-50 ppm Model 10HS
Heating tape	Brisket flexible heating tape, 115 volts, 576 watts, 1-inch wide, 72 inches long
Multiple selector 24	12 points, Omega Engineering, Inc.

TABLE XI (Continued)

Felt insulation	Ceramic fiber insulation, max. 2300°F, Refractory Products Company
Beaded heaters	115 volt, 400 and 800 watts, 12 and 24 feet length, max. 2000°F, Marsh beaded heaters
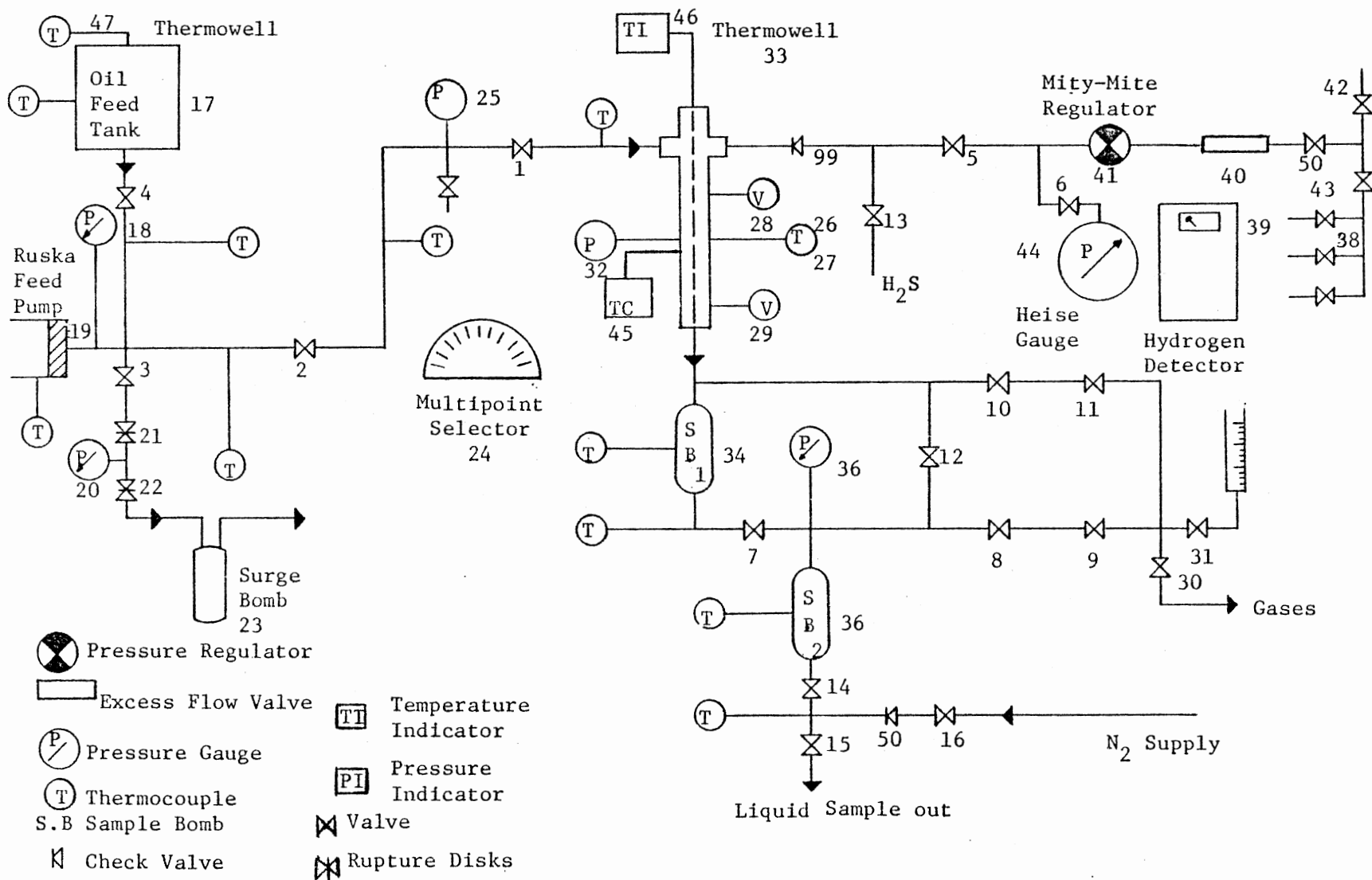
Figure 19. Numbered Experimental System

20 shows the reactor details. A 1/8-inch O.D. stainless teel tubing with one end shut was used as a thermowell. The thermowell was secured in the middle of the reactor by means of a 1/4-inch to 1/8-inch reducing union which was drilled for easy sliding on the thermowell tubing. Stainless steel screens of 50 mesh size were used to hold the catalyst and inerts in the reactor. A 1/2-inch swagelok cross was connected to the top of the reactor and two 1/2-inch to 1/4-inch reducers were connected to the two sides. The bottom of the reactor was fitted with a 1/2-inch to 1/4-inch reducer to enable it to be connected to the sample bomb.

Reactor Heating System

The heaters consisted of three specially designed solid aluminum blocks with a 1/2-inch diameter hole in the center. The blocks were split in the middle and hinged at one end for easy mounting and removal. The blocks were grooved with 3/8-inch wide and 5/8-inch deep slots, and beaded heaters were placed in these slots. The blocks were of different lengths, as shown in Table XII.

The top and bottom heaters were controlled by powerstats. The middle block--the longest one--was controlled by a Hewlett-Packard temperature programmer. The chromel-alumel control thermocouple was placed in a small hole in the middle aluminum block. An iron-constantan thermocouple was placed in a 1-inch deep hole located halfway down the middle heating block, and was connected to the temperature indicator through a multipoint selector for easy temperature monitoring. The top and bottom heaters were used to counter end-effect heat losses. Control with powerstats was maintained by balancing heat input with heat loss to achieve the required temperature
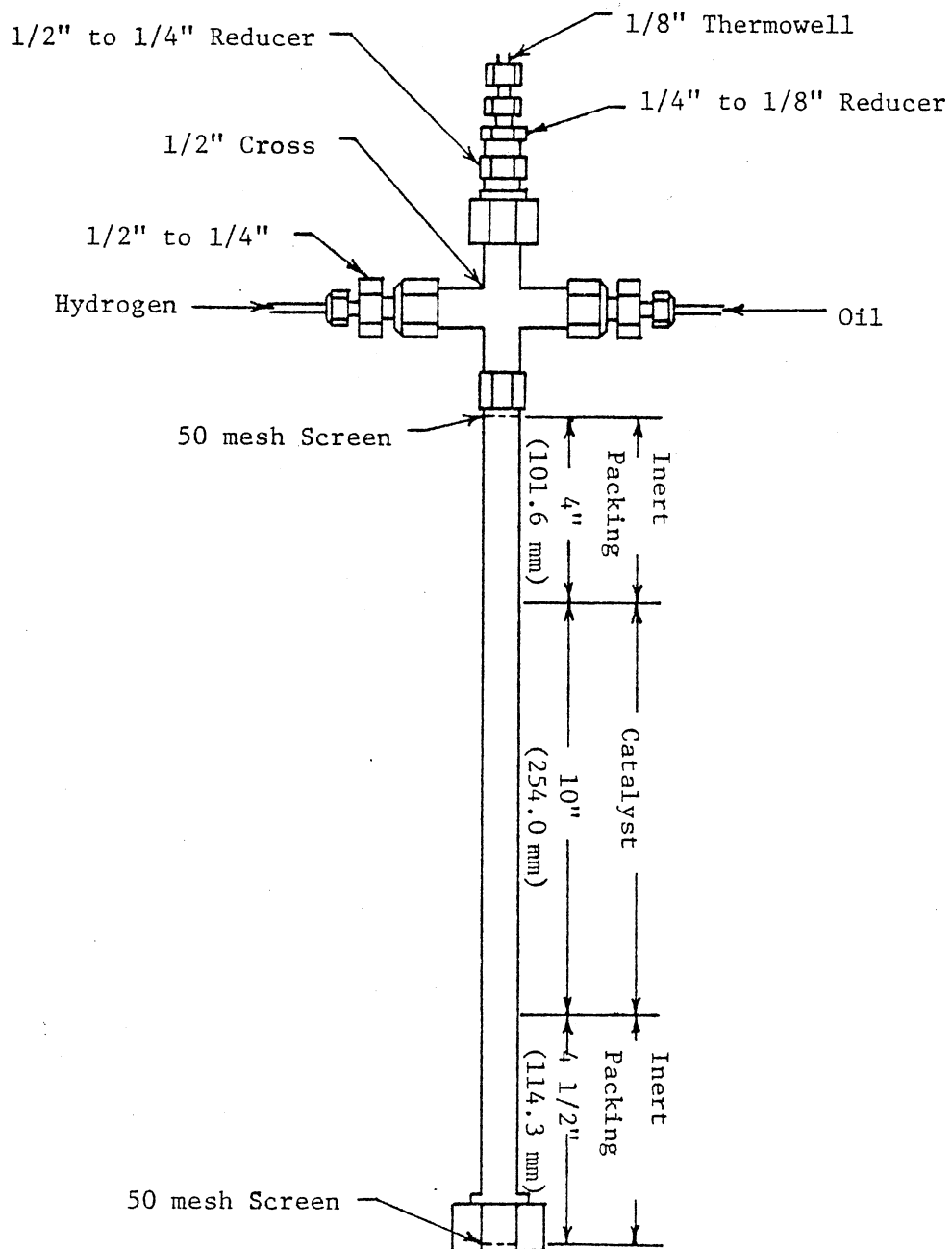
Figure 20. Reactor Design

TABLE XII

REACTOR HEATER CONFIGURATION

Block Number from Reactor Inlet	Block Height in Inches	Mode of Control
I	4	Powerstat
II	10	Hewlett-Packard Temperature Programmer
III	4	Powerstat

profile.

The aluminum blocks were held in place by metal strips. Felt fabric in the form of rectangular boxes, split in the middle, were used for insulating the reactor. Fiberglass insultation was wrapped around the reactor and held in place by means of asbestos tape. Electrical connections for the heaters were made through breaks in the insulation. Care was taken to carefully pack any gaps with fiberglass.

Temperature Measurement

The reactor temperature profile was measured with a Conax J-type grounded tip, iron constantan thermocouple. This was done by first placing the temperature selector switch at the desired point and then sliding the thermocouple along the thermowell. The response was noted on the Doric DS-350 digital readout. A callibration chart was prepared to convert the K-type digital output of the Doric into the actual J-type readout. This was necessitated due to the nonavailability of K-type thermocouples in the size range required for the present experimental system. In the future, matched thermocouple and temperature readout should be used. The thermocouples in the oil feed system, reactor and separation system were connected to a multipoint selector 24. This selector had the capability of accepting the output of up to twelve thermocouples, selecting one of them and feeding the signal into a DS-350, Doric digital temperature readout.

Pressure and Flow Control

The system pressure was monitored on a 0-3000 psig Heise gauge 44. The pressure indicated by this was taken as the nominal reactor pressure.

The inlet pressure to the reactor was controlled by using an internally loaded Mitey-Mite pressure regulator 41. The pressure upstream of the pressure regulator was maintained by the manifold regulator 38. A pressure differential of 80-100 psig was maintained between the manifold pressure and the outlet pressure of the regulator.

The gaseous flowrate was maintained by means of four valves--8, 9, 10 and 11. Valves 8 and 10 were Vee-tip type valves designed to take a major portion of the pressure drop. Micro-metering valves 9 and 11 were used for fine control of the gas flow. The gas flow was monitored downstream from the control valves by means of a 0-100 ml bubble flow meter 37. In order to avoid gases always flowing through the flow meter, a bypass line was connected to the bubble meter, through valves 30 and 31.

Oil and Hydrogen Feed Systems

The oil feed system consisted of a stainless steel feed tank 17 and a Ruska positive displacement pump 19. The oil feed lines were all wrapped with flexible heating tape and insulated with fiberglass to preheat the heavier oils. The oil cylinder of the Ruska pump and the feed tank were heated and insulated in a similar manner. The temperature of the oil lines was controlled manually by means of powerstats; care was taken not to overheat any section. The temperature along the whole length of the feed lines was monitored by means of thermocouples connected to the multipoint selector 24, which could be used to select any one of the various points for display on the Doric digital readout. Rupture disks 2 and 22, rated at 1800 and 2300 psig, respectively, were installed on the feedline to prevent damge to the

pump in case of oil-lines becoming clogged. The rupture disks were installed closest to the pump exit and were connected to a 2400-ml sample bomb by means of a 1/2-inch pipe. A pressure gauge 20 was connected between the two rupture disks. In case of a rupture in the first disk, the pressure would be indicated on the pressure gauge 20. The pressure in the oil lines was monitored on three pressure gauges 18, 25 and 36.

The hydrogen was fed directly from the gas bottles through a manifold, which allowed the changing of hydrogen bottles without interrupting the run. An excess flow valve 40 was provided close to the manifold system, which could shut off the hydrogen gas in case of excessive flow such as a line rupture. A quarter turn valve 50 was installed upstream to the excess flow valve 40. This provided for rapid manual cutoff of hydrogen supply to the system in case of an emergency.

Sampling System

The sampling system was designed to obtain samples without causing an interruption of the normal operation. The system consisted of two sample bombs 34 and 35, each of 300 cc capacity, rated at 1800 psig and placed in series. Figure 21 shows the sample bomb design. The bottom end of the reactor was connected to the sample bomb 34, using a 1/4-inch stainless steel tube. The entry of the 1/4-inch stainless steel tube into the bomb was made possible by drilling a hole in the 1/2-inch to 1/4-inch swagelok reducer. The seal on the tube was made by a swagelok fitting on the 1/4-inch tube. Vapor and liquid separated within the bomb, and the liquid collected and settled at the bottom.

Hydrogen + Oil

Hydrogen

Oil
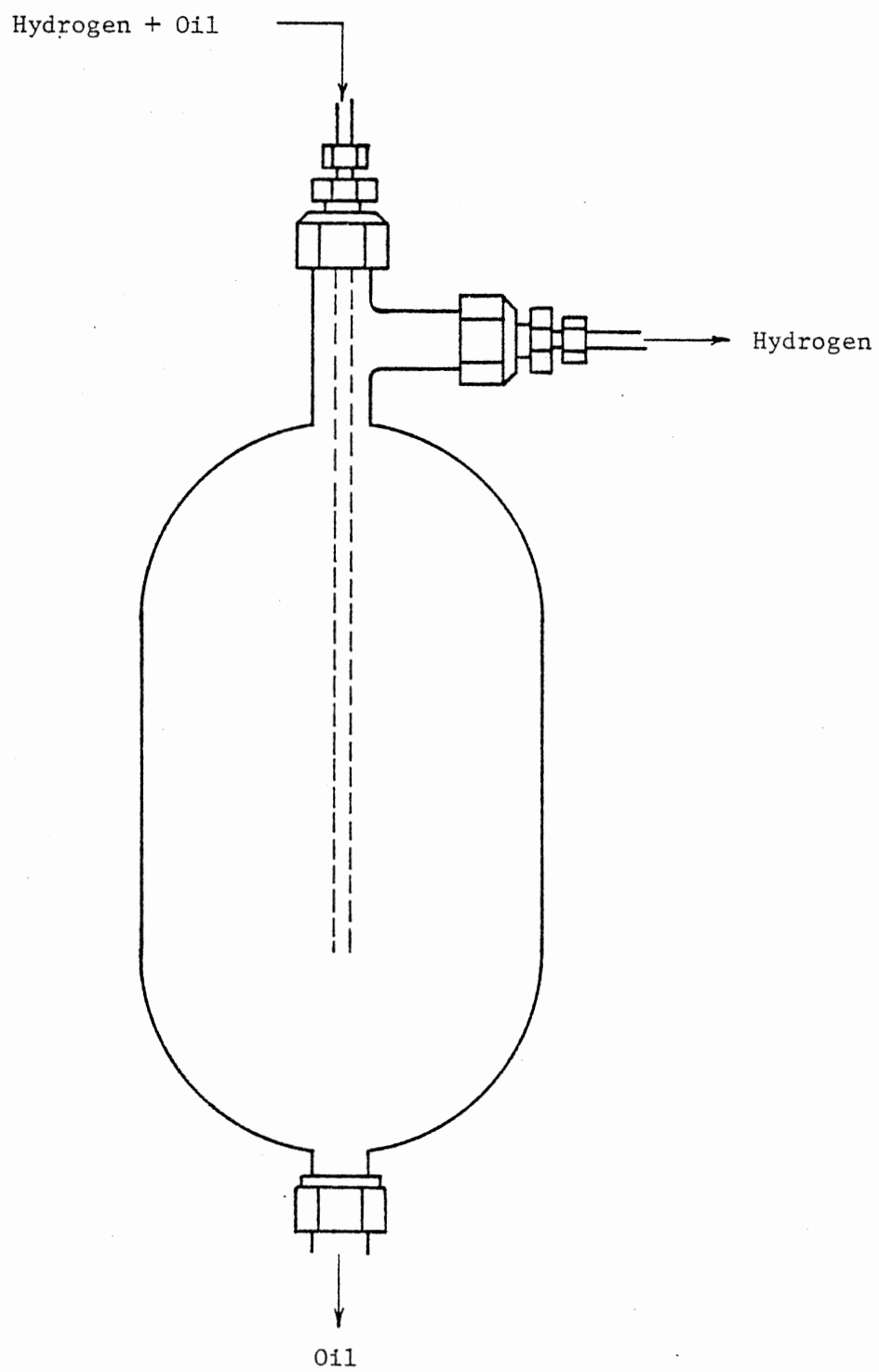
Figure 21. Sample Bomb

Sample bomb 35 was placed in series with sample bomb 34. The liquid flowed down from bomb 34 into bomb 35. Valve 7 was placed between the two bombs in order to isolate one from the other. A Bourdon type pressure gauge 36 monitored the pressure in the second

Both bombs were wrapped with flexible heating tape, connected to powerstats for temperature control and insulated with fiberglass. Thermocouples were connected to the multipoint selector 24 to monitor the temperature in the sampling system.

Gas Detectors

A combustible gas detector, MSA Model 501, was installed with two detector heads located over the hydrogen bottles. A red light would come on in case the hydrogen concentration in the room reached 50% of the lower explosive limit. The system was checked before conducting an experiment.

A portable hydrogen sulfide detector was kept handy during the catalyst presulfidation and while taking the liquid sample. It provided a digital output of the instantaneous, average and maximum hydrogen sulfide concentration during an interval. This detector was set to sound an alarm at 17-20 ppm concentration of hydrogen sulfide; the alarm frequency increased with the increase in concentration.

Inert Gas Purging Facility

The liquid product samples were purged with nitrogen gas in the second sample bomb 34 to remove the ammonia and hydrogen sulfide dissolved in the liquid sample. Nitrogen was supplied to the sample bomb 34 directly from the supply cylinder. Nitrogen entered bomb 35 through

valves 16 and 14, and escaped to the atmosphere through valves 8, 9, and 30. Check valve 50, was provided to avoid flow of the product liquid sample into the nitrogen feedline.

Experimental Procedure

A stepwise description of the experimental procedure follows. The sequence of the steps involved in the actual experiment are the same as those given here.

Catalyst Preparation and Loading

Two commercially available catalysts, HDN-30 and Ketjenfine-124, were used in the present study. Both catalysts were 1/16-inch extrudes. The reactor was packed at the two ends with 10-20 mesh size porcelain boiling chips. The catalyst was packed in the middle to minimize the end effects. The reactor was packed as follows:

1) A fifty-mesh size screen was wedged between the bottom of the reactor and 1/2-inch union.

2) The thermowell was held centrally inside the reactor.

3) The 10-20 mesh size porcelain boiling chips were poured into the reactor while vigorously tapping the reactor for uniform packing around the thermowell. For every run, the bottom of the reactor was packed with fresh porcelain boiling chips to a height of 4.5 inches (12.7 cm).

4) The catalyst was next poured into the reactor by following the procedure described above. For every experimental run the reactor was packed with fresh catalyst to a height of 10 inches (25.4 cm).

5) The 10-20 mesh size porcelain boiling chips were next poured

into the reactor, making sure to distribute them evenly by tapping the reactor vigorously. For every run, the top of the reactor was packed with fresh porcelain to a height of four inches. A 50-mesh screen with a hole in the middle for the thermowell was slipped over the top of the porcelain chips.

6) The packed reactor was next fitted with a 1/2-inch cross, as shown in Figure 20. The thermowell was secured by means of a 1/8-inch swagelok fitting.

7) The packed reactor was secured into the system by connecting a check valve, 49 and a 1/4-inch to 1/8-inch reducer connected to the hydrogen gasline. The oil line was connected to the other end through a 1/2-inch to 1/4 inch reducer.

8) The system was pressure tested before installing the heating blocks. Each fitting in the entire system was checked for leaks by gradually pressurizing the system with nitrogen gas. The system pressure was raised to 1600 psig--100 psig higher than the operating pressure. Snoop leak detector solution was used for detecting any leaks. The system was kept under pressure for one hour. In case the pressure drop was greater than 20 psig, the system was depressurized and all suspected fittings tightened. Silver goop was used on all fittings to prevent seizing.

9) The beaded heating wires were properly positioned into the grooves. The wires were tested for short circuit by a volt-ohm meter. One wire of the volt-ohm meter was connected to the aluminum block and the other to the heating wire. In case any resistance was detected, the wires were reinstalled, making sure the metal wires were completely insulated from the aluminum block by means of the porcelain beads. The

heating blocks were installed around the reactor and secured in place by means of metal strips. The heating wires were connected to the controllers and electrical connections insulated by glass tape. The thermocouples were connected to the middle heating block and the reactor insulated by felt and glass wool insulation.

Catalyst Activation

This consisted of two steps--calcination and sulfiding--as described below.

Calcination

This step was meant to remove adsorbed water from the catalyst. The reactor was gradually heated to $900^{\circ}F$ ($482^{\circ}C$) at a rate of $3^{\circ}F/$ min and maintained at this temperature for one hour. Nitrogen gas at the rate of 200 cc/min was passed through the reactor. The temperature profile was recorded every half hour. The heaters were next turned off and the temperature allowed to fall to about $500^{\circ}F$. The heaters were turned on and the temperature was stabilized at $500^{\circ}F$ ($260^{\circ}C$), while maintaining the nitrogen gas flow rate at 200 cc/min. The system was ready for sulfidation after 12 hours of calcination at $500^{\circ}F$.

Sulfidation

The nitrogen supply to the system was cut off after 12 hours. All of the valves except valves 5, 10, 11, and 30 were closed. The H_2S supply valve, 13, was opened and a mixture of 5.14% H_2S in H_2 was passed through the reactor at a pressure of 0-4 psig, while maintaining the temperature constant at $500^{\circ}F$ ($260^{\circ}C$). The H_2S-H_2 mixture gas flow rate

was maintained by adjusting micrometer valve 11 at 200 cc/min for a period of 90 minutes. The Heise Pressure gauge and the Mity-Mite pressure regulator were eliminated from the system during sulfidation by closing valve 49. The system was flushed with nitrogen gas for 20 minutes at a pressure of 250 psig and a gas flow rate of 20 cc/min. A summary of the valve positioning during catalyst activation is given in Table XII.

TABLE XIII

SUMMARY OF VALVE POSITIONING DURING THE CATALYST ACTIVATION

Valve Number	Calcination Position*	Sulfidation Position*
6	open	closed
5	open	closed
50	open	closed
43	open	closed
10	open	open
11	open	open
30	open	open
31	open**	open**
7	closed	closed
13	closed	open

*All valves kept closed unless specified.

**Opened only when measuring gas flowrate.

Startup Procedure

After activation of the catalyst, the heaters were turned on and the temperature stabilized at the operating value. In the meantime, feed tank 17 was filled with oil and Ruska pump feed rate set at the operating liquid flow rate. In the present study, no heating of the oil lines was necessary because of the light coal liquid used. Nitrogen gas flow rate of 20 cc/min at 200 psig was maintained. The Ruska pump 19 was filled with oil by closing valves 2 and 3 and opening valve 4. The Ruska pump mode 2236 WII was equipped with a rapid traverse motor for easy filling of the cylinder. Ruska pump Model 2242 BI was filled manually, keeping the feed clutch in neutral position. Two Ruska pumps were used during this study. Pump Model 2236 WII broke down after two experimental runs, necessitating the use of Ruska pump Model 2242 BI.

When the temperature inside the reactor was within $10^\circ F$ ($5.6^\circ C$) of the desired value, the nitrogen supply was cut off. The system was pressurized with hydrogen gas to the desired pressure by gently turning the Matheson pressure regulator (connected to hydrogen manifold, 38) in clockwise direction and monitoring the pressure increase in the Heise gauge 44. In case of excessive flow, the excess valve, 40, would automatically shut off; the flow was restored by closing the shut-off valves 50 and 43, and opening valve 42 to depressurize the hydrogen gas line. By opening valve 50, normal flow would be restored.

Ruska pump 19 was pressurized manually with valves 1 and 3 closed, to the desired pressure, while carefully monitoring the pressure on the pressure gauge 18. Valve 1 was opened and the pump traversed through 20 cc manually before being turned on. This operation took approximately

2-3 minutes. This was done to make sure that the hydrogen and oil hit the catalyst at approximately the same time. Valves 3, 8, 9, 10 and 11 were opened and hydrogen gas flow rate adjusted to the desired value.

Normal Operation

The system was considered to be operating normally when the pressure and temperature had stabilized. A maximum variation of $\pm$ 20 psig was considered normal; the pressure fluctuations were negligible throughout all runs. A temperature variation of $\pm$ $3^{o}F$ ($1.5^{o}C$) along the axis was considered normal before the oil hit the catalyst. During normal operation, the temperature profile, pressure gauge readings, setting of temperature programmer and controller, gas flow rate, pump reading, and hydrogen gas bottle pressure were recorded every two hours but were read every hour. The temperature profile was recorded from the bottom to the top of the catalyst bed at 1-inch intervals.

During normal operation, hydrogen entered the top of the reactor through valve 5; oil entered through valve 1 and flowed concurrently through the packed bed. The unreacted hydrogen, product oil and other gaseous products flowed into the sample bomb 35 which was placed immediately below the reactor. Here the gases and liquids were separated and the liquid and some of the gases flowed into the sample bomb 36 through valve 7. The gases in sample bomb 35 escaped through valves 8 and 9, and were joined by gases escaping from sample bomb 34, coming out of valves 10 and 11. Throughout the normal operation, sample bomb connecting valve 12 was kept closed. The gases were metered with a 0-100 cc bubble meter, placed inside the fume hood. The hydrogen gas flow rate was fixed at the desired value by adjusting the micrometer

valves 9 and 11. The gases were allowed into the bubble flowmeter
through valve 31 during the routine 2-hour check for the rest of the
time valve 31 was kept closed and the gases vented to the atmosphere
through valve 30. A summary of the valve positions during normal
operation is given in Table XIV.

TABLE XIV

VALVE POSITION SUMMARY DURING NORMAL OPERATION

Valve Number	Position	Valve Number	Position
5	open	14	close
7	open	15	close
8	open (1/4 turn)	16	close
9	open	30	open
10	open (1/4 turn)	31*	close
11	open	1	open
12	close	2	open
13	close	3	open

*Opened when measuring hydrogen gas flow rate.

Sampling Procedure

The system was designed with the objective of removing the
liquid product sample without disturbing the normal operation. The

second sample bomb, 35, was isolated from the system by closing valves 7 and 12. Sample bomb 35 was next depressurized by opening micrometer valve 9 slightly. The pressure of sample bomb 35 was monitored on pressure gauge 36. When the pressure in the bomb was released completely, the liquid was purged with nitrogen at 200 psig for 15-20 minutes. Nitrogen gas entered the bottom of bomb 35 through valves 16, 50 and 15, and left through valves 8, 9 and 30. After 15-20 minutes of purging, the nitrogen gas supply was cut off and bomb 35 allowed to depressurize to a pressure of 50 psig. Valve 8 was quickly closed. Valves 14 and 15 were closed and opened alternately to collect the liquid sample in sampling bottles. Valves 14 and 15 were closed when the pressure gauge 36 indicated a pressure drop.

The sample bomb was repressurized by nitrogen gas at 1500 psig. In case the pressure indicated by pressure gauge 36 was lower than the system pressure, micrometer valve 12 was opened until the pressure equalized. Pressure bomb 35 was reconnected to the system by carefully opening valve 7. The hydrogen flow rate was adjusted by opening valves 8 and 9. A summary of the valve positions is given in Table XV.

Shut-down Procedure

The pump was switched off and valves 1, 2 and 7 were closed. The heaters were turned off and the reactor allowed to cool. The hydrogen gas supply was cut off after 15 minutes and the pump depressurized. The liquid sample was collected during this period after purging with

TABLE XV

SUMMARY OF VALVE POSITIONS DURING SAMPLING
OPERATION AND PUMP REFILLING

Valve Number	Position	Valve Number	Position
A) Nitrogen Purging:			
16	open	15	close
7	close	8	open
12	close	9	open
14	open	30	open
B) Liquid Sample Collection:			
16	close	7	close
14	open (partially)	8	close
15	open (partially)	10 & 11	open
C) Sample Bomb 35, Repressurizing:			
16	open	7	close
15	close	12	(momentarily) open
14	open	8	close
D) Pump 19, Refilling:			
4	open	1	close
3	close		
2	close		

nitrogen gas. The reactor was allowed to cool down to room temperature, insulation was removed, the heating blocks were taken out, and the reactor was disconnected from the system. The reactor tube was labelled for future reference.

APPENDIX B

EXPERIMENTAL PROCEDURE

The experimental procedures for the various analytical work are described briefly in this Appendix. A complete list of all of the chemicals and gases used are given in Table XVI.

Sulfur Analysis

An automatic sulfur analysis system, purchased from Leco Laboratory Equipment Corporation, was used to determine sulfur content of the samples. The procedure for sulfur analysis, given below, is based on that given in the Leco Bulletin. The following steps are followed:

1) Solution Preparation: Three solutions, i.e., starch, HCl and KlO_3 are needed for the sulfur analysis. The starch solution is prepared by adding two grams of arrowroot starch to 50 cc of distilled water. This mixture is then added to 150 cc of boiling distilled water; this mixture is allowed to boil for one or two minutes and then allowed to cool to room temperature. Six grams of KI are then added to the starch solution, and stirred vigorously until all of the KI is dissolved. Fresh solution is prepared daily.

The HCl solution is prepared by diluting 15 cc of concentrated HCl solution with one liter of distilled water. The solution can be prepared in large quantities and kept for a period of one month.

Potassium iodate solution is prepared by dissolving 0.444 grams of KlO_3 to prepare a one-liter solution in distilled water. This solution can also be made in large quantities and kept for a period of one month.

2) Machine Warmup: The Leco induction furnace and titrator are turned on and allowed to warm up for 30 minutes. The titrant receiver is filled with HCl solution to a predetermined level. After 30 minutes of warmup period, oxygen is allowed to bubble through the HCl solution

TABLE XVI

LIST OF GASES AND CHEMICALS USED

Hydrogen	purity, 99.5%, 2300 psig (Sooner Supplies)
Nitrogen	purity, 99.5%, 2300 psig (Sooner Supplies)
Hydrogen sulfide	5.14% mixture in H_2, 2000 psig (Matheson)

Sulfur Analysis

Oxygen	purity, 99.5%, 2300 psig (Sooner Supplies)
Magnesium oxide	analytical grade, Fischer Scientific Company
Potassium iodate	analytical grade, Fischer Scientific Company
Potassium iodide	analytical grade, Fischer Scientific Company
Concentrated HCl solution	Fischer Scientific Company
Sodium azide	Fischer Scientific Company
Iron chips	Leco Corporation, part #501-007
Tin accelerator	Leco Corporation, part #501-076
Crucible	Leco Corporation, part #528-036
Crucible porous lid	Leco Corporation, part #528-012
Alumina	Alcoa Chemicals, supplied by Sargent Welch Company

Nitrogen Analysis

Oxygen	high purity (99.99%), 2700 psig (Linde)
Helium	chromatographic (99.995%), 2500 psig (Linde)
Aluminum capsules	Perkin Elmer, part #009-0709
Platinum gauze	80 mesh, Perkin Elmer, part #240-1147
Silver gauze	40 mesh, Perkin Elmer, part #240-0092
Magnesium perchlorate	reagent grade, Perkin Elmer, part #240-1119
Silver vanadate	reagent, Perkin Elmer, part #240-1117
Tungstic anhydride	Perkin Elmer, part #240-1238
Colorcarb	Perkin Elmer, part #240-0115
Copper	60-100 mesh, Perkin Elmer, part #240-0017
Silver oxide-silver tungstate on chromium	reagent, Perkins Elmer, part #240-0113
Silver tungstate-magnesium oxide	Perkin Elmer, part #240-1344
Cyclohexanone-2-4-dinitrophenyl-hydrazone	B.D.H. Chemicals
Quartz tube (9mm 1.D x 11.2 mm O.D.)	Thermal American Quartz

in the titrant receiver for 15 minutes. A resistance heating wire wrapped around the glass tube connecting the titrator and the induction furnace is also turned on.

3) <u>Sample Preparation</u>: The sample for analysis is prepared in the following manner:

(a) Add 0.282 ± 0.005 gm MgO to a crucible supplied by the Leco Corporation.

(b) Add 0.1 ± 0.005 gm sample oil on the MgO layer in the center of the crucible. For liquid samples where blowouts occur, smaller quantities of oil are recommended.

(c) Add 0.282 ± 0.005 gm MgO to cover the oil in the crucible.

(d) Add 1.5 ± 0.005 gm iron chips on top of the MgO layer.

(e) Add 0.77 ± 0.005 gm tin accelerator on top of the iron chips.

(f) Add two scoops of alumina (Al_2O_3) on top of the tin accelerator.

The crucible is then covered with a porous lid supplied by the Leco Corporation. The igniter switch on the furnace is turned on.

4) <u>Setting the End Point</u>: This is done to establish reference color for the titrator. The titration vessel is filled with HCl solution up to the predetermined level and 2 cc of the starch solution is added. Oxygen is allowed to bubble through the vessel at a rate of 1.1 to 1.2 liters per minute. The end point control knob is turned to the extreme left position, and the double arrow switch to the end point position. The end point control switch is then turned clockwise slowly until the color of the solution in the titration vessel turns medium

blue by automatic addition of $K10_3$. The set point control knob is set at this position and not disturbed until the necessity to do so arises.

5) <u>Blank Determination</u>: The samples were prepared exactly according to the procedure outlined in step 3, except that no oil was added. The blank determination takes care of the sulfur present in the crucible and the other chemicals used in the analysis. This reading is deducted from the buret reading obtained on analyzing a sample.

The titration vessel is filled with HCl solution to the premarked level. Two cc of starch solution is added, and oxygen is allowed to bubble through the mixture at a rate of 1.2 liters/min. The double throw switch is put at the end point. No more addition of $K10_3$ solution and a medium blue color of the solution in the titration receiver establishes the end point. The titrator double throw switch is now turned to the neutral position. The oxygen supply to the titration receiver is cut off and the buret is refilled with $K10_3$ solution. About 0.7 grams of sodium azide (two scoops) are added to the mixture in the titration receiver . This avoids the interference by nitrogen oxides and chlorine. The prepared crucible is placed in the combustion tube and combusted in an atmosphere of pure oxygen. The double throw switch is turned to the titrate position. The unreacted oxygen together with the gaseous combusion products bubbles through the titration receiver. The titration is assumed over when no more addition of $K10_3$ takes place from the buret.

6) <u>Determination of Furnace Factor</u>: The calibration factor is determined as follows:

$$\text{furnace factor} = F = \frac{(\text{weight of sample})(\% \text{ S content})}{(\text{buret reading} - \text{blank reading})}$$

A coal liquid of known sulfur content is used for calculating the furnace factor. In this study, Rasyn coal-derived liquid with 0.54 wt % sulfur was used as the reference liquid.

7) <u>Chemistry of Analysis</u>: The following reactions are involved in the determination of the end point:

$$KIO_3 + 5KI + 6HCl \rightarrow 3I_2 + 6KCl + H_2O$$

$$I_2 + starch \rightarrow blue\ complex$$
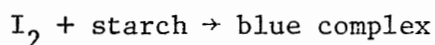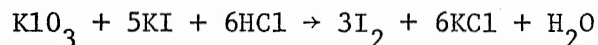
The gaseous products pass through the titration vessel and the SO_2 tends to decolorize the solution by undergoing the following reaction:

$$SO_2 + I_2 + H_2O \rightarrow H_2SO_4 + 2HI$$
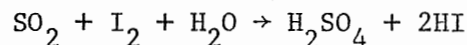
To maintain the color at the end point setting, an amount of KIO_3 is added from the buret. When no more addition takes place, tritration is considered to be over.

8) <u>Analysis of an Unknown Sample</u>: The sample is prepared according to step 3 and is run in the same way as for determination of the furnace factor. The weight percent sulfur in the sample is calculated as follows:

$$weight\ percent\ sulfur = F\ \frac{(buret\ reading\ -\ blank\ reading)}{Weight\ of\ sample}$$

A sample is normally analyzed twice or until consistent readings are obtained.

Nitrogen and Hydrogen Analysis

A brief description of the working of the nitrogen analysis system used in this study is given in Chapter III. The stepwise procedure is as follows:

1) <u>Calibration</u>: The instrument is calibrated before the samples are analyzed. First, blank values for both nitrogen and hydrogen are found by analyzing an empty platinum sample boat. The empty boat is placed in combustion ladle and inserted into the combustion tube. The analysis is started by pressing the start switch of the analyzer and allowed to go through complete analysis cycle. The blank values are calculated from the recorder output as follows:

$$\text{Nitrogen:} \quad (\text{Blank})_N = (\text{Read})_N - (\text{Zero})_N$$

$$\text{Hydrogen:} \quad (\text{Blank})_H = (\text{Read})_H - (\text{Zero})_H$$

The calibration factors for nitrogen and hydrogen are determined once the nitrogen and hydrogen blanks have been found. This is done by analyzing a sample of known nitrogen and hydrogen content. In this study, the calibration standard is Cyclohexanone-2-4-dinitrophenhyl-hydrazone $(C_6H_{10}NNHC_6H_3(NO_2)_2)$. This chemical compound has a molecular weight of 278.27 and nitrogen, hydrogen and carbon content of 20.14, 5.07, and 51.79 wt %, respectively.

Two to three mg sample of Cyclohexanone-2-4-dinitrophenylhydrazone is carefully weighed into a platinum boat. The sample is next analyzed. The calibration factor is calculated from the recorder output as follows:

$$\text{Nitrogen:} \quad K_N = \frac{(Read)_N - (Zero)_N - (Blank)_N}{(Percentage\ of\ N)(Sample\ Weight)}$$

$$\text{Hydrogen:} \quad K_H = \frac{(Read)_H - (Zero)_H - (Blank)_H}{(Percentage\ of\ H)(Sample\ Weight)}$$

2) <u>Blank Determination</u>: For calibration purposes a platinum boat is used, cyclohexanone-2-4-dinitrophenylhydrazone being a solid. Aluminum capsules are employed for analyzing liquid samples. Empty aluminum capsules are sealed in an atmosphere of helium with the Perkin-Elmer Capsule Sealing Unit Model 042-1250. The blank is determined as described in Section 1).

3) <u>Analysis of Unknown Samples</u>: One to three mgs of oil is weighed into the aluminum capsule. The capsule is sealed in an atmosphere of helium. The sealed capsule is placed in the ladle and the ladle passed into the combustion tube. The analyzer is started by pressing the start switch. The recorder output is used to find the nitrogen and hydrogen contents as follows:

$$Wt\ \%\ N = \frac{(Read)_N - (Zero)_N - (Blank)_N}{K_N\ (Weight\ of\ the\ Sample)}$$

$$Wt\ \%\ H = \frac{(Read)_H - (Zero)_H - (Blank)_H}{K_H\ (Weight\ of\ the\ Sample)}$$

Ash Content in Oil

The routine procedure consists of the following steps:

1) Thoroughly clean the crucible with concentrated HCl and distilled water.

2) Heat the crucibles to 775-800°C for two hours in a furnace.

3) Allow the crucibles to cool down to room temperature and then weigh. Carry on steps 2) and 3) until a constant crucible weight is obtained.

4) Weigh the crucibles with 3-5 gms of sample oil.

5) Heat the crucibles in the furnace at a rate of about 200°C/hr.

6) Stabilize the temperature in the range of 775-800°C and maintain this temperature for one hour.

7) Allow the crucibles to cool down to room temperature, and then weigh.

8) Repeat steps 3) through 7) until no further change occurs in the weight upon repeated heating.

The ash content in the oil is given by

Wt % ash in oil = (w/W) x 100

where w = final weight of residue left in the crucible, and

W = initial weight of the oil sample.

Distillation

The procedure is based on the ASTM D-1160 standard. It consists of the following steps:

1) Turn water heater on and connect temperature recorder to the thermocouple.

2) Load cold trap with acetone and dry ice.

3) Turn on pump for circulating hot water. Allow the cooling water to circulate through the vapor condenser.

4) Take 100 ml of liquid sample in the flask. Make sure to add

boiling chips to the liquid before clamping the flask to the unit. Place glass thermometer in thermowell.

5) Turn on the vacuum pump and adjust pressure to 50 mm of Hg by adjusting the vacuum line valve.

6) Turn on the powerstat; initial setting of the powerstat is determined by operator (recommended 60 or higher).

7) Lower face shield and be sure to wear goggles.

8) Record pot temperature and vapor temperature indicated by the temperature recorder in the logbook.

9) Collect approximately 10% of total sample in each test tube (10 cc). Record vapor and pot temperature when test tube is changed.

10) Powerstat settings are increased to give a uniform distillate rate.

11) Shut down. Turn off vacuum pump and powerstat.

12) Let the system cool to approximately 100°C. Repressurize slowly by opening the by-pass valve.

13) Collect the liquid sample in the vapor trap. Collect bottom liquid sample.

14) Clean the flask by boiling acetone in it. Cleanup is best accomplished by atmospheric distillation of 20-30 ml of acetone.

APPENDIX C

CONVERSION OF DEW POINT TEMPERATURE AT 50 mm Hg

TO EQUIVALENT ATMOSPHERIC DATA
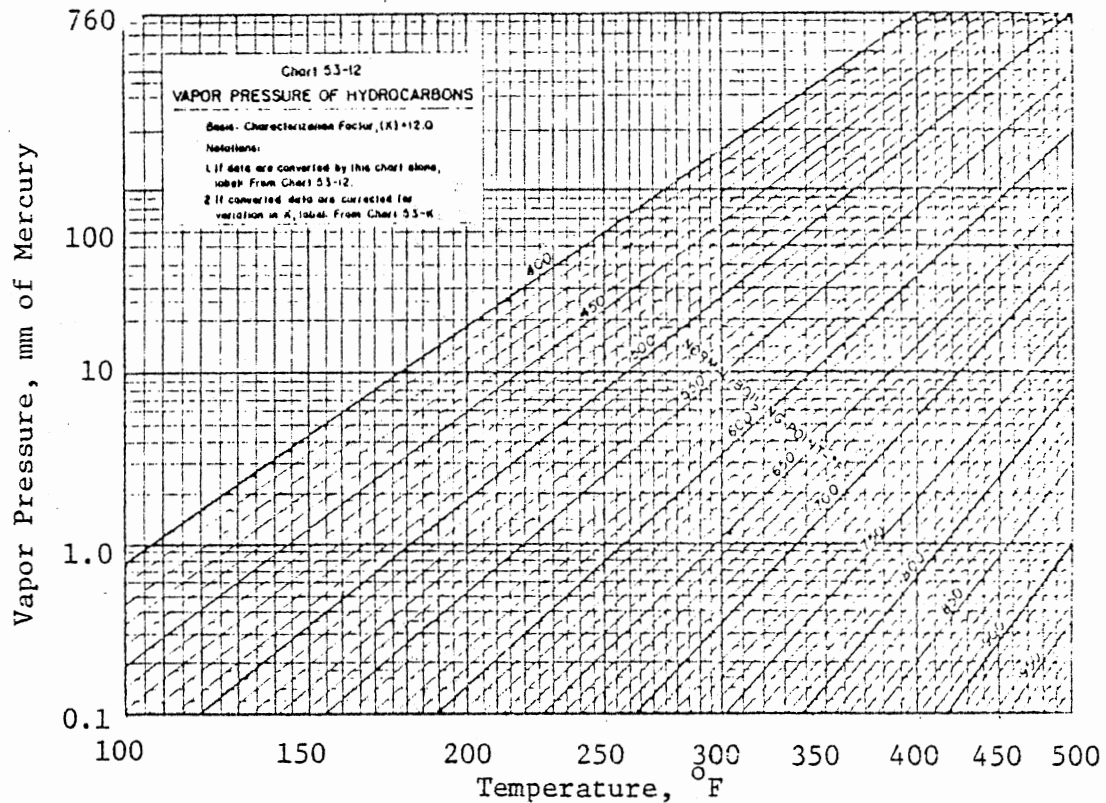
Figure 22.   Vapor Pressure of Hydrocarbon (^{O}F)

The boiling point (^{O}F) at 760 mm Hg is determined from observed temperatures (^{O}F) at 50 mm Hg by using Chart 52-12 (ASTM D-2892). The procedure is as follows:

1) Locate the boiling point at 50 mm Hg on the abscissa.

2) Locate the 50 mm Hg pressure on the ordinate.

3) Draw an isotherm at the point of intersection parallel to the normal boiling point isotherms. This temperature represents the normal boiling point (^{O}F).

APPENDIX D

EXPERIMENTAL DATA

The data obtained from the five experimental runs, ZBA, ZBB, ZBC, ZBD and ZBE, are listed in this Appendix. Experimental data were taken at 1500 psig and the temperatures of $616^{O}F$ ($324^{O}C$) and $815^{O}F$ ($435^{O}C$). Pamco Process Solvent oil was used in all five experimental runs. Commercial Co-Mo-alumina and Ni-Mo-alumina catalyst were used separately and in combination as zonal-catalyst beds. The product oil was analyzed for sulfur, nitrogen, and hydrogen concentrations.

TABLE XVII

RESULTS FROM RUN ZBA WITH HDN-30 CATALYST

Sample[*] Number	Temp[a] ^{o}F(^{o}C)	Pressure (psig)	Space Time[b] (Vol. hrly)	Hydrogen (SCF/BBL)	Hours[c] on Oil	%S[d]	%S[e] Removal	%N[d]	%N[e] Removal	%H[d]
Feed						0.438		0.977		7.110
ZBA-2	615(324)	1500	1.024	6730	15	0.255	43	0.593	37	9.076
ZBA-4	615(324)	1500	1.024	5510	35	0.278	36	0.793	19	8.497
ZBA-6	615(324)	1500	1.024	4592	40	0.235	47	0.829	15	7.950
ZBA-7	615(324)	1500	1.024	5510	43	0.251	44	0.819	16	7.944
ZBA-10	615(324)	1500	2.048	5510	55	0.251	44	0.827	15	7.718
ZBA-13	615(324)	1500	2.048	6730	65	0.257	42	0.857	12	7.360
ZBA-15	615(324)	1500	2.048	6730	70	0.207	54	0.845	14	7.491
ZBA-17	615(324)	1500	0.512	2525	78	0.371	17	0.867	11	7.431
ZBA-18	615(324)	1500	0.512	2525	80	0.309	31	0.925	-5	7.340
ZBA-19	615(324)	1500	1.024	3122	84	0.261	37	0.779	20	7.345
ZBA-24	615(324)	1500	1.024	4426	96	0.286	36	0.890	9	8.551

[*]Footnotes found on page 163.

TABLE XVIII

RESULTS FROM RUN ZBB WITH KETJENFINE-124 CATALYST

Sample[*] Number	Temp[a] °F(°C)	Pressure (psig)	Space Time[b] (Vol. Hrly)	Hydrogen (SCF/BBL)	Hours[c] on Oil	%S[d]	%S[e] Removal	%N[d]	%N[e] Removal	%H[d]
Feed						0.438		0.977		7.110
ZBB-2	815(435)	1500	2.048	6730	20	0.048	90	0.161	84	10.439
ZBB-3	815(435)	1500	2.048	6730	30	0.020	96	0.125	87	10.048
ZBB-4	815(435)	1500	2.048	6730	40	0.020	96	0.111	88	9.366
ZBB-5	815(435)	1500	2.048	6730	50	0.032	92	0.090	91	9.986
ZBB-6	815(435)	1500	2.048	6730	60	0.041	91	0.116	88	10.027
ZBB-7	815(435)	1500	2.048	6730	70	0.020	96	0.125	87	9.174
ZBB-8	815(435)	1500	1.024	6730	78	0.050	88	0.320	67	10.155
ZBB-9	815(435)	1500	1.024	6730	88	0.052	88	0.525	46	9.947
ZBB-10	815(435)	1500	1.024	6730	94	0.061	86	0.371	62	9.380
ZBB-11	815(435)	1500	2.048	6730	99	0.073	84	0.402	58	9.872
ZBB-12	815(435)	1500	2.048	6730	104	0.081	82	0.336	66	9.960

[*]Footnotes found on page 163.

TABLE XIX

RESULTS FROM RUN ZBC WITH HDN-30 CATALYST

Sample[*] Number	Temp[a] $^oF(^oC)$	Pressure (psig)	Space Time[b] (Vol. Hrly)	Hydrogen (SCF/BBL)	Hours[c] on Oil	%S[d]	%S[d] Removal	%N[d]	%N[e] Removal	%H[d]
Feed						0.438		0.977		7.110
ZBC-2	815(435)	1500	2.048	6730	20	0.107	76	0.129	87	10.659
ZBC-3	815(435)	1500	2.048	6730	30	0.20	96	0.062	94	10.849
ZBC-4	815(435)	1500	2.048	6730	40	0.020	96	0.031	96	10.455
ZBC-5	815(435)	1500	2.048	6730	50	0.020	96	0.133	86	9.323
ZBC-6	815(435)	1500	2.048	6730	60	0.046	90	0.067	93	9.692
ZBC-7	815(435)	1500	2.560	6730	70	0.020	96	0.067	93	10.858
ZBC-8	815(435)	1500	2.560	6730	75	0.020	96	0.023	97	10.037
ZBC-9	815(435)	1500	2.560	6730	83	0.020	96	0.068	93	10.381
ZBC-10	815(435)	1500	1.024	6730	89	0.108	76	0.624	36	8.912
ZBC-11	815(435)	1500	1.024	6730	94	0.050	86	0.541	45	8.134
ZBC-12	815(435)	1500	1.024	6730	98	0.099	77	0.635	35	8.330
ZBC-13	815(435)	1500	2.048	6730	106	0.020	96	0.266	73	9.243
ZBC-14	815(435)	1500	2.048	6730	111	0.069	85	0.293	70	9.116
ZBC-15	815(435)	1500	2.048	6730	117	0.038	92	0.380	61	9.449

[*]Footnotes found on page 163.

TABLE XX

RESULTS FROM RUN ZBD WITH KETJENFINE-124 AND HDN-30 CATALYST

Sample[*] Number	Temp[a] $^oF(^oC)$	Pressure (psig)	Space Time[b] (Vol. hrly)	Hydrogen (SFC/BBL)	Hours[c] on Oil	%S[d]	%S[e] Removal	%N[d]	%N[e] Removal	%H[d]
Feed						0.438		0.977		7.110
ZBD-2	815(435)	1500	2.048	6730	20	0.026	94	0.116	88	10.493
ZBD-3	815(435)	1500	2.048	6730	30	0.020	96	0.118	86	9.349
ZBD-4	815(435)	1500	2.048	6730	40	0.020	96	0.131	87	10.070
ZBD-5	815(435)	1500	2.048	6730	50	0.028	94	0.091	91	9.481
ZBD-6	815(435)	1500	2.048	6730	60	0.020	96	0.127	87	11.286
ZBD-7	815(435)	1500	2.560	6730	70	0.020	96	0.083	92	10.843
ZBD-8	815(435)	1500	2.560	6730	80	0.020	96	0.070	93	10.094
ZBD-9	815(435)	1500	2.560	6730	88	0.020	96	0.125	87	10.009
ZBD-10	815(435)	1500	1.024	6730	95	0.065	85	0.504	48	8.231
ZBD-11	815(435)	1500	1.024	6730	100	0.020	96	0.576	41	8.595
ZBD-12	815(435)	1500	1.024	6730	104	0.030	93	0.314	68	9.210
ZBD-13	815(435)	1500	2.048	6730	109	0.020	96	0.193	80	10.042
ZBD-14	815(435)	1500	2.048	6730	114	0.020	96	0.143	85	8.401
ZBD-15	815(435)	1500	2.048	6730	120	0.020	96	0.314	68	8.543

[*]Footnotes found on page 163.

TABLE XXI

RESULTS FROM RUN ZBE WITH HDN-30 CATALYST

Sample[*] Number	Temp[a] °F(°C)	Pressure (psig)	Space Time[b] (Vol. hrly)	Hydrogen (SCF/BBL)	Hours[c] on Oil	%S[d]	%S[e] Removal	%N[d]	%N[e] Removal	%H[d]
Feed						0.438		0.977		7.110
ZBE-2	815(435)	1500	2.048	6730	20	0.020	96	0.125	87	10.624
ZBE-3	815(435)	1500	2.048	6730	30	0.038	91	0.063	94	10.652
ZBE-4	815(435)	1500	2.048	6730	40	0.048	89	0.050	95	10.202
ZBE-5	815(435)	1500	2.048	6730	50	0.020	96	0.077	92	10.102
ZBE-7	815(435)	1500	2.048	6730	70	0.020	96	0.045	95	9.786
ZBE-8	815(435)	1500	2.048	6730	80	0.020	96	0.074	92	9.996
ZBE-9[**]	815(435)	1500	2.048	6730	90	0.029	93	0.106	89	10.747
ZBE-10	815(435)	1500	2.048	6730	100	0.020	96	0.217	78	9.401
ZBE-11	815(435)	1500	2.048	6730	110	0.029	93	0.224	77	9.836
ZBE-12	815(435)	1500	2.048	6730	120	0.039	91	0.213	78	10.060
ZBE-13	815(435)	1500	2.048	6730	125	0.020	96	0.281	71	9.030

[*] Footnotes found on page 163.

[**] Oil flow was cut off for 2.5 hours due to power failure.

FOOTNOTES

[a] Nominal reactor temperature.

[b] This is a volume hourly space time (volume of catalyst/volume of oil per hour).

[c] Total hours which the catalyst has been contacted with oil at reaction conditions.

[d] Percent of sulfur, nitrogen or hydrogen in liquid product.

[e] % removal = 100 (fraction in feed less fraction in product)/(fraction in feed).

2.

VITA

Opinder Kishan Bhan

Candidate for the Degree of

Master of Science

Thesis: AN INVESTIGATION OF THE ACTIVITY OF ZONAL CATALYST BEDS FOR HYDRODESULFURIZATION AND HYDRODENITROGENATION OF A COAL-DERIVED LIQUID

Major Field: Chemical Engineering

Biographical:

   Personal Data: Born in Srinagar (Kashmir), India, on March 17, 1956, to Mohini and Prof. Brij Kishan Bhan.

   Education: Graduated from C.M.S. High School, Srinagar, Kashmir, India, in 1972; received the Bachelor of Engineering degree in Chemical Engineering from the University of Kashmir, Srinagar, Kashmir, in August, 1978; completed requirements for the Master of Science degree in Chemical Engineering at Oklahoma State University, Stillwater, Oklahoma, in May, 1981.

   Professional Experience: Engineering Trainee at Bhabha Atomic Research Center, Bombay, India, 1977; worked at Ozark Mahoning Company, Tulsa, Oklahoma, during the summer of 1979; Graduate Teaching Assistant, School of Chemical Engineering, Oklahoma State University, January, 1979, to January, 1980; Research Assistant, School of Chemical Engineering, Oklahoma State University, January, 1980, until present.